1983

Studies In Surface Photochemistry

Linda Joanne Johnston

CANADIAN THESES ON MICROFICHE

I.S.B.N.

THESES CANADIENNES SUR MICROFICHE

National Library of Canada
Collections Development Branch

Canadian Theses on
Microfiche Service

Ottawa, Canada
K1A 0N4

Bibliothèque nationale du Canada
Direction du développement des collections

Service des thèses canadiennes
sur microfiche

NOTICE

The quality of this microfiche is heavily dependent upon the quality of the original thesis submitted for microfilming. Every effort has been made to ensure the highest quality of reproduction possible.

If pages are missing, contact the university which granted the degree.

Some pages may have indistinct print especially if the original pages were typed with a poor typewriter ribbon or if the university sent us a poor photocopy.

Previously copyrighted materials (journal articles, published tests, etc.) are not filmed.

Reproduction in full or in part of this film is governed by the Canadian Copyright Act, R.S.C. 1970, c. C-30. Please read the authorization forms which accompany this thesis.

AVIS

La qualité de cette microfiche dépend grandement de la qualité de la thèse soumise au microfilmage. Nous avons tout fait pour assurer une qualité supérieure de reproduction.

S'il manque des pages, veuillez communiquer avec l'université qui a conféré le grade.

La qualité d'impression de certaines pages peut laisser à désirer, surtout si les pages originales ont été dactylographiées à l'aide d'un ruban usé ou si l'université nous a fait parvenir une photocopie de mauvaise qualité.

Les documents qui font déjà l'objet d'un droit d'auteur (articles de revue, examens publiés, etc.) ne sont pas microfilmés.

La reproduction, même partielle, de ce microfilm est soumise à la Loi canadienne sur le droit d'auteur, SRC 1970, c. C-30. Veuillez prendre connaissance des formules d'autorisation qui accompagnent cette thèse.

THIS DISSERTATION
HAS BEEN MICROFILMED
EXACTLY AS RECEIVED

LA THÈSE A ÉTÉ
MICROFILMÉE TELLE QUE
NOUS L'AVONS REÇUE

NL-339 (r. 82/08)

Canada

STUDIES IN SURFACE PHOTOCHEMISTRY

by

Linda Joanne Johnston

Department of Chemistry

Submitted in partial fulfillment
of the requirements for the degree of
Doctor of Philosophy

Faculty of Graduate Studies
The University of Western Ontario
London, Ontario
May, 1983

ABSTRACT

The behaviour of photochemically generated radical pairs on a silica gel surface was compared with results obtained in other restricted environments and in solution. Particular emphasis was placed upon the adsorbed radicals' surface mobility as measured by the amount of nongeminate recombination of the original radical pair.

Benzyl radical pairs were generated by photolysis of 4-methylbenzyl-4-methoxyphenyl acetate, 1-(4-methylphenyl)-3-(4-methoxyphenyl)-2-propanone and 4,4'-methoxymethyl-dibenzyl sulfone adsorbed on silica gel. The amounts of geminate recombination determined from the dibenzyl product ratios indicated that substantial movement occurs for adsorbed benzyl radicals. The surface mobility was influenced by both photolysis temperature and the radical pair multiplicity but was relatively insensitive to changes in surface coverage, partial dehydroxylation of the silica gel and the presence of coadsorbates on the surface. The observation of rearranged starting materials among the products produced by photolysis of adsorbed dibenzyl ketone and dibenzyl sulfone indicated the increased restrictions to radical motion on the shorter timescale of the phenyl-acetyl-benzyl and benzyl sulfonyl-benzyl radical pairs. The substantial ^{13}C enrichment of dibenzyl ketone recovered after partial photolysis on silica gel provided further evidence for restrictions to the motion of adsorbed

phenylacetyl-benzyl radical pairs. The relative rates of the Type I cleavage of a number of monosubstituted dibenzyl ketones were measured by CIDNP.

Cyanopropyl radicals generated photochemically from adsorbed azobisisobutyronitrile yielded both carbon-nitrogen and carbon-carbon coupling products, indicating that the surface did not restrict the rotational motion of these radicals, as previously claimed. Deuterium labelling experiments indicated that there was predominantly geminate recombination of singlet cyanopropyl radical pairs, although some radicals were sufficiently translationally mobile to escape from their original partners. The longer-lived radical pairs generated by triplet sensitization yielded mainly nongeminate recombination.

ACKNOWLEDGEMENTS

I thank Dr. de Mayo for his guidance and encouragement throughout the course of this research. Thanks go also to Dr. Wong for his advice and help, particularly with respect to the CIDNP and ^{13}C experiments. Brad Frederick's help with some of the sulfone work is gratefully acknowledged. I would also like to thank everyone in 202, 203 and 204 and the others in the chemistry department who have helped in various ways and have made my stay at Western an enjoyable one. Finally, a special thank-you to Sandy Tamowski for the typing of this manuscript.

TABLE OF CONTENTS

LIST OF TABLES

LIST OF FIGURES

List of Figures (continued)

CHAPTER 1

INTRODUCTION

Surface photochemistry has until recently been a relatively unexplored area, despite its obvious potential in probing surface structures and photochemical reaction mechanisms. Surprisingly little is known about the general physical behaviour of commonly encountered organic molecules in their ground states when adsorbed on the surface of adsorbents such as silica gel, alumina or porous Vycor. Investigations of the reactivity and mobility of radicals generated from adsorbed precursors are also scarce.

In general, the behaviour of adsorbed radicals and molecules is more complex than that of the same species in homogeneous systems. A number of parameters require consideration in investigations of surface photoprocesses. Firstly, the adsorbed species may adopt a conformation different from that normally observed in solution. Such conformational changes may alter absorption and emission spectra, may permit normally forbidden transitions to occur and may change the rates of various photophysical processes. Variations in product stereochemistry or in partitioning of an intermediate along two reaction pathways may also be envisaged. Secondly, the surface "viscosity" is expected to influence several processes, the most important of which, with respect to this research, is the surface mobility of

the adsorbed species.‡ Rotational and diffusional movement may both be affected by the adsorbent. Until recently, few studies have dealt with the questions, "How much movement can occur for adsorbed species?" and "On what timescale does this motion take place?". Answers to these questions will demonstrate the feasibility of bimolecular processes occurring for adsorbed species. Thirdly, the consequences of the surface roughness and irregularity must be considered. For example, surface irregularities may appear as nonuniform distributions of strong adsorption sites. Finally, the adsorbed molecule's inherent chemical reactivity may be modified since the electronic polarisation and polarisability may both be affected by the binding forces on the surface.

The primary purpose of this research was to investigate the behaviour of radicals generated photochemically from adsorbed molecules in comparison with their behaviour in other inhomogeneous environments (e.g., micelles) and in solution. Silica gel was chosen as the adsorbent for the investigations of adsorbed radicals. It was selected for the following reasons: silica gel is relatively unreactive towards most organic compounds; its surface properties have been extensively studied and reviewed;[1,2,3] and it does not give energy transfer upon irradiation as does alumina.

---

‡It should be noted that the term "viscosity" as it is used here refers primarily to restriction of motion of an adsorbate on the surface. It will vary for different adsorbates and is, therefore, not an inherent property of the solid as is viscosity for a liquid.

1.1 Surface Structure of Silica Gel

The term silica includes all structures with the composition SiO_2, as well as various hydrated species, $SiO_2 \cdot X\ H_2O$. Each silicon atom is surrounded by four oxygens to give a tetrahedral $[SiO_4]^{4-}$ unit. Silicas exhibit primarily covalent bonding along with smaller amounts of ionic and $d\pi$-$p\pi$ silicon-oxygen bonding. Although there are several structurally well defined crystalline silicas (e.g., quartz), only the porous, amorphous silicas will be considered here. The latter are formed by polycondensation of polysilicic acids to form particles which have an irregular three-dimensional network of SiO_4 tetrahedra with the residual valences on the surface occupied by hydroxyl groups. Adsorbent characteristics such as the particle size and density, the surface area, and the number, size and shape of the pores are determined by various experimental parameters (e.g., pH, temperature, presence of electrolytes, etc.) during the condensation process.

The specific surface area of porous silica includes both internal and external surface areas. The internal surface area corresponds to the area of the pore walls and is several orders of magnitude larger than the geometric surface area of the particles. As a result, the usual 100-600 m^2/g surface areas represent predominantly internal surfaces. Because the pore sizes and diameters vary considerably (i.e., from micropores of <1 nm in diameter to macropores of >100 nm in diameter), the entire silica surface may not be accessible to larger organic molecules.

Surface areas are most commonly measured using the BET (Brunauer, Emmett and Teller) nitrogen adsorption method.

The surface of silica gel consists of three species, the hydroxyl groups, the siloxane bonds and physically adsorbed water molecules. All three are usually present but the amount of each depends very strongly on the heat treatment which the surface has received and on the method used to prepare the silica gel. Figure 1 illustrates the various arrangements of the functional groups on the surface. Despite the vast amount of literature on the subject, there is no general concensus regarding the number and type of surface species. The difficulty in specifying and/or duplicating a particular type of silica gel has added to the confusion.

Fully hydroxylated silica gel is capable of physically adsorbing water in amounts which vary with temperature, water vapor pressure and sample surface area. Fripiat and Uytterhoeven,[4] among many others, have investigated the amounts of physisorbed water present at various temperatures; above 230°C the concentrations become negligible in comparison to those of the hydroxyl groups. The temperature at which surface water can be removed without concomitant hydroxyl condensation has not been well established. Quoted values[5] range from 100 to 350°C and Iler[3] has suggested that only low temperature drying under vacuum is satisfactory. The concentrations of physisorbed water are generally evaluated by measuring the weight loss upon annealing at a temperature at which the silanols are

Figure 1. Surface structure of silica gel: A - vicinal, hydrated hydroxyls; B - geminal hydroxyls; C - isolated hydroxyls; D - siloxane bonds; D - vicinal hydrogen-bonded hydroxyls.

A

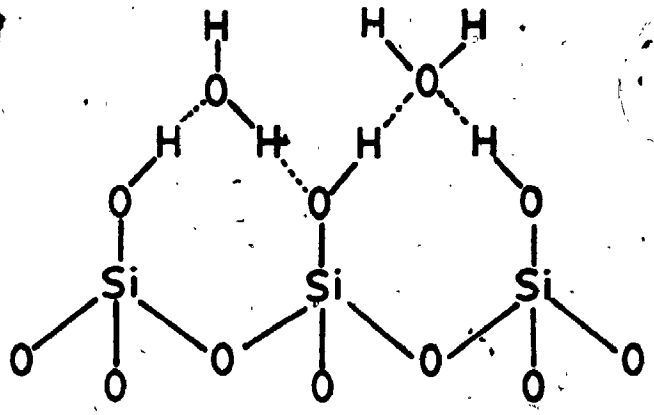

B

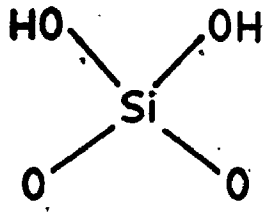

C D C

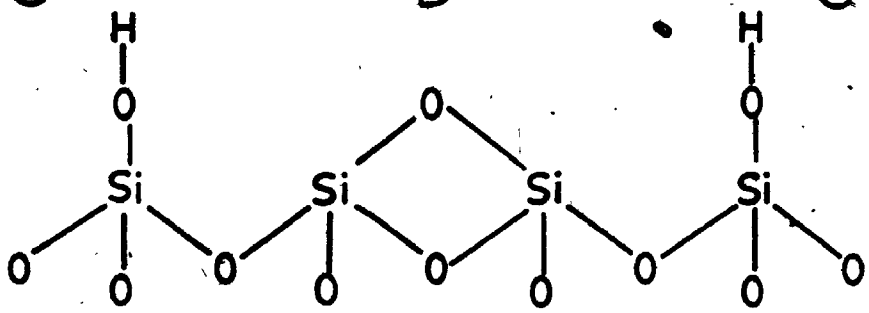

D

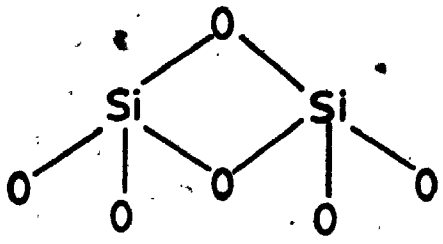

E

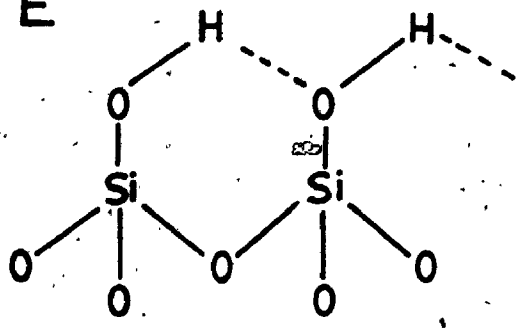

not condensed. Infrared spectroscopy,[6] alone or in conjunction with thermogravimetric techniques, has been the most frequently used means of investigating physically adsorbed water.

It is now generally accepted that there are 4-5 hydroxyls/nm^2 on the surface of silica gel from which physisorbed water has been removed.[3] These silanols are not uniformly distributed. One theory[7] classifies them as nonhydrogen-bonded hydroxyls (>0.31 nm apart) and bound hydroxyls (0.24-0.31 nm separations) which have hydrogen bonds of varying strengths. A second theory[8] defines isolated and paired hydroxyl groups, the latter including both geminal and vicinal silanols (see Figure 1). However, the postulated geminal hydroxyl groups have been suggested by others[3] to be internal uncondensed hydroxyls.

The various types of silanols have been studied extensively by infrared spectroscopy and a comprehensive review of the subject has been presented by Kiselev.[6] Additional methods for quantitatively determining silanol concentrations include deuterium exchange techniques and reaction of the active hydrogens with, for example, trichlorosilanes to form covalently bound surface species. One study[9] has indicated that the silica gel has ~3.2 hydrogen bonded and ~1.6 internal hydroxyls/nm^2. More recently Tsuchyla[9] has reported that infrared spectra of hydrogen bonded species actually include three types of perturbed silanols. Contributions from oxygen (A), hydrogen (B), and both hydrogen and oxygen (C) hydrogen bonded

hydroxyls could be distinguished in addition to the sharp absorption due to isolated silanols.

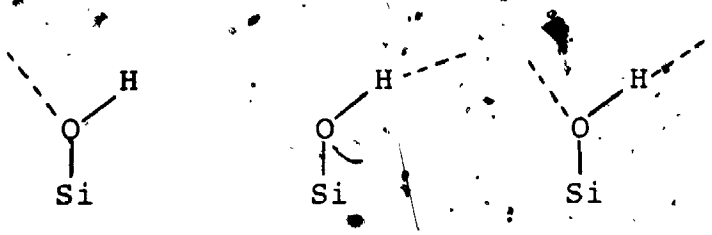

A B C

Both surface and internal hydroxyl groups are removed by condensation to form siloxane bonds plus water (1).[2,3,4]

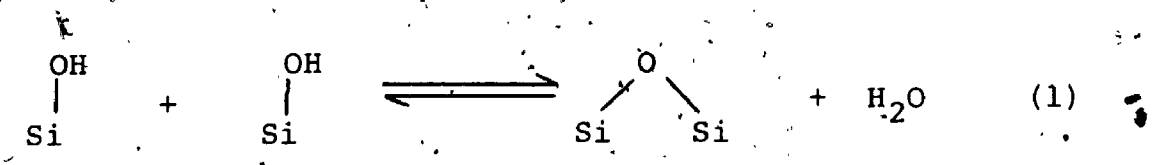

(1)

The dehydration is reversible but rehydration occurs slowly for highly dehydroxylated surfaces as adsorption of a water molecule at an adjacent silanol must precede addition of water to a siloxane linkage.[3] At 500-600°C all but the isolated hydroxyls are removed; an estimated 1 hydroxyl/nm^2 remains at 800°C.[3] The complete dehydroxylation which occurs when silica is annealed at ~1100°C has been postulated to occur by lateral movement of surface silicon atoms bearing isolated hydroxyls.[1] Destruction of the pore structure by sintering also occurs under these conditions and leads to substantially reduced surface areas. Internal silanols are removed over a wide temperature range and this process has been suggested to occur by proton migration across strained oxygen bridges to give adjacent condensable hydroxyls.[11]

The concentration of the third surface species, siloxane bonds, varies with the heat treatment which the silica has received. Siloxanes cover most of the surface when silica has been annealed at a high temperature. As a result, such surfaces are hydrophobic and inefficient in adsorbing polar molecules. The strained siloxane linkages are reported to form small amounts of free radicals.[12] In addition, siloxylated surfaces have been shown to possess definite oxidizing properties.[13]

1.2 Adsorption on Silica Gel

Adsorption of molecules on a surface may be divided into two categories: physisorption and chemisorption. The latter involves a bonding interaction between an adsorbate and the surface atoms to yield a chemically bound species. It usually requires an activation energy and has a heat of adsorption in excess of 80 kJ/mol. Only physisorbed molecules will be considered here. Physical adsorption occurs through (1) London-type dispersion forces arising from induced dipole interactions, (2) induction forces (interactions between permanent or induced molecular dipoles) and (3) charge transfer interactions, such as hydrogen bonding, between the adsorbate and the surface atoms. These processes do not require activation energies and have heats of adsorption of 8-40 kJ/mol.

The adsorption interactions between silica and adsorbates have been studied for a large number of molecules.[14] Nonspecific interactions such as London forces

occur to some extent for most molecules and provide the major adsorption interaction for nonpolar species. They are relatively insensitive to the water content or degree of dehydroxylation of the surface. On the other hand, specific interactions are observed for molecules with localized centres of high electron density (i.e., π electrons) or polar functional groups. Hydrogen bonding to the silanol groups is the major specific interaction for a silica gel surface and contributes much more to the adsorption interaction for polar species than do dispersion forces. The hydrogen bonding interaction for several molecules is illustrated in Figure 2. It should be noted that the magnitude of a hydrogen bond to a π system is only ~9 kJ/mol[15,16] as compared to ~40 kJ/mol for that to a heteroatom.

The strength of adsorption of molecules on silica gel will, in general, increase with increasing polarity of the substrate. For example, Basila[17] has demonstrated the importance of hydrogen bonding to surface silanols in the adsorption of substituted benzenes. The magnitude of the adsorption interaction was shown to be a function of both the frequency shift of the hydroxyl stretching vibration and the adsorbate ionization potential. Isolated silanols are expected to interact more strongly with most adsorbates than are hydrogen bonded hydroxyls. Since water interacts strongly with the surface silanols, silica gel from which physically adsorbed water has been removed will have the greatest adsorption capacity. Conversely, adsorption on

silica which has large amounts of physisorbed water or on dehydroxylated silica will be less efficient, particularly for polar molecules. Some adsorption may occur by hydrogen bonding of compounds to surface adsorbed water but this is expected to be weaker than the interaction with hydroxyl groups.

The importance of hydrogen bonding to hydroxyl groups in the adsorption process on silica gel has been well established. Other factors in the adsorption process are also important in any investigation of the adsorbed species. Because the silanol groups are of different types and are not uniformly distributed over the surface[1], inhomogeneous arrangements of adsorbed molecules may occur. Preferential interactions between adsorbate molecules rather than with the surface can also contribute to inhomogeneity in the adsorbed phase. In an extreme case, one could imagine small islands of tightly packed adsorbed molecules in the midst of large areas of bare surface. Furthermore, the initial adsorbate distribution is not necessarily the most stable; equilibration may occur if the species is sufficiently mobile on the surface.

Secondly, there may be "active sites" on the surface where certain molecules will be particularly strongly adsorbed.[18] For example, Snyder and Ward[18a] have suggested that adjacent pairs of strongly hydrogen bonded hydroxyls are the most reactive in adsorption of aromatics on silica gel. Others have suggested that isolated silanols are more reactive. In any case, the strength of adsorption will

depend on the hydroxyl environment and this is not uniform throughout the sample. Moreover, the large size of most organic compounds in comparison to the spacing between adjacent silanol groups implies that an adsorbed molecule may interact with more than one silanol group,[15] as illustrated in Figure 2. Depending on the number and type of surface sites with which it is in contact, an adsorbate may experience a range of adsorption interactions. This has been pointed out by Dacey[18b] who envisages a wide range of energy barriers for activated diffusion of molecules adsorbed on a heterogeneous surface.

Additional variables in the adsorption process include the orientation of the molecule at the surface and the amount of surface area that is actually accessible to a particular adsorbate. It has been shown that for adsorbent pore diameters of 1 nm or less some of the surface available to nitrogen adsorption is unavailable to larger adsorbates such as dibenzyl or naphthalene.[18a]

1.3 Mobility of Small Adsorbed Molecules

Small molecules might be expected to show considerable translational mobility when adsorbed on a surface but this hypothesis has not been extensively tested. Nitrogen has been shown to migrate easily on tungsten;[19] the results suggest that surface migration becomes important at half the temperature at which evaporation is observable. Similarly, surface mobility of benzene has been observed.[20,21] Studies of electronic spectra and entropies of adsorption suggest

Figure 2. Bonding on the silica gel surface.

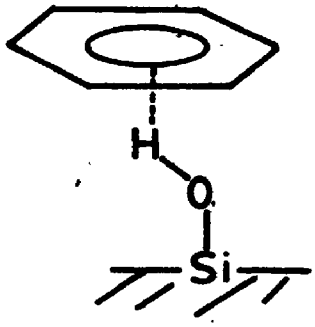
H
O
Si

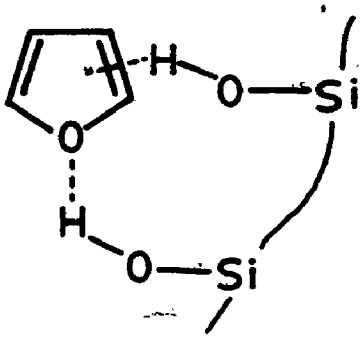
H
O
Si
O
H
O
Si

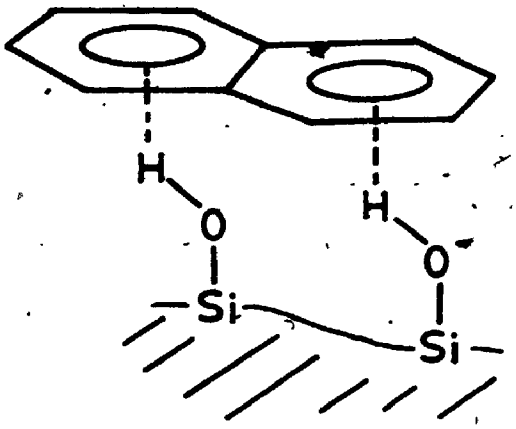
H
O
Si
H
O
Si

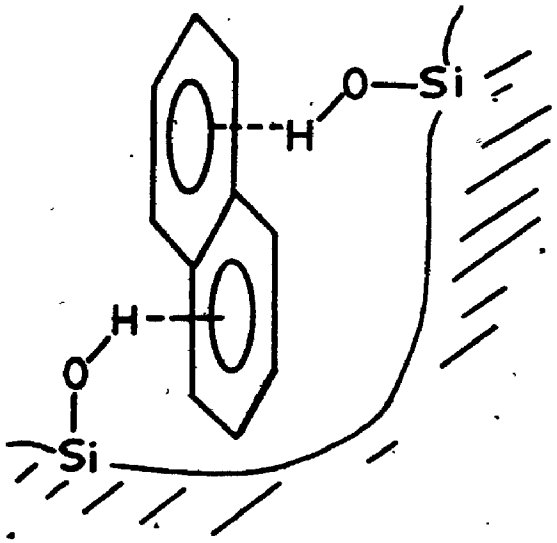
O
Si
H
H
O
Si

that a mobile adsorption model is more suitable than a site adsorption model for benzene.[20] Measurement of the diffusion coefficients for benzene adsorbed on Aerosil plugs using NMR spin echo techniques[21] gave values which, at high coverages, were similar to those for liquid benzene. However, part of the surface diffusion was thought to result from molecular mobility in the pore volume. Activation energies for diffusion of benzene on Aerosil were in the 14.5-21 kJ/mol region.

NMR studies have also been undertaken for other small molecules adsorbed on surfaces.[22,23] Proton relaxation times for methanol-d_0, d_1 and d_3 adsorbed on porous glass[22] were shown to depend on coverage. The observed distribution of correlation times was claimed to be characteristic of molecular motion, both rotational and diffusional. Carbon-13 NMR spectra were obtained for a number of small molecules adsorbed on silica gel.[20] For trans-2-butene and acetone the decrease in spin-lattice relaxation times relative to those of the same molecules in the liquid state was partially attributed to an increased efficiency of dipole-dipole relaxation caused by slower molecular motion of the adsorbed molecules. It is unclear whether a distinction can be made between rotational and translational movement in either of the above experiments.

1.4 Mobility of Adsorbed Radicals

There have been few investigations of the mobility of adsorbed radicals. The available data come from electron

paramagnetic resonance studies of relatively stable radicals, such as nitroxides, adsorbed on a variety of inorganic solids. Hoffman et al.[29] have measured EPR spectra of the di-t-butyl nitroxide radical adsorbed on silica, alumina and mixed silica-alumina adsorbents. The observed hyperfine splittings were consistent with radical adsorption at two sites, the hydroxyls and aluminum(III) ions, on the alumina and the silica-alumina surfaces. Equilibration of samples on these surfaces at various temperatures produced changes in the relative amounts of the signals for adsorption at the two sites. This site equilibration could result from either rotational or translational motion if the radical is large relative to the spacing between the two adsorption sites. The inhomogeneous environment of the radicals makes it difficult to distinguish between these possibilities. Spectra of the nitroxide adsorbed on silica indicated that the radical was immobile at (and below) 77 K; the broad range of correlation times at higher temperatures were indicative of radicals with varying degrees of mobility.[24b]

EPR spectra of the 2,2,6,6-tetramethylpiperidin-1-oxy radical adsorbed on silica, alumina and gallium oxide have been measured by Evreinov and coworkers.[25] As with the nitroxide discussed above, the spectra of this iminoxy radical adsorbed on alumina showed components due to adsorption at Lewis acid and hydroxyl sites.[25a] The spectra on silica gel exhibited line broadening characteristic of hindered rotation of the radical; an activation energy of ~2

kJ/mol was calculated from changes in the correlation time with temperature.[25b] Although the spectra were insensitive to the degree of dehydroxylation of the surface, coadsorption of donor molecules (e.g., H_2O, NH_3, pyridine) led to increases in the radical mobility.[25c] The increased mobility in the presence of these donors was attributed to to occupation of the stronger adsorption sites by the donor and the lack of change in the EPR spectra of the adsorbed radical upon coadsorption of nonpolar molecules lends support to this hypothesis. The authors have suggested that both translational and rotational motion occur but their results do now show any necessity for the former.

The EPR spectra of methyl radicals generated on porous glass have been recorded.[26] The sharp line widths at 77 K indicated a rapid tumbling motion of the radical.[26a] At higher temperatures the signal decay was attributed to surface diffusion of the radicals followed by recombination. The more complex spectra at low radical concentrations were assigned to a combination of physically trapped methyl radicals and radicals formed by interaction of a methyl radical with a surface impurity site.[26b,d]

1.5 Absorption Spectra of Adsorbed Molecules

Absorption spectra for a large number of organic molecules adsorbed on a variety of adsorbent surfaces have been measured.[26-30] Most have been obtained with transparent adsorbents or with slurries of the adsorbent in an inert solvent with a refractive index similar to that of

the absorbent (in order to obtain sufficiently transparent samples). However, recent advances in techniques such as reflectance and photoacoustic spectroscopy have now made photophysical investigations of opaque materials possible. In general, weakly adsorbed molecules have absorption spectra which are similar to those in solution but which often show broader, less well-resolved bands. Absorption maxima are usually shifted in the direction expected for a polar solent, a fact for which Leermakers has provided ample evidence.[29] Red shifts occur when the excited state of the adsorbed molecule has an increased dipole or is more polarizable than the ground state (e.g., ketone π-π^* states); in the reverse case blue shifts occur (e.g., ketone n-π^* states). The magnitude of the observed shifts is a function of the strength of interaction of the molecule with the surface. For example, large blue shifts were observed by Leermakers[29b] for the charge transfer transitions of the strongly adsorbed alkylpyridinium iodides in silica gel-cyclohexane slurries. The λ_{max} of the absorption band of 1-ethyl-4-carbomethoxypyridinium iodide gave the silica gel a Kosower Z value of 88, which indicated that the polarity of the surface was intermediate between that of water and methanol.

The shifts in the absorption spectra which occur upon adsorption may lead to an inversion in the usual energy levels for two excited states. An interesting example of this effect was discovered in the isomerization of 2,4-cyclohexadienones in a silica gel-solvent slurry.[31]

Inversion of the π-π^* and n-π^* triplets for the adsorbed dienones resulted in the observation of a previously unknown isomerization of these molecules to bicyclic ketones. Similar effects upon excited state energy levels have also been observed for the triplet states of α,β-unsaturated cyclopentenones.[32]

1.6 Radical Reactions of Adsorbed Molecules

Several radical reactions, most of which were photochemically initiated, have been carried out for molecules adsorbed on solid surfaces. Adsorbent-solvent slurries were used for the earlier experiments; thus, these examples are complicated by the fact that at least some reaction occurred in the solvent. In an early example the Type I cleavage isomesityloxide was carried out in a silica gel slurry,[33] although no comparison with solvent results was given. Two other examples come from Leermakers' extensive investigations of adsorbed molecules in silica gel slurries.[29,34] He has examined the photolysis of azobisisobutyronitrile and tetramethyl-1,3-cyclobutanedione in these media.[29b,34] For the former the failure to observe any of the unsymmetrical coupling product formed in solution photolyses was taken as evidence for restricted rotation of the cyanopropyl radicals produced by homolysis of the azo compound on the surface. This system has been reinvestigated during the course of this research and the previous findings have been shown to be in error, as discussed in Chapter 5.

Irradiation of the above cyclobutanedione in a silica gel-cyclohexane slurry resulted in a large decrease in the quantum yield for photodecomposition, as compared to solution.[34] The lower quantum yield was attributed to the "super cage" effect of the surface. The rate of diffusional decay of the initial alkyl-acyl radical pair was slower on the surface than in solution and, thus, recombination of the radicals to regenerate starting material predominated over irreversible loss of carbon monoxide and subsequent product formation.

The photolysis of a number of alkyl ketones adsorbed on porous Vycor glass has been examined in some detail by Anpo and coworkers.[35,36] In contrast to results obtained in solution, a large preference for geminate recombination of the radicals was observed in the Type I reactions of adsorbed alkyl ketones. The Type II reaction of 2-pentanone was also affected by the surface; the amount of Type II cleavage decreased for photolysis on Vycor which had been degassed at 800°C rather than at 100°C. This effect was ascribed to a greater stabilization of the Type II biradical on the hydroxylated and, therefore, more polar surface which remained after low temperature degassing.

Anpo et al.[35] have also examined the effect of adsorption upon the excited state lifetimes of a number of alkyl ketones. The shorter lifetimes for the adsorbed ketones were thought to result from an increased radiationless deactivation rate owing to surface-adsorbate interactions. The correlation between the decrease in the

lifetimes and the strength of the interaction of the ketone with the Vycor surface supported this explanation. Energy transfer from one ketone to another and quenching of phosphorescence and photochemistry for the adsorbed ketones were also examined.

The photo-Fries rearrangement has been demonstrated for aromatic esters adsorbed on dry silica gel and in silica gel-pentane slurries (2).[32] The reaction in solution

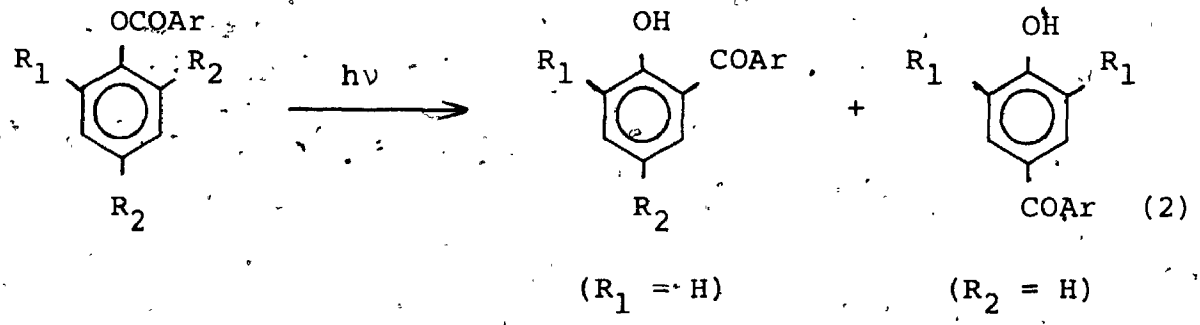

(2)

involves homolysis from the singlet state followed by recombination, in the solvent cage, of the radical pair. The observation of both ortho and para products upon photolysis of the adsorbed esters required that movement occur during the lifetime of the singlet radical pair. Product yields for some esters were higher than in solution and reflected the slower diffusional separation of the radical pair on the surface.

The first clear example of a major deviation from solution results in the reaction pathway for an adsorbed molecule has been recently reported by de Mayo et al.[38] Irradiation of benzoin methyl ether and benzoin isopropyl ether on dry silica gel led to large changes in the product

distributions from those obtained in methanol. Previously undetected Type II products and the rearranged product, 1 resulting from geminate recombination of the radical pair formed by Type I cleavage were isolated (Scheme 1). The products from benzoin isopropyl ether photolysis on silica gel at -80°C were ~71% Type I, of which ~60% was the rearranged product, 1, and ~24% Type II. In contrast, in methanol at -80°C only 18.3% rearranged Type I product was formed and no Type II products were observed. The large amount of geminate recombination product,1, indicated that translational movement for the triplet radical pair produced by Type I cleavage was restricted on the surface, particularly at low temperature. However, rotational motion was relatively facile and resulted in the formation of rearranged Type I products. The substantial amounts of Type II reaction and the Type II cyclisation to cleavage ratios implied that the surface had imposed upon the ether a conformation which was different from that in solution and from which hydrogen abstraction could occur.

Leffler et al.[39] have investigated the photochemical and thermal radical decomposition of azocumene on silica surfaces. The previously unobserved rearranged cumyl dimers, 2 and 3, were formed in 2-6% yields in addition to the normal coupling and disproportionation products (3). Catalytic sites for rearomatization were postulated for the production of these dimers since they were formed only by geminate recombination. In fact, trapping and deuterium labelling experiments indicated that most radicals

Scheme 1

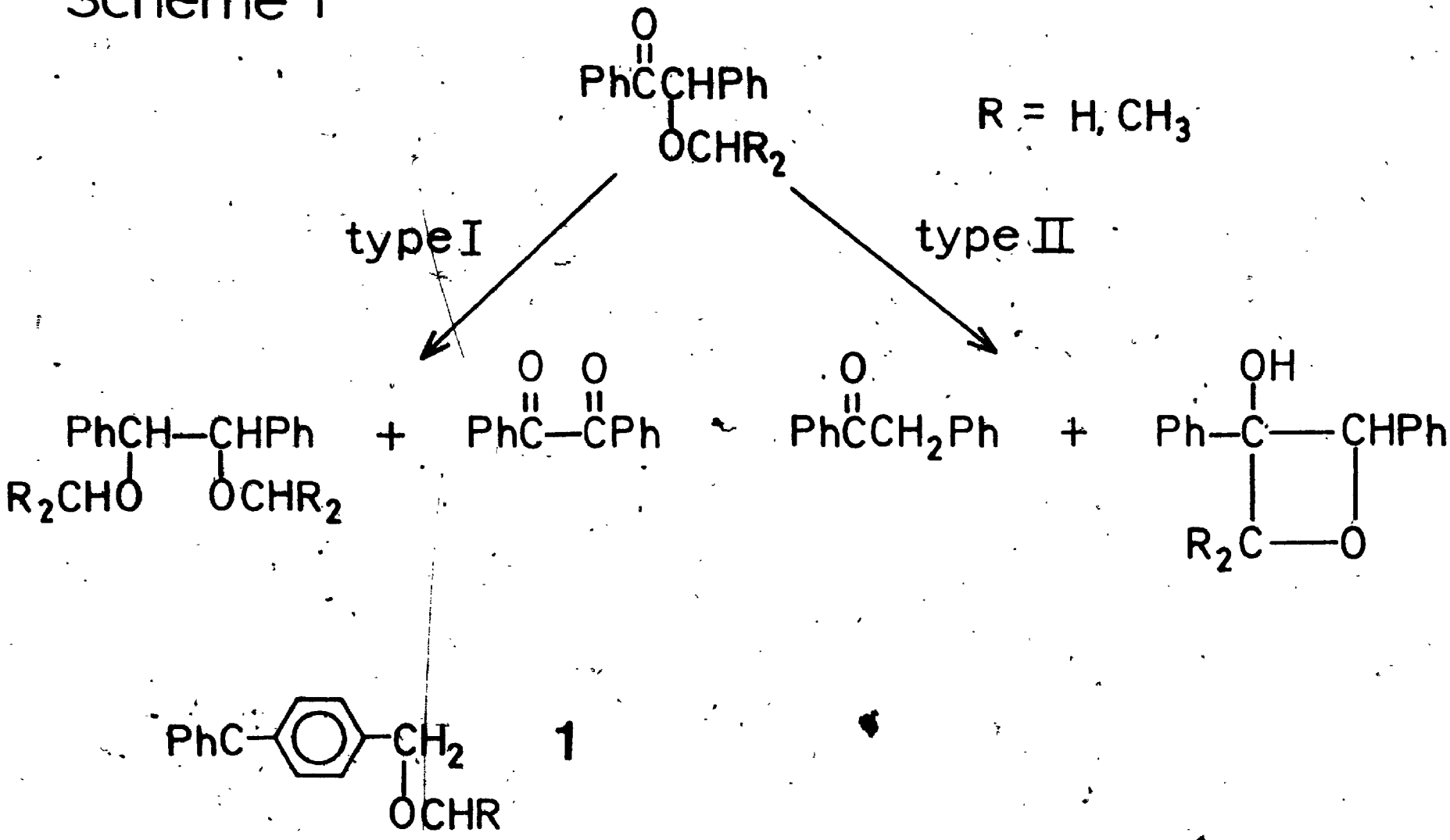
PhCCHPh
O
OCHR2
R = H, CH3
type I
type II
PhCH—CHPh
R2CHO OCHR2
PhC—CPh
O O
PhCCH2Ph
O
Ph—C—CHPh
OH
R2C—O
PhC
CH2
OCHR
1

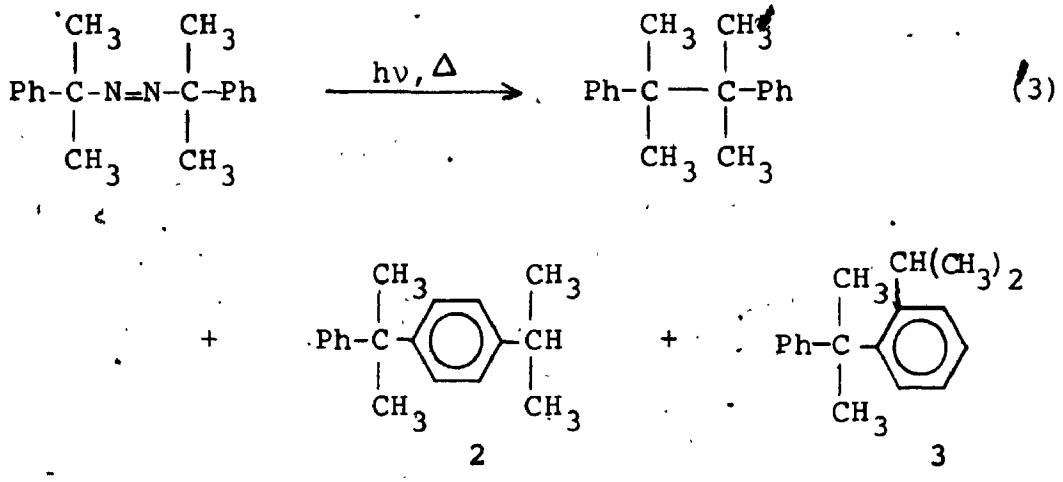

(3)

2 + 3 + disproportionation products

recombined or disproportionated in their original geminate pair, although some were sufficiently translationally mobile to escape geminate reaction. A greater amount of rotational mobility on the surface was indicated by EPR spectra of the adsorbed cumyl radicals. The authors have also suggested that small changes in the thermal decomposition kinetics of azocumene at different surface coverages or in the presence of coadsorbates provide some evidence for preferred adsorption sites. This conclusion seems questionable since only small variations in the decomposition rate were observed.

The photolysis of diacyl peroxides such as 4 adsorbed on silica gel has also been examined by Leffler and coworkers.[40] Although the surface decomposition was faster and produced different products than did the solution reaction, the presence of both radical and ionic pathways greatly complicated the analysis. The authors have, nevertheless, suggested that the radicals' translational

motion was constrained and that a variety of nonequivalent adsorption sites were present on the surface. Decreased yields of products resulting from neophyl to phenyl-t-butyl radical rearrangements (4) supplied further evidence for restriction of the internal motion of the radicals.

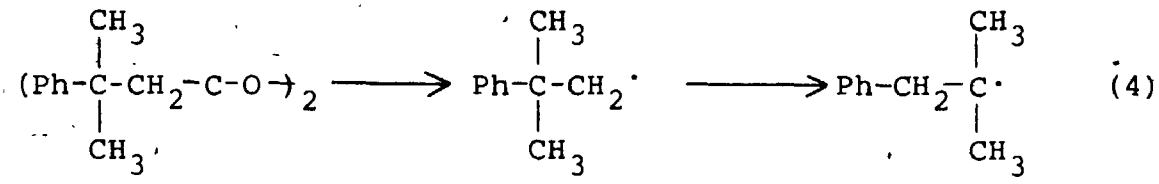

(4)

4

1.7 Photophysics of Adsorbed Molecules

A number of photophysical studies of adsorbed hydrocarbons have provided information concerning the adsorbate's mobility and its interaction with the surface. For example, oxygen quenching of the fluorescence and phosphorescence of aromatic hydrocarbons on porous glass and silica has been examined.[41] The static quenching model proposed to explain the results did not require that movement of the molecules occur. Oelkrug[42] has supplied evidence from fluorescence studies for both physi- and chemisorbed species for aromatics adsorbed on alumina, titanium oxide and gallium oxide. He and coworkers have also used fluorescence and excitation measurements to probe the strength of the interaction of 1-naphthol with the surfaces of several adsorbents.[43]

A detailed investigation of the photophysics of pyrene adsorbed on silica gel, alumina, porous Vycor glass and calcium fluoride has been reported by de Mayo and

coworkers.[44,45] In contrast to solution results, the decay of monomer emission was nonexponential for pyrene adsorbed on all the above surfaces. The decay could, however, be analyzed by assuming a double exponential rate expression. In all cases the average lifetime of adsorbed pyrene was shorter than that in cyclohexane solution, indicating that the surface-pyrene interactions were increasing nonradiative decay rates. All attempts to reproduce the solution single exponential decay on the surface by varying experimental parameters such as surface coverage, sample aging, excitation and emission wavelengths and sample temperature were unsuccessful. These results led to the conclusion that there was an inhomogeneous interaction between pyrene and the surface. Thus, pyrene molecules were not uniformly distributed and those adsorbed on different sites had different lifetimes which resulted in the observed multiexponential emission decays.

Fluorescence from pyrene adsorbed on silica gel was quenched by 2-halonaphthalenes[44] by both static and dynamic quenching mechanisms, the latter indicating diffusional motion of either an excited pyrene or a quencher molecule or of both. Control of the quenching rate for this system by the frequency of diffusional formation of an encounter complex was demonstrated.

On silica gel at higher coverages ($>10^{-5}$ mole/gram) the emission spectrum of pyrene showed an additional excimer-like band which was attributed to ground state bimolecular associations. The same emission was present and was

considerably more intense in the fluorescence of pyrene adsorbed on porous Vycor. Its absence for samples of pyrene on alumina and calcium fluoride showed that no ground state complexes were present for pyrene adsorbed on these solids. For silica gel samples the ratio of the excimer-like to monomer fluorescence intensity varied with the time elapsed after sample preparation. The sites initially occupied by pyrene on the surface did not, therefore, represent the equilibrium situation although diffusion resulted in its eventual attainment. The surface diffusion rate was increased by both shaking the sample and raising its temperature. Several types of experiments indicated that inter- as well as intra-granular motion was occurring for pyrene (and other aromatic hydrocarbons) adsorbed on silica gel but not for the much more polar Rose Bengal molecule.

The effect of coadsorbed molecules such as glycerol, 1-decanol and 1-adamantanol on the fluorescence of pyrene adsorbed on silica gel was also examined.[45b] More intense and better resolved emission spectra were obtained when glycerol and 1-decanol were present. When either of these two coadsorbed substances was added in small amounts (<10% coverage) nonexponential pyrene monomer emission was observed. However, the emission became a single exponential when the alcohol coverage was increased to 50%. Apparently the decanol and glycerol bond preferentially to strong adsorption sites and large amounts of these molecules produce a reasonably uniform surface on which the remaining weak adsorption sites provide a homogeneous environment for

pyrene molecules. At high decanol or glycerol coverages the excimer emission decay was a double exponential with a negative preexponential A_2 which indicated a "growing-in" of the excimer formation. Under these conditions the excimer emission did not originate from ground state complexes but arose from dynamic excimer formation in the excited state.

Singer et al.[49] have also recently reported the results of a study of the pyrene monomer and excimer system on silica and silylated silica. As in the previous study, shorter pyrene lifetimes, nonexponential emission decays, and excimer emission from both static and dynamic formation pathways were observed. However, pyrene adsorbed on the modified surface experienced a different microenvironment from that of pyrene on silica and was more uniformly distributed on the surface.

Recently, two examples of flash photolysis studies of adsorbed molecules have appeared.[47,48] In the first, the longer triplet lifetime and large shift in the triplet-triplet absorption spectrum of pyrene adsorbed on porous glass suggested that there was a strong interaction between the more polar (with respect to the ground state) triplet states and the surface.[47] Secondly, Wilkinson et al.[48] have used diffusive reflectance flash photolysis techniques to measure triplet-triplet absorption spectra for several hydrocarbons adsorbed on alumina. The spectra were attributed to transitions to charge transfer states of the surface-adsorbate systems. Nonexponential triplet decays for some molecules furnished evidence for a variety of

adsorption sites on the alumina surface.

1.8 Photodimerization of Adsorbed Molecules

Photodimerizations of adsorbed molecules have been studied and have also provided some information about the mobility and reactivity of adsorbed molecules. Some of the earliest examples may be found in Leermakers' work with silica gel slurries. Irradiation of cyclopentenone in a cyclohexane-silica gel matrix resulted in much lower yields of dimer than in solution.[49] Most of the dimer was thought to be formed in the supernatant solution phase. These results were rationalized in terms of the adsorbed enone being so tightly bound to the surface that bimolecular cycloaddition could occur only for contiguous molecules for which motion was not required for reaction to occur.

Contrary to the above findings, 2-methyl-1,4-naphthoquinone, 5, adsorbed on dry silica gel underwent efficient photochemical dimerization.[50] Four dimers were formed on the surface whereas only two resulted from irradiation in the crystalline solid state. It was not demonstrated whether dimer formation for adsorbed 5 occurred via nearest neighbour reactions or involved movement of the quinone on the surface. Similarly, photodimerization of 3-methyl-4-nitro-5-styrylisoxazole, 6, adsorbed on silica gel and in a cyclohexane-silica gel slurry occurred efficiently to produce four dimer products,[51] whereas only one was formed in the solid state. Again, it was unclear whether or not motion of the adsorbed molcules preceded reaction.

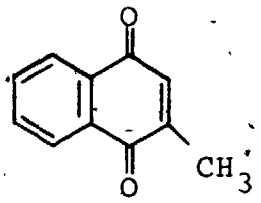

5

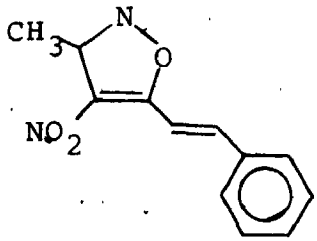

6

A detailed study of the dimerization of acenaphthylene has been reported by de Mayo and coworkers.[44,52] Irradiation of 7 adsorbed on dry silica gel yielded both cis

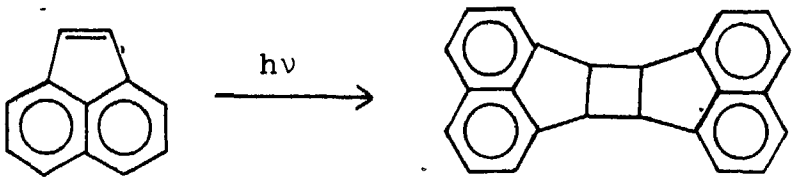

(5)

7 cis and trans

and trans dimers (5) with both singlet and triplet states involved in product formation, as in solution. Variations in the cis:trans ratios with surface coverage indicated that the singlet could react only when it was beside another molecule whereas the longer-lived triplet could move and encounter a ground state molecule with which to react before being deactivated. Coadsorption of the structurally similar acenaphthene altered the number of nearest neighbour acenaphthylene molecules, as evidenced by the changes in the cis:trans ratios. An inhomogeneous distribution of molecules of 7 on the surface was indicated.

The dimerization of 7 was sensitized by Rose Bengal, Eosin Y or Acridine Orange at low sensitizer coverages

(Ø.1%).[44] The observed efficiences (one Rose Bengal molecule sensitized >57 molecules of 7) required that translational movement of both the monomer and the dimer occur. Acenaphthylene dimerization could be quenched by the triplet quencher ferrocene and a value of $7.Ø2 \times 1Ø^{15}$ $dm^2.mol^{-1}.s^{-1}$ was obtained for the rate constant for diffusion of a molecule of ferrocene and acenaphthylene toward each other. It was suggested that, at the concentrations used, acenaphthylene can move ~2 Å during its singlet lifetime but ~3ØØ Å during its triplet lifetime.

Dimerization of 9-cyanophenanthrene has also been carried out on silica gel.[44] Higher product yields with increased temperatures led to the conclusion that an activation energy for diffusional motion of the adsorbed molecules was being observed. The longer singlet lifetime of cyanophenanthrene as compared to acenaphthylene allowed movement to precede bimolecular reactions of the former in its singlet state. In summary, these results for the dimerization of adsorbed molecules have demonstrated that bimolecular reactions of adsorbed molecules do occur. The extent of reaction will depend on the excited state lifetime, the strength of interaction of the molecule with the surface, the distribution of the adsorbed molecules and the presence of coadsorbed species.

1.9 Bimolecular Reactions of Adsorbed Molecules

There are few examples of bimolecular reactions, other than dimerizations, for adsorbed molecules; in most cases

only one of the reactants is bound to the surface. Stearic acid adsorbed at monolayer coverage on dry alumina has been photochlorinated.[53] The marked preference for end group chlorination suggested that the molecules were closely packed and standing acid-end-down on the surface. Autoxidation of fatty acid monolayers on silica gel has been investigated.[54] The efficiency of inhibition of the oxidation reaction by coadsorbed antioxidants required that either the fatty acid, the antioxidant or a radical chain carrying species have substantial surface mobility at 60°C. In a related experiment[55] it was shown that palmitic acid adsorbed on silica gel could be transferred from one particle to another through the vapor phase. Temperatures of 80-100°C and times of several hours were required to achieve ~4% transfer between silica plates separated by 0.1 mm. It was concluded that this "vapor phase hopping" could account for at least some of the mobility observed in the adsorbed fatty acid autoxidation experiments.

1.10 Unimolecular Reactions of Adsorbed Molecules

Several unimolecular photochemical reactions, such as isomerizations, of adsorbed molecules have been examined. Leermakers[56] observed that the photostationary state for photochromic spiropyrans was affected by adsorption. Contrary to solution results, the photochemical transformation of adsorbed spiropyran (dry silica gel) from its colorless to colored form was shown to be reversible.[57] The photoisomerization of thioindigo adsorbed on alumina was

also examined.[58] Although the trans → cis conversion occurred readily, the reverse reaction was not detected, perhaps because, as suggested by the authors, there was extra stabilization of the cis-thioindigo on the surface.

Several groups have examined the cis-trans isomerization of adsorbed stilbene. Leermakers[55] observed changes in the photostationary state from that in solution upon adsorption of stilbene in a silica gel slurry. Similar effects for stilbene adsorbed on alumina were attributed, by Moesta,[28] to specific surface effects. However, irradiation of stilbene on alumina has been reported to produce a largely reversible photochromic change rather than the expected isomerization.[60] Formation of an intermediate involving bonding of stilbene to an active surface site, probably a hydroxyl group, was suggested.[60b]

Phenylethylenes adsorbed on alumina have been shown to undergo photocyclization to dihydrophenanthrenes.[28] The reaction occurs for several molecules which do not cyclize in solution. Apparently the surface orients the two rings in a nearly planar configuration from which they may be linked by photoreaction. Isomerization of 2-butenes adsorbed on porous Vycor has also been observed under direct and sensitized irradiation conditions.[61]

Also of interest with respect to the photochemistry of adsorbed species are two recent reports on the measurement of quantum yields on solid surfaces. The method developed by Guenther et al.[62] has been employed only for photoreactions in solid-solvent slurries but that of de Mayo

and coworkers[63] has been applied to the photodimerization of acenaphthylene adsorbed on dry silica gel.[52]

The investigations to be described are mainly concerned with the behaviour of adsorbed radicals in comparison with that in other inhomogeneous environments and in solution. Substituted and unsubstituted benzyl radical pairs generated photochemically from ketones, esters and sulfones were examined as were cyanopropyl radical pairs. Particular emphasis was placed upon the diffusional mobility of these radicals (as measured by the amount of nongeminate recombination for the radical pairs), the rotational motion of the adsorbed radicals and modifications of the usual solution behaviour caused by adsorption of the radical or its precursor.

CHAPTER 2

BENZYL RADICAL PAIRS

2.1 Introduction

The solution photochemistry of dibenzyl ketones,[64-66] benzyl acetates,[67-69] and dibenzyl sulfones[70,71] has been extensively investigated. All have been shown to undergo photoextrusion reactions via radical pathways as outlined in the general mechanism given in Scheme 2 for the unsubstituted molecules, 8, 9 and 10. Absorption of light produces an excited molecule which may either decay to the ground state or undergo C-X bond homolysis to produce a radical pair with the same multiplicity as its excited state precursor. Cleavage may occur from either a singlet or triplet state, or from both, depending on the substrate. The initial radical pair has two pathways available to it. It may recombine to produce starting material or an isomer of the original molecule. Alternatively, it may loose the fragment X to generate a benzyl radical pair which decays predominantly by combination to form dibenzyl, 11. Variations in this general scheme are to be expected with changes in the multiplicity of the excited substrate, the rate of loss of X, the diffusional behaviour of the radical pairs in a particular environment and the reactivity of the radicals towards disproportionation and hydrogen abstraction.

Scheme 2

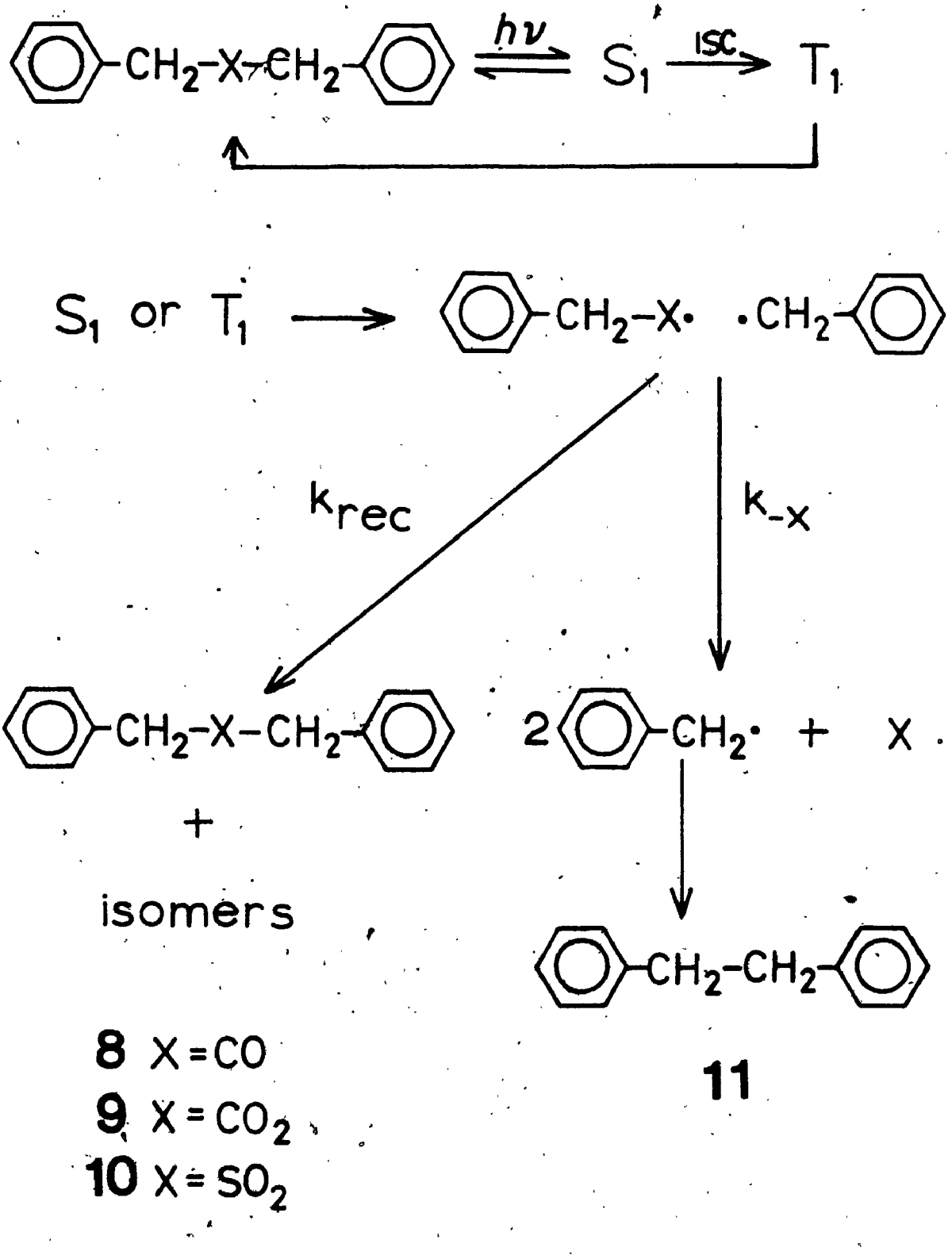

8 X = CO
9 X = CO_2
10 X = SO_2

11

Preliminary investigations of the Photo-Fries rearrangement of adsorbed molecules[37] have indicated that a more detailed examination of the behaviour of adsorbed radical pairs was required. Molecules 8, 9 and 10 and their substituted analogues appeared to be good choices for such a study since they cleave facilely to produce benzyl radical pairs which give quantitative yields of dibenzyl products.

Studies of the Type I photolysis of dibenzyl ketone, 8,[64-66] have shown that excitation is followed by rapid intersystem crossing to a short-lived triplet ($\tau_T \sim 10^{-10}$ s)[65] which undergoes α cleavage to produce a phenylacetyl-benzyl radical pair. Geminate recombination of this radical pair to regenerate starting material was suggested to explain the measured photodecarbonylation quantum yields of less than unity (0.70±0.1 in benzene).[65] The observation of CIDNP emission for the methylene protons of 8 during its photolysis confirmed that some geminate recombination was occurring.[66a,b] However, in solution, the main decay pathway for the initial phenylacetyl-benzyl radical pair is diffusional escape from the original solvent cage. Decarbonylation of the free phenylacetyl radicals then occurs. The rate of decarbonylation, k_{-CO}, has been estimated to be $\sim 10^8$ s^{-1} at room temperature[65] from quenching studies. A later estimate of $k_{-CO} < 10^7$ s^{-1} was reported by Turro et al.[72] on the basis of quantitative CIDNP measurements and computer-simulations. Recently, two groups have measured the absolute rate constant for the decarbonylation of the phenylacetyl radical by laser flash

photolysis:[73] values of 9.1×10^6 s^{-1} [73a] and 6.4×10^6 s^{-1} [73b] in isooctane and 5.2×10^6 s^{-1} [73a] in methanol were obtained. The benzyl radicals combine to form dibenzyl; essentially quantitative yields of both carbon monoxide and dibenzyl are observed. The statistical dibenzyl product ratios obtained upon photolysis of unsymmetrical dibenzyl ketones indicate that cage recombination of benzyl radicals does not occur. Furthermore, the absence of emissive CIDNP effects for dibenzyl formed from photolysis of 8 in the presence of a thiol scavenger and the absorptive CIDNP signals in the absence of scavenger also suggest that dibenzyl is formed via a random, noncage process.[72] The lifetime of the phenylacetyl-benzyl radical pair is limited by recombination, which is presumably controlled by the rate of intersystem crossing and by diffusion, but not by decarbonylation.

The photodecarboxylation of benzyl phenylacetate, 9,[67,68] and a number of methyl and methoxy substituted derivatives[67-69] has been investigated. The reaction efficiency varies considerably for different substituents and solvents but is always lower than that for the decarbonylation of dibenzyl ketones; for example, $\Phi(9)$ is 0.31 in dioxane[68b] and 0.19 in methanol.[67] Although it has been concluded that a radical process is involved in the photolysis of these esters, the multiplicity of the excited state involved and the nature of the decarboxylation step are less certain. Early claims[68a,b] that the photolysis of a number of phenylacetates, including 9, involved triplet

precursors have been disproved for naphthylmethyl phenylacetates. The reaction has been shown to occur from the singlet for these esters and it is likely that the photolysis of 9 and its derivatives follows a similar pathway.[70]

Givens et al. have attempted to develop a general mechanistic scheme for the photochemistry of benzyl phenylacetates and other arylmethyl esters. They have suggested that decarboxylation proceeds by initial cleavage of the carbon-ether oxygen bond[68d] since very low reactivities were observed for esters in which the excited chromophore was not adjacent to this bond.[68c] Partial photolysis of chiral α-methylbenzyl phenylacetate showed complete retention of stereochemistry in the recovered starting material.[68d] It was, therefore, proposed that loss of carbon dioxide occurred too rapidly to permit any recombination of the original benzyl-phenylacetoxy radical pair. Although the decarboxylation is expected to be rapid,‡ these results would also be consistent with a recombination reaction which was sufficiently fast that rotation (and resulting racemization) could not compete. The matter is further complicated by the observation of

---

‡ The rate of decarboxylation of acetoxy radicals has been measured; $k\text{-}co_2 = 1.6 \times 10^9\ s^{-1}$ (60°C), $E_a = 6.6$ kcal/mole,[74] and $k\text{-}co_2 = 2\text{-}3 \times 10^9\ s^{-1}$ (110°C).[75] Phenylacetoxy radicals would be expected to have shorter lifetimes.

oxygen scrambling between the ether and carbonyl oxygens for several esters (Φ_{scram} = Ø.Ø2 for 9 in dioxane).[68d] This scrambling was said to occur by a 1,3-sigmatropic migration with retention of configuration at the migrating carbon, rather than by recombination of the initial radical pair, but little evidence has been presented to support this hypothesis.

In contrast to dibenzyl ketones, substantial cage effects were observed for the photolysis of unsymmetrically substituted benzyl phenylacetates.[68b,69] Givens et al.[68b] have reported that 4'-methylbenzyl-4-methoxyphenylacetate, 12, gives the three possible dibenzyls (13, 14 and 15) in ratios of 1:2.5:1 in dioxane (η = 1.Ø87 × 10^{-3} N s m^{-2}) and 1:5.Ø7:1 in 2-propanol (η = 1.765 × 10^{-3} N s m^{-2}). The high yield of unsymmetrical coupling product 14 indicates a substantial amount of geminate recombination in the more viscous solvent and provides further support for a singlet excited state precursor.

The photoextrusion of sulfur dioxide from several arylmethyl sulfones has been examined by Givens et al.[70] The excited state multiplicities for the sulfones, unlike the analogous ketones and esters, depended on the substrates' structures. For example, dibenzyl sulfone, 1Ø, showed both singlet and triplet reactivity (Ø.59 < Φ_s < 1.Ø, depending on the value taken for Φ_{ISC}; Φ_T = Ø.18) whereas 1-naphthylmethyl benzyl sulfone reacted only from the triplet (Φ = Ø.Ø9). Although difficulties in identifying sulfur dioxide have prevented it from being unequivocally

established as the extruded fragment in sulfone photolyses,[71] the radical nature of the process has been demonstrated. Product dibenzyls derived from both geminate and random free radical combination as well as reduced cage effects in the triplet sensitized, as opposed to the direct decompositions, supported the proposed radical mechanism.

Photolysis of chiral α-methylbenzyl sulfone[70b] resulted in racemization of the starting material, indicating that stepwise cleavage of the sulfone had occurred. The initial benzylsulfonyl-benzyl radical pair could have either lost sulfur dioxide or recombined and produced racemized sulfone. There was apparently little recombination with benzyl migration from sulfur to oxygen since no evidence for sulfinate ester formation was found upon photolysis of 10.[70a]

2.2 Choice of Substrates

The unsymmetrical molecules 12, 16 and 17 were selected for a preliminary investigation of the behaviour of adsorbed radical pairs on the silica gel surface. Three dibenzyl products were expected from each (6). The ratio of the three products resulting from coupling of the benzyl radicals would provide a measure of the amount of nongeminate combination of the radical pairs; this would then serve as a useful probe for translational radical movement on the surface. All three substrates were synthesized and purified, as outlined in Chapter 6.

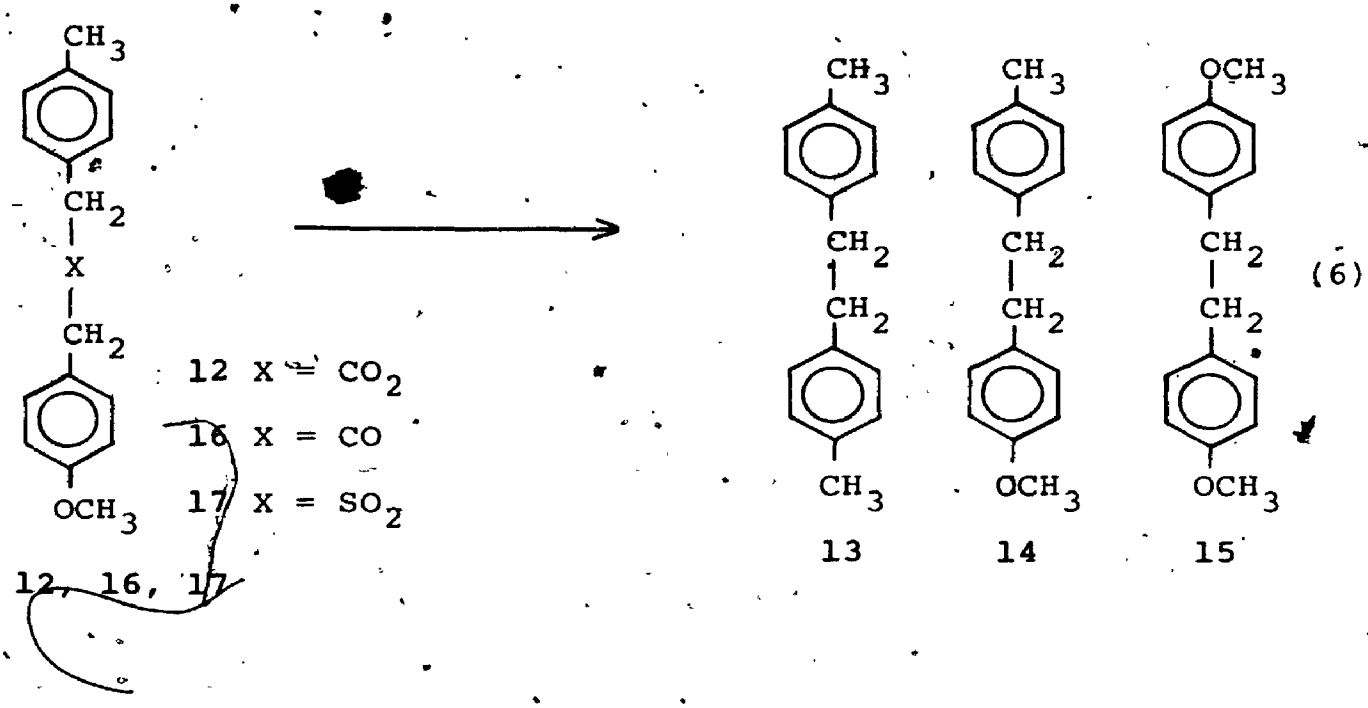

(6)

2:3 Solution Photolyses: 16, 17

The photochemistry of ketone 16 and sulfone 17 had not previously been examined and both were, therefore, first photolyzed in solution. As expected, quantitative yields of the three dibenzyl products, 13, 14 and 15, were obtained from 16. The dibenzyl distribution (Table 1) for the ketone differed from that of ester 12 in that the statistical (1:2:1) ratio expected for random combination of free radicals was obtained in the relatively viscous solvent, 2-propanol. Even at -78°C the approximately statistical product distribution indicated that most of the radicals escaped from the solvent cage before recombining.

Irradiation of sulfone 17 gave the same products, 13, 14 and 15. The ratios (Table 1) were similar in dioxane, 2-propanol and acetone and indicated that more geminate recombination had occurred for 17 than for ketone 16. Givens[70a] had claimed that the cleavage of dibenzyl sulfones

Table 1. Photolysis[a] of ketone 16, ester 12 and sulfone 17 in solution.

	Solvent	Dibenzyl Ratio		
		13	14	15
16	2-propanol	1.0	2.0	1.0
	2-propanol[b]	1.0	2.2	1.0
12	dioxane[c]	1.0	2.5	1.0
	2-propanol[c]	1.0	5.07	1.0
17	dioxane	1.05	2.65	1.0
	acetone	1.1	2.7	1.0
	2-propanol	1.1	2.9	1.0

[a] 16, 150 W xenon lamp; 12 and 17, Rayonet reactor, 253.7 nm, except 17 in acetone, 300 nm.

[b] -78°C (Methanol/dry ice).

[c] From reference 68b.

could be sensitized by acetone. However, the amounts of cage reaction observed here for the sensitized and direct irradiation conditions were very similar, although the sensitized irradiation was considerably less efficient (based upon the times required to obtain similar conversions). Furthermore, comparison of the triplet energies of acetone (331-343 kJ)[76] and toluene (347 kJ)[76] indicated that sensitization of 17 by triplet acetone should not be very efficient. Both the product ratios and the unfavorable triplet energies suggested that the photolysis of 17 in acetone had not occurred by triplet sensitization. The sulfone product distribution was intermediate between those for the ketone (triplet) and ester (singlet) and, therefore, implied a mixture of singlet and triplet reaction upon direct irradiation, as found previously for dibenzyl sulfone.[70].

2.4 Monolayer Coverages of Adsorbed Molecules

Concentrations of adsorbed species are expressed in terms of monolayer coverage, the fraction of the total adsorbent surface area covered by the adsorbate. The amount of substrate required for monolayer coverage may be determined in two ways: by calculation from the known surface areas of the adsorbent and adsorbates, assuming a certain orientation of the molecules at the surface, and by measurement of an adsorption isotherm. The latter method may be more reliable for large molecules as it does not require any knowledge of the molecular orientation or

packing; in addition, all of the surface area as measured by a small molecule (e.g., methanol or nitrogen) may not be accessible to a large organic molecule, a fact which may lead to errors in calculations of monolayer coverages. Both methods have been used here.

Langmuir adsorption isotherms were measured for ester 12 and ketone 16 by equilibrating cyclohexane solutions of each with silica gel samples and determining the equilibrium solution concentrations of the adsorbate. Values for 100% monolayer coverage were then obtained from a plot of moles adsorbed (N) versus equilibrium solution concentrations (C_{eq}), as shown in Figure 3. Monolayer coverages which were the same within experimental error were obtained for 12 and 16 (0.9 mmol substrate/g silica gel). The values for 100% coverage obtained as the reciprocals of the slopes of plots of C_{eq}/N versus C_{eq} (Figure 4) for both (0.98 mmol/g for 16 and 17) were in agreement with those extrapolated from the plots in Figure 3.

An adsorption isotherm was not measured for sulfone 17. It was assumed that it would exhibit similar adsorption behaviour to 12 and 16; hence, all coverages quoted for 17 were calculated on the basis of 0.9 mmol/g as 100% coverage.

The surface areas for most molecules used were determined from space filling models, assuming a relatively flat molecular orientation, and are listed in Table 2.

---

* Determined by Dr. K. Okada,[44] in these laboratories, using the methanol adsorption method of Hoffman et al.[77]

Figure 3. Adsorption isotherms for ketone 16 (O) and ester 12 (●) on silica gel; N (mmol/g) versus C_{eq} (M).

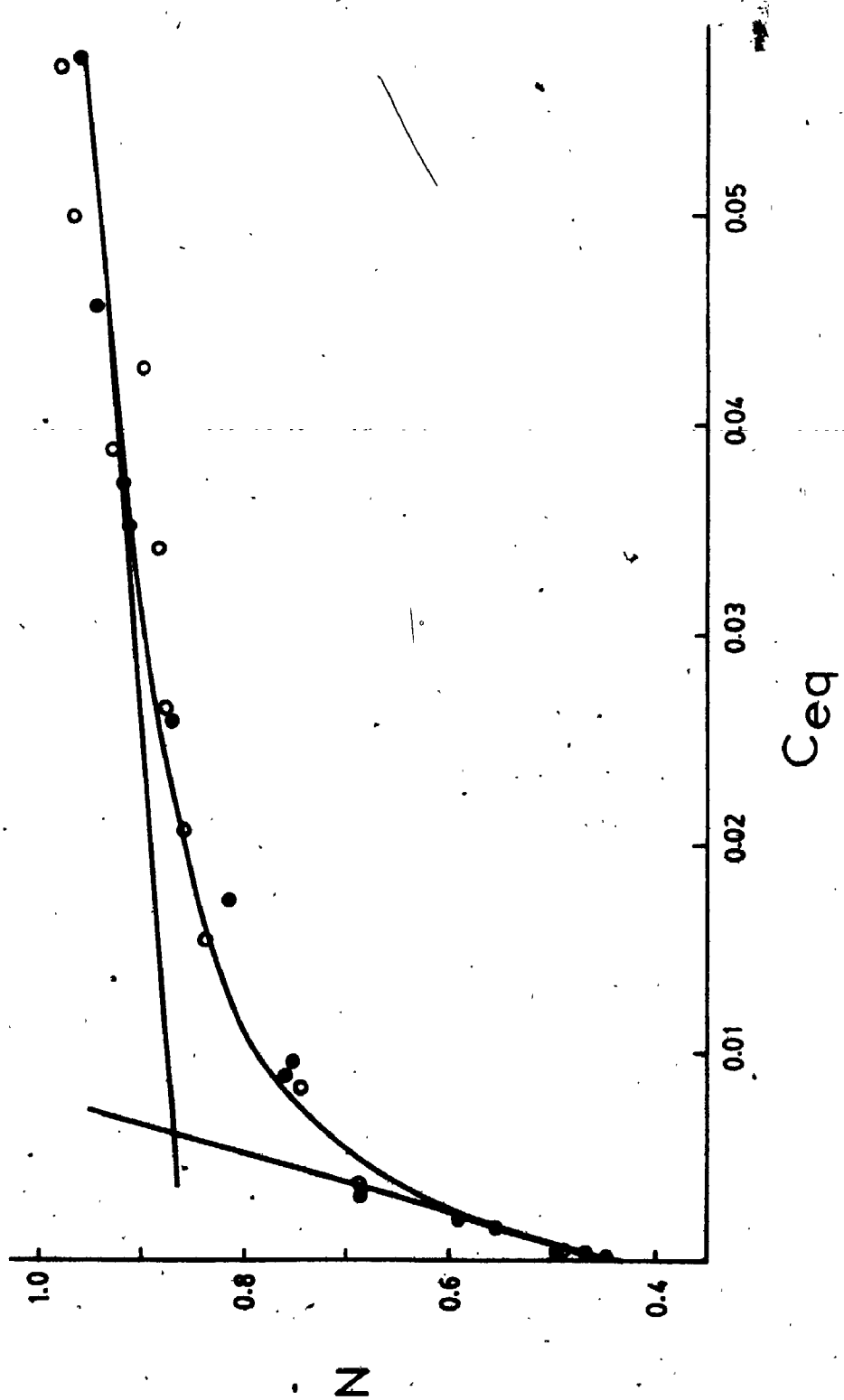
1.0
0.8
0.6
0.4
N
0.01
0.02
0.03
0.04
0.05
Ceq

Figure 4. C_{eq}/N (ℓ^{-1}) versus Ceq (M) for ketone 16 (O) and ester 12 (●).

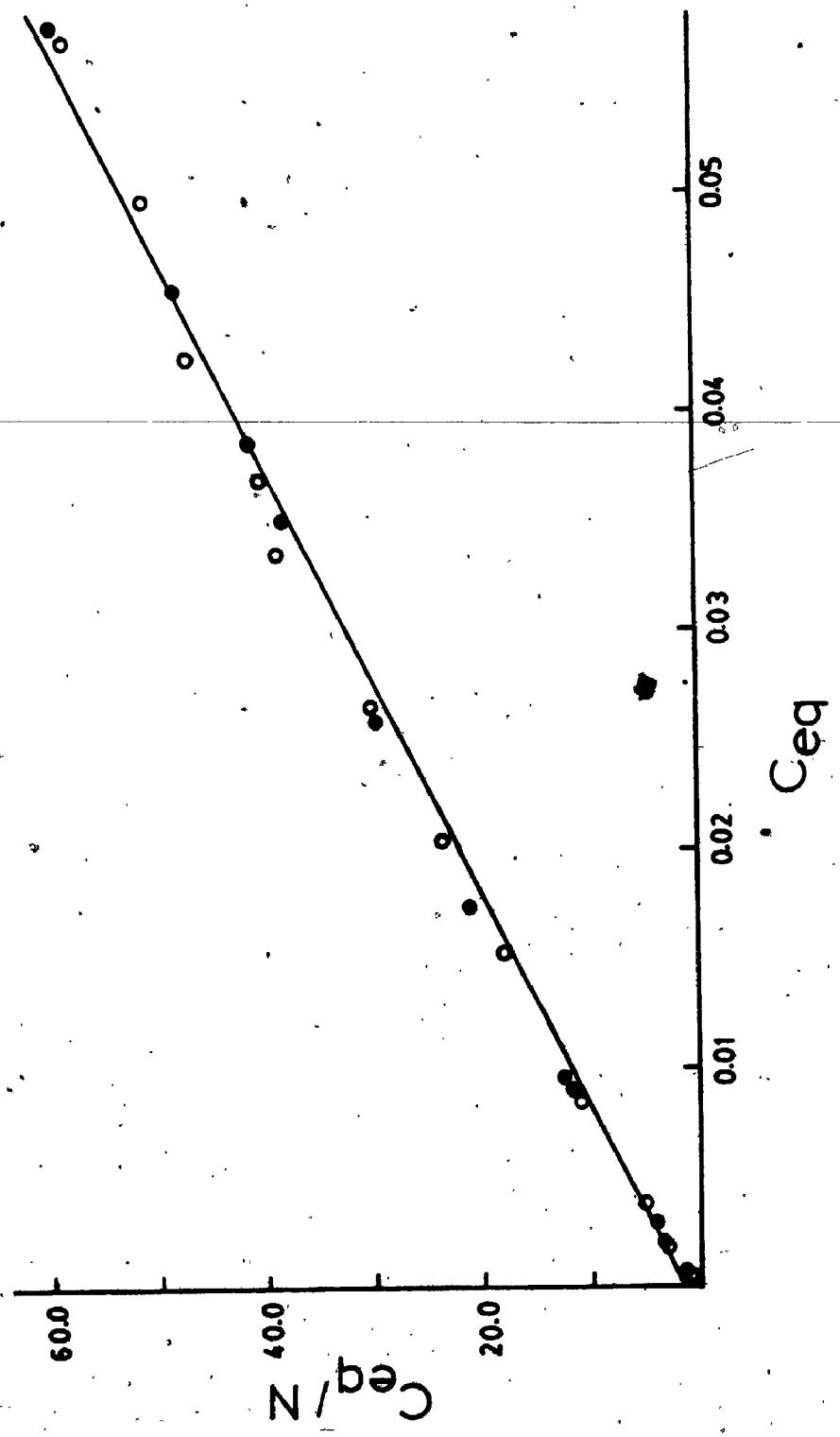
60.0
40.0
20.0
Ceq/N
0.01
0.02
0.03
0.04
0.05
Ceq

Table 2. Molecular areas and calculated monolayer coverages.

	Molecular Area (nm^2)	Monolayer Coverage[a] (mmol/g)
16	Ø.94	Ø.99
12	Ø.98	Ø.95
pinacol	Ø.4Ø	2.3
cyclohexane diol	Ø.37	2.5
azobisisobutyronitrile	Ø.55	1.7
decanol	Ø.65	1.4
benzophenone	Ø.71	1.3

[a] Calculated based on a surface area of 56Ø m^2/g.

Monolayer coverages were calculated (7) using a value of 560 m^2/g for the surface area of the silica gel.* For 12 and 16 the calculated values, Ø.95 and Ø.99 mmol/g, respectively, (Table 2) agreed well with those obtained from

$$\text{Monolayer Coverage} = \frac{\text{Surface area adsorbent } (m^2/g)}{\text{Surface area adsorbate } (m^2/mol)} \quad (7)$$

the adsorption isotherms. This suggests that the molecules are reasonably flat on the surface and that most of the surface is available to them.

2.5 Silica Gel Photolyses: 12, 16 and 17

Samples of 12, 16 and 17 adsorbed on silica gel at various coverages were irradiated. A considerable number of experiments was required to determine the best techniques for sample preparation, degassing and irradiation procedures. These are outlined in the experimental section. In general, the silica gel was dried at 200°C at <1 torr for >5 hours before use and was not exposed to the atmosphere during the sample preparation. The substrate was adsorbed from a methylene chloride solution. Following solvent removal the sample was degassed ($<10^{-5}$ torr) and either sealed under vacuum (20°C experiments) or placed under an oxygen-free nitrogen atmosphere (low temperature experiments) and then sealed. The addition of nitrogen to degassed samples prior to irradiation at low temperature was required for adequate temperature equilibration of the

sample (see 6.3.4). After the samples had been irradiated, the products were extracted and analyzed.

As in solution, dibenzyls 13, 14 and 15 were formed in good yield (75-100%) when 12, 16 or 17 were photolyzed on dry silica gel. The dibenzyl ratios obtained under various conditions are listed in Table 3. At room temperature for ketone 16 the product distribution was not far removed from the statistical. However, in contrast to results obtained in solution, there was some recombination of benzyl radicals with their original partners. For example, at 10% coverage the dibenzyl ratio indicated that 23% of the radicals combined in the original geminate pair. The remaining radicals must have separated from their original partners and found a radical from another ketone molecule with which to react. These results require that translational movement of the benzyl radicals occur even if the ketone molecules are unevenly distributed on the surface (e.g., small pools of ketone molecules and large areas of "bare" silica gel). The amount of movement, but not the necessity for its occurrence, will depend upon the adsorbate distribution. An estimate of the amount of motion required if the adsorbate was uniformly spread over the surface can be obtained from the calculated mean separation of molecular centres. This varies from ~11.2 nm to ~1.4 nm over the 1-50% coverage range to zero at 100% coverage.

The fraction of geminate combination did not increase upon increasing the coverage of 16 from 10 to 50%. If the radical mobility was restricted in the presence of

Table 3. Photolysis of ketone 16, ester 12 and sulfone 17 on dry silica gel.[a]

	Coverage (%)	Temperature (°C)	Dibenzyl ratio[b] 13	14	15
12	1	20	1.0	6.1	1.0
	10	20	1.4	5.5	1.0
	50	20	1.0	4.1	1.1
	10	-55		>96%	
16	1	20	1.2	3.7	1.0
	10	20	1.0	3.2	1.0
	50	20	1.0	3.1	1.0
	2	-55	1.2	9.0	1.0
	10	-55	1.0	6.3	1.0
	50	-55	1.0	6.2	1.0
	10	-165		>95%	
17	2	20	1.2	8.3	1.0
	10	20	1.0	6.2	1.0
	50	20	1.2	6.4	1.0
	~10	-55	1.0	30	1.2

[a] 20°C photolyses: 16, 150 W high pressure xenon lamp; 12 and 17, Rayonet, 254 nm; -55° and -165° photolyses: 1000 W high pressure xenon lamp.

[b] All product ratios are the average of two or more experiments.

additional ketone molecules, the fraction of geminate combination would be expected to increase at higher coverages. This was not observed, indicating that ketone molecules do not interfere with the translational movement of the benzyl radicals.

Lowering the photolysis temperature to -55°C gave a larger amount of the unsymmetrical dibenzyl, 14, although the product distribution still required some radical movement. Further lowering of the temperature to -165°C gave >95% of 14. At this temperature on the time-scale of the experiment the ketone is presumably immobile; the benzyl radicals may also be so, but on warming become mobile between this temperature and -55°C where the product ratios require movement. These results reflect the increased restrictions placed upon radical movement on the surface at low temperatures, and demonstrate that there is an activation energy for this radical motion.

Photolysis of ester 12 on dry silica gel at 10% coverage gave a dibenzyl distribution similar to that obtained in 2-propanol solution. As with ketone 16, the product ratios did not change appreciably from 1 to 50% coverage. However, more geminate recombination to produce the unsymmetrical dibenzyl, 14, was always observed for the ester than for the ketone at the same coverage at room temperature. These differences were more pronounced at low temperature: at -55° >96% of the unsymmetrical dibenzyl was obtained from 12 whereas much lower temperatures were required before similar results were obtained from 16. It

is apparent that less translational movement occurs before recombination for radicals generated from 12 than for those from 16.

As shown in Table 3 the dibenzyl product ratios for sulfone 17 resembled those for the ester but showed slightly more geminate recombination at room temperature. Again, as with the ester, there appeared to be less translational motion for benzyl radicals generated from the sulfone than for the same radicals produced from the ketone. The above results lead to the conclusion that translational motion on the surface of silica gel competes more effectively with radical recombination for 16 than for 12 or 17. The benzyl radicals formed from all three are the same; only the distances between the radical centres and their multiplicities differ. The radical pair is formed with the greatest separation from 12 and should, therefore, be the most likely to diffuse apart and exhibit more nongeminate recombination. The opposite is observed so an explanation based on the multiplicity of the radical pair is favoured. The decomposition of 16 occurs from a triplet,[64] whereas 12 is thought to decompose by a singlet pathway.[68] The singlet radical pair generated from 12 should recombine faster than the triplet pair from 16 and, thus, should show more geminate recombination, as the results indicate. Similarly, the increase in unsymmetrical dibenzyl formation for the ester as compared to the ketone in 2-propanol must also reflect this difference in spin multiplicity of the benzyl radical pair.

The situation with sulfone 17 is less clear. The surface results, since they are similar to those obtained with the ester, suggest a singlet precursor. However, dibenzyl ratios for 17 in solution are intermediate between those of the ester and ketone and provide evidence for a mixture of singlet and triplet pathways, as do the sensitization results. If a primarily singlet decomposition is occurring for the sulfone on the surface, the increase in geminate recombination for 17 as compared to 12 may reflect the slightly greater separation for the radical pair generated from the former.

The results for the adsorbed versus the solution phase sulfone may be a reflection of changes in the relative amounts of singlet and triplet excited states. For example, changes in the rates of either intersystem crossing or radiationless deactivation processes could decrease the amount of triplet reaction occurring for the adsorbed sulfone. Previously observed variations in excited state energy levels[31,32] and in excited state lifetimes[35] due to changes in radiationless deactivation rates have been well documented for adsorbed molecules and provide support for the above hypothesis. More information concerning the multiplicity of excited state sulfones is obviously needed before any conclusions can be reached.

The results obtained for adsorbed 12, 16 and 17 demonstrate that translational motion occurs for benzyl radicals adsorbed on the silica gel surface. This movement requires an activation energy to overcome the surface -

adsorbate interaction; depending on the strength of this interaction, a wide range of activation energies may be needed for movement from different adsorption sites. When interaction of a molecule with two (or more) hydroxyls is possible, translational motion need not require the simultaneous disruption of all bonding, as would motion which occurred by vaporization. Furthermore, if the molecule moves toward a silanol group, bonding to it may occur as the original silanol bonding is disrupted. According to this model, the most rapid translational motion is to be expected for surfaces with large numbers of silanols or for ones with very few silanols.

The effectiveness of translational motion in competing with recombination was shown to depend on the radical pair multiplicity (and, as a result, on its lifetime). Movement of the radicals was, however, unaffected by increased coverages of starting material. An increased amount of adsorbate might be expected to either interfere with or to increase radical movement. The latter would presumably occur because the probability of a molecule being adsorbed at a stronger binding site would be lower at higher coverages. Neither effect was observed for benzyl radicals over the 1-50% coverage range.

The increased non-statistical distribution of products from 12, 16 and 17 at low temperature illustrates the greater restriction to motion on the surface under these conditions. An estimate of the effective surface "viscosity" of the silica gel at room temperature may be

obtained for singlet derived benzyl radicals for which the surface product ratios have been shown to resemble those in 2-propanol. It should be noted that this apparent viscosity changes when either the radical pair multiplicity or the photolysis temperature is varied. Consequently, a surface viscosity can only be expressed with reference to a particular adsorbate and specified conditions. It will be very sensitive to the nature of the surface-adsorbate interaction and the activation energy required to overcome this binding.

Some evidence for nonequivalent radical adsorption sites had previously been presented by Leffler.[39,40] Preferential adsorption at sites with stronger surface-adsorbate interactions would be expected to result in higher yields of the unsymmetrical dibenzyl at low coverage. However, the similar product distributions at low and high coverages for each substrate suggest that the environment of the radical pairs is similar at these coverages. At least for these systems over the 1-50% coverage range at room temperature, the sites of attachment are effectively equal.

The absence of evidence for preferential adsorption sites and the insensitivity of the amount of geminate recombination to changes in surface coverage may, in light of recent results,[78] be caused by the presence of sufficient water to fill the active surface sites. Although the present experiments were carried out under "dry" conditions (see 6.2), some water would have been added in even the dry solvent. Typically the methylene chloride after drying

contained 10 ppm water; the use of 4 ml/g silica would, thus, result in the addition of 0.5 mg water/g. Recently, the addition of similar amounts of water to dry silica gel has been shown to produce dramatic changes in the emission spectra for pyrene adsorbed at low coverage on silica gel.[78] These results indicate that only a small number of the adsorption sites are responsible for the observed effects. The coverages used for 12, 16 and 17 may be too large to permit detection of effects caused by such a small fraction of active sites, even if such sites are not filled with water.

Turro and Baretz[79] have recently reported results for the photolyses of the unsymmetrical ketone, 1,3-diphenylbutan-2-one, adsorbed on porous glass and on silica gel TLC plates. The observed product ratios indicated "cage" effects of 38% and 9%, respectively. The authors attributed their results to the constraints imposed upon the diffusional separation of geminate radical pairs by the "super-cage" environment. It should be noted that this usage of the word "cage" to refer to a surface is somewhat misleading, since, on the surface, a radical pair is not surrounded by a solvent cage as it is in solution.

2.6 Photolysis of 12 and 16 on Modified Surfaces

Several experiments aimed at determining the effects of modification of the silica gel surface were also undertaken. Firstly, the silica gel was heated at 750°C, at which temperature most of the surface silanols are thought to be

removed. Because the major adsorption interaction is with the hydroxyls, an extensively dehydroxylated silica might be expected to provide less restriction to movement of adsorbed radicals or molecules. Photolysis of ketone 16 on dehydroxylated silica gel at two coverages at room temperature gave dibenzyl products in the ratios shown in Table 4. The small decrease in the unsymmetrical product yield from that on the normal hydroxylated surface is consistent with an increased radical mobility on the dehydroxylated silica. Since there are fewer adsorption sites on the latter, they are more easily filled and the remainder of the radicals move more easily.

Irradiation of ester 12 (0.45 mmol/g) on this silica gel also showed only a small variation in the dibenzyl distribution: 1.2:4.4:1 for the dehydroxylated surface versus 1.0:4.1:1.1 for the hydroxylated surface. However, the change is in the opposite direction to that observed with ketone 16. In any case, the dehydroxylated surface does not produce large changes in the radical mobility. Assuming that approximately one isolated hydroxyl/nm^2 remains on the silica surface[3] and using the calculated area of 0.98 nm^2 for ester 12, each substrate molecule should still be able to interact with one or two silanols. The results for the dehydroxylated silica are, therefore, reasonable.

Secondly, the effect of coadsorbates on the translational mobility of benzyl radicals on the silica gel surface was examined. Coadsorbates might be predicted to

Table 4. Photolysis of ketone 16 on modified silica gel.

Coverage	Silica Gel[a]	Temperature (°C)	Dibenzyl Ratio 13 : 14 : 15
0.09 mmol/g[b]	Dehydroxylated	20	1.1 : 2.7 : 1.0
0.45 mmol/g[b]	Dehydroxylated	20	1.1 : 2.7 : 1.0
2%	A, 0.45 mmol/g	-55	1.0 : 11 : 1.0
2%	A, 0.093 mmol/g	-55	1.1 : 8.8 : 1.6
2%	A, 0.020 mmol/g	-55	1.0 : 8.0 : 1.2
2%	B, 0.33 mmol/g	-55	1.0 : 11.4 : 1.2[c]
2%	B, 0.06 mmol/g	-55	1.0 : 6.3 : 1.4[c]

[a] Coadsorbates: A-Cyclohexane diol; B - 2,3-dimethylbutane - 2,3-diol (pinacol).

[b] Monolayer coverage is expected to be different for dehydroxylated silica gel. The coverages used would correspond to 10 and 50% for "normal" silica gel.

[c] Product recovery (as dibenzyls) was <40% in these experiments.

influence radical mobility in several ways: they could interfere with and, thus, decrease translational motion; they could adsorb preferentially on stronger adsorption sites (if they exist), leaving the substrate the weaker sites from which the radicals could more easily escape; or they could change the substrate distribution on the surface. Two diols which were expected to be quite strongly adsorbed were chosen as the coadsorbates. The ketone photolyses on silica gel in the presence of these diols were carried out at 2% coverage at -55°C. It was anticipated that changes in the dibenzyl ratios could most readily be detected under these conditions.

Dibenzyl ratios obtained after photolysis of 16 on dry silica gel in the presence of coadsorbed cyclohexane diol, 18, and pinacol, 19, are shown in Table 4. Small variations from the product distribution obtained on silica gel alone were observed in the presence of coadsorbed cyclohexane diol. The increase in the amount of unsymmetrical product for the higher coverage of 18 (0.45 mmol/g is ~20% coverage, by calculation) was consistent with some interference by the diol with movement of the benzyl radicals. When the amount of 18 was reduced, the percentage of geminate combination also decreased. In the presence of pinacol the product distribution changed more than with 18 as the coadsorbate. However, the dibenzyl product recovery was low (20-40%) in these experiments and the ratios were not reproducible. A search for the missing material showed small amounts of volatile material but the amounts were insufficient to

obtain a good mass balance. The pinacol appeared to interfere with the radical recombination; results obtained in its presence were, therefore, considered unreliable and were not pursued any further.

2.7 Micelle Photolyses: 12 and 16

For comparison with results obtained both in solution and on the silica gel surface, substrates 12 and 16 were photolyzed in potassium dodecanoate micelles. The micelle, in localising molecules within a small volume, provides a restricted environment in which reaction can occur. It was, therefore, of interest to compare results for photolysis of ester 12 and ketone 16 in micelles to those for the silica gel adsorbed molecules. The results are listed in Table 5.

When ester 12 was photolyzed in aqueous potassium dodecanoate, the unsymmetrical dibenzyl 14 derived from geminate combination accounted for most of the products. At 0.76 mM 12 (N = 0.64, average number of ester molecules/micelle) the dibenzyl mixture was 97% 14 and, at 3.00 mM 12, 14 still comprised 88% of the dibenzyls. Evidently the micelle prevented the radicals from diffusing apart so that a large percentage recombined with their original geminate partners.

The nongeminate products could be derived from photolysis of two ester molecules in the same micelle, from aqueous photolysis or from combination, in the aqueous phase, of radicals which had diffused out of the micelle. At 3 mM 12 there are an average of 2.52 molecules per

Table 5. Photolysis[a] of ester 12 and ketone 16 in 0.08 M potassium dodecanoate micelles.

	Concentration (mM)	Dibenzyl Ratio 13	14	15
12	0.76	1.0	72	1.1
	1.21	1.4	44	1.0
	1.51	1.0	31	1.0
	2.02	1.2	26	1.0
	2.52	1.0	23	1.4
	2.52[b]	1.0	31	1.1
	2.52[c]	1.0	36	1.2
	3.00	1.1	15	1.0
16	0.60	1.4	15	1.0
	0.83	1.2	7.5	1.0
	1.01[d]	1.0	6.4	1.2
	1.01[e]	1.0	48	1.0

[a] Rayonet reactor (254 nm).

[b] 0.01 M KBr

[c] 0.10 M KBr

[d] N = 0.85

[e] 0.16 M surfactant; N = 0.35

micelle; if a Poisson distribution is assumed, 72% of the micelles contain more than one ester molecule. Nevertheless, the probability of the simultaneous photolysis of two molecules in a single micelle is negligible; i.e., the probability of a second photon striking a micelle during the lifetime of the benzyl radical pair is very low. Addition of an efficient free radical scavenger which is soluble only in the aqueous phase and is negatively charged so that it will be repelled by the micelle surface would be expected to decrease the fraction of products formed in the aqueous phase. Photolysis of 12 (2.52 mM) in potassium dodecanoate micelles gave dibenzyl products which were 90.5%, 93.6% and 94.2% 14 at Ø M, Ø.Ø1 M and Ø.1Ø M potassium bromide, respectively (Table 5). The increase in the unsymmetrical product in the presence of bromide ion suggested that some product was indeed formed in the aqueous phase. However, some nongeminate reaction still occurred with Ø.1Ø M scavenger. This probably resulted from inefficient trapping by bromide ion of radicals in the aqueous phase.

Shortly after the completion of these experiments, Turro et al.[8Ø] published the first of their extensive micellar studies of dibenzyl ketone photochemistry. Photolysis of benzyl 4-methylbenzyl ketone in aqueous hexadecyltrimethylammonium chloride produced dibenzyl products which, above the critical micelle concentration, were primarily the unsymmetrical dibenzyl. The results were attributed to the "restricted dimensionality" of the

micelle.[80]

Similar results were obtained when ketone 16 was photolyzed in micellar solution (Table 5). Lower substrate: surfactant ratios were required to obtain the degree of selectivity observed for the micellar ester photolysis. The triplet nature of the benzyl radical pair could permit more time for escape from the micelle to compete with geminate recombination. Alternatively, greater solubility of the ketone than of the ester in water could also be responsible for the differences between 12 and 16. Turro has shown that a significant number of benzyl radicals are scavenged by copper sulfate during micelle photolysis of dibenzyl ketones.[80]

Comparison of the results obtained for 12 and 16 in micelles and on the surface indicates that the selectivity in dibenzyl formation is much greater for the former system. The micellar environment is more effective in preventing the diffusion apart of the benzyl radicals than is the silica gel surface at room temperature. Escape from a micelle is relatively slow: for example, the rate of escape of toluene from hexadecyltrimethylammonium chloride micelles was estimated to be $\sim 5 \times 10^5$ s^{-1};[81] a value of $\sim 4 \times 10^6$ s^{-1} has been determined for the exit rate of the cyclohexadienyl radical.[82] Hence the micelle is able to localise the radical pair until reaction occurs. The restrictions to translational motion and, thus, to diffusional separation of benzyl radicals on a silica gel surface are considerably less stringent.

2.8 Photolysis of Dibenzyl Ketone

Photolysis of dibenzyl ketone, 8, in micellar solution has been shown by Turro and coworkers[83] to produce small amounts of a rearranged starting material, 1-phenyl-4'-methyl-acetophenone, 20. This product presumably arises via recombination of the original acyl-benzyl radical pair with subsequent rearomatization, as shown in (8). Although 5-10%

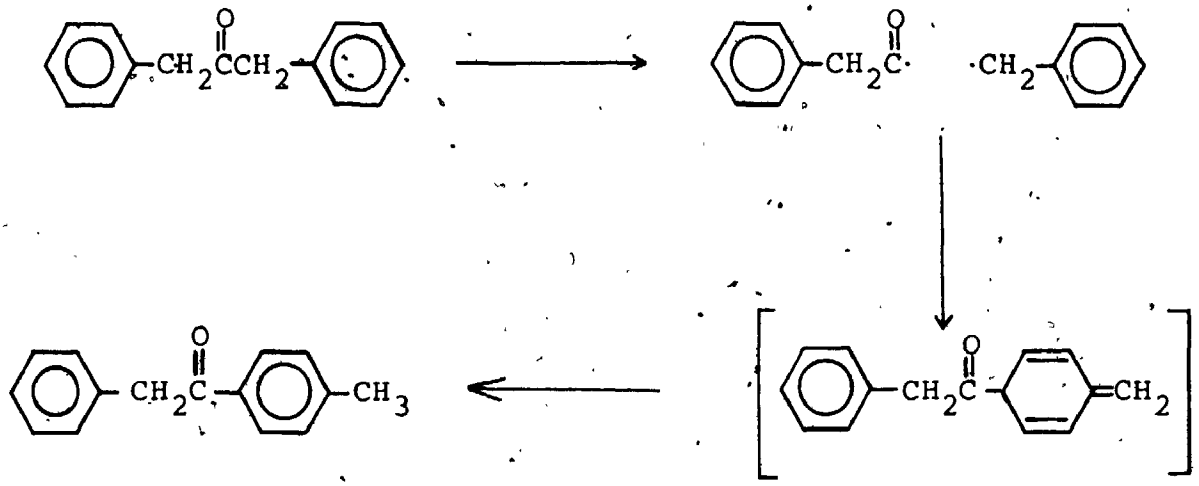

20 (8)

yields of 20 are reported for photolysis of 8 in hexadecyltrimethylammonium chloride micelles, the isomer has not been observed in solution photolyses.[83b]

It seemed plausible, on the basis of the above findings, that photolysis of 8 on dry silica gel would also produce isomer 20. Irradiation of 8 on silica gel at 20°C did indeed yield small amounts of 20 along with the major product, dibenzyl. The isomer was isolated and its identity confirmed by comparison with an authentic sample. Typical yields were from 1-2% for irradiation of 8 on silica

(irrespective of the manner of drying) at 20°C; photolysis at -55°C resulted in higher yields of 3-4%. At both temperatures the percentage of 20 decreased considerably at higher conversions (e.g., 0.1-0.4% for >97% reaction), presumably due to its photodecomposition. Irradiation of 8 in aqueous micellar potassium dodecanoate gave results similar to those obtained by Turro et al.,[83] 11% yields of the dibenzyl ketone isomer were obtained at low conversions.

There appeared to be no obvious reason for the formation of the para isomer 20 but not the analogous ortho compound, 1-phenyl-2'-methylacetophenone, 21. Formation of

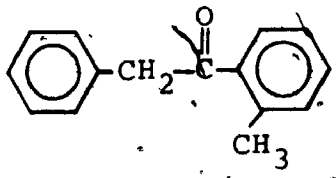

21

21 requires less movement of the radicals and should be at least as favorable as recombination to give 20. Therefore, evidence for the presence of 21 in the reaction products from photolysis of 8 in micelles and on the silica gel surface was sought. The GC retention times of 8 and 21 were identical on the SE 30 column normally used for analysis of reaction products but the two were separable from each other, and from 20, on a carbowax column. Analysis of the reaction products obtained in micelle solution showed the presence of isomer 21 (~2-4% yields) as well as 20. Lesser amounts (<0.5%, estimated) of 21 were also detected in silica gel reaction mixtures at 20 and -55°C. The

observation of both ortho and para rearranged starting material is consistent with the earlier observation of both ortho and para products in the photo Fries rearrangement on dry silica gel.[37]

2.9 Photolysis of Dibenzyl Sulfone

Solution photolysis of dibenzyl sulfone, 10, has been reported to produce dibenzyl as the only isolated product (although in less than quantitative yields) in benzene[70,71] and ethanol.[71] Givens et al.[70a] have suggested that little recombination or benzyl migration from sulfur to oxygen occurs since no evidence for sulfinate ester formation was found.

Photolysis of 10 on silica gel at room temperature yielded small amounts of a rearranged starting material in addition to the major isolated product, dibenzyl, 11. The isomer was isolated from a silica gel reaction mixture and was shown by comparison with an authentic sample to be sulfinate 22. The sulfinate is presumably formed by

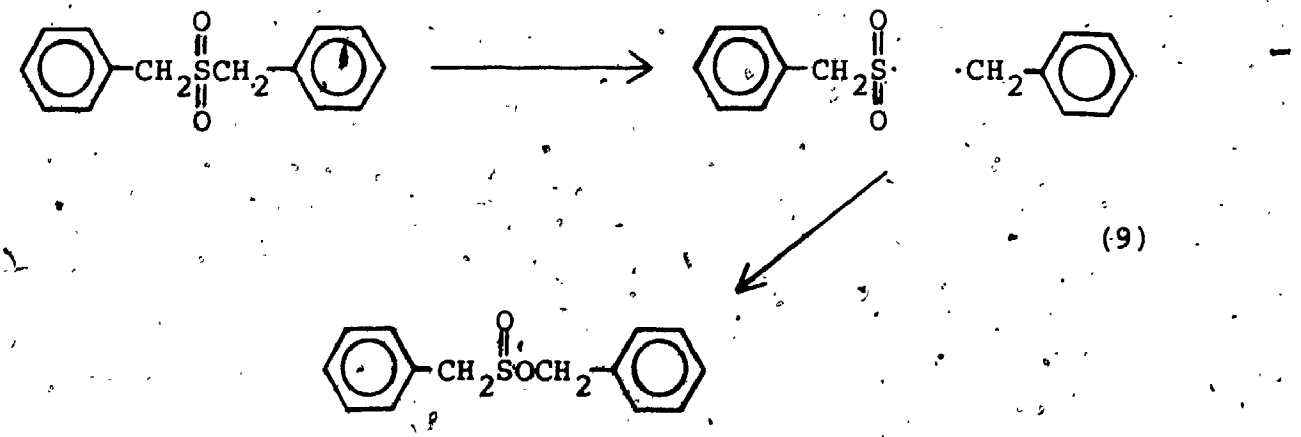

(9)

22

recombination of the benzyl sulfonyl-benzyl radical pair (equation 9) before its destruction by either desulfonylation or diffusional separation. Sulfinates have been detected among the photolysis products from other sulfones, such as 23[84] and 24.[85] However, sulfinate formation was not thought to occur via a radical pathway for either of these sulfones.

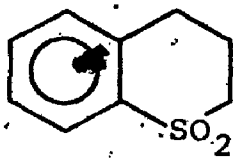

23

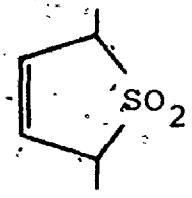

24

Yields of dibenzyl, 11, and sulfinate 22 produced upon photolysis of 10 in solution and on silica gel are presented in Table 6. On silica gel at 20°C 11 and 20 accounted for ~40% and <5%, respectively, of the decomposed sulfone; decreasing the photolysis temperature to -55°C gave an increased yield of the sulfinate (10%). In contrast, photolysis of 10 in methanol at either 20° or -77°C gave much lower yields of 22 (~0.5%). The total yield of 22 and 11 was usually less than half the molar quantity of sulfone consumed for both the silica gel and solution experiments. These low product recoveries may result from formation of toluene-α-sulfinic acid or toluene-α-sulfonic acid; this has been proposed previously to explain the low yields of dibenzyls formed by photolysis of dibenzyl sulfones.[71] The isolation or identification of acidic products was not attempted.

Table 6. Photolysis[a] of Dibenzyl Sulfone, 10.

Conditions	Temperature (°C)	Conversion (%)	Products (Mole%)[b] 11	22
Silica Gel[c]	25	45	38	5.0
Silica Gel	25	59	45	3.0
Silica Gel	25	69	36	2.7
Silica Gel	-55	30	24	10
Methanol, 0.011 M	20	52	35	0.4
Methanol, 0.0034 M	-77	52	64	0.6

[a] Rayonet (254 nm) except for silica gel at -55° for which a 1000 W xenon lamp was used.

[b] Based on amount of sulfone recovered.

[c] 0.250 mmol 10/g silica gel; silica gel was not dried before use.

The decreased yield of sulfinate at higher conversions for the silica gel experiments suggested that 22 was not stable on the silica gel surface. To test for this possibility two samples of 22 adsorbed on silica gel were prepared; one sample was kept in the dark for 24 hours and the other was irradiated using the same conditions as those used for sulfone photolyses. Both samples were then extracted and analyzed by GC. The dark sample showed ~80% sulfinate recovery with some additional low boiling material also detected. For the irradiated sample the extracted material contained 63% unreacted 22 in addition to dibenzyl and dibenzyl sulfone, 10 (13% and 8%, respectively, based on sulfinate consumed). A number of other compounds were also evident in the GC traces but none of these were identified. GC analysis of an irradiated methanol solution of 22 also indicated the presence of dibenzyl 11, dibenzyl sulfone and a number of unidentified compounds.

The above results indicate that recombination of the initial radical pair formed by photolysis of dibenzyl sulfone does occur with benzyl migration from sulfur to oxygen when the sulfone is adsorbed on silica gel. The yields of 5% and 10% at 20 and -55°C represent lower limits for the amount of rearranged material since the instability of 22 on silica gel as well as its photolability have been demonstrated. The surface is apparently able to restrict the translational motion of the radicals so that recombination of the radical pair can compete more effectively with its diffusional separation on the surface

than in solution.

2.10 Intergranular Transfer of Adsorbed 16

Evidence has been presented for translational motion of adsorbed benzyl radicals. It was also of interest to determine whether movement could occur for adsorbed molecules, and in particular, whether movement from one particle to another was possible. To test for this, silica gel, 35-70 mesh, was divided into coarse and fine particles using a 50-mesh sieve. Ketone 16 was adsorbed on one type of silica gel, an equal amount of the other was added, and the mixture was shaken for a certain length of time. The sample was then reseparated into fine and coarse particles and the amount of 16 on each was determined. The results listed in Table 7 indicated that intergranular transfer of adsorbed 16 had occurred. The rate of transfer was slower than that found for either acenaphthylene or pyrene adsorbed on silica gel[44] which suggests that the ketone is more strongly bound to the surface than are aromatic hydrocarbons.

Table 7. Intergranular motion of adsorbed ketone 16.

Silica Gel	Time of Shaking (hours)	Observed % 16	
		35-50 mesh	50-70 mesh
35-70 mesh[a]	0.1	46	54
35-50	0.25	90	10
35-50	2	82	18
35-50	10.5	83	17
50-70	0.25	6	94
50-70	2	11	89
50-70	10.5	16	84

[a] Ketone was adsorbed on equal amounts of 35-50 and 50-70 mesh silica gel at the same time.

CHAPTER 3

^{13}C ENRICHMENT OF DIBENZYL KETONE

3.1 Introduction

Virtually all methods of isotope separation are based upon differences in mass or related properties. However, Lawler and Evans,[86] in 1971, predicted that the separation of isotopes based upon differences in the magnetic moments rather than the masses of nuclei should be possible. Their prediction was derived from the radical pair theory[87,88] which had recently been developed to interpret CIDEP and CIDNP effects. In 1976 Buchachenko's observation[89a] of ^{13}C enrichment during the photolysis of dibenzylketone confirmed that magnetic effects could lead to isotope separation. Since then a number of radical reactions have been shown to be influenced by magnetic isotope and magnetic field effects.[83b,89-92]

A basic premise of the radical pair theory is the postulate that the chemical behaviour of a radical pair may be influenced by the spin of magnetic nuclei. One of the major mechanisms for intersystem crossing (ISC) in a radical pair containing magnetic nuclei is the electron-nuclear hyperfine coupling (hfc) interaction. As a result, the presence of a magnetic nucleus will increase the ISC rate of the radical pair; the extent to which it does so will be greatest for nuclei which have large hfc constants. For

example, a triplet radical pair containing a magnetic isotope with a large hfc constant (e.g., ^{13}C) will undergo more rapid ISC because of the additional electron-nuclear hfc contribution than will the same triplet pair containing a nonmagnetic isotope (^{12}C). If ISC to a singlet radical pair followed by recombination competes with diffusion apart and further nongeminate reaction of the radicals, then the cage products are expected to be enriched in the magnetic isotope while the escape products will be impoverished.

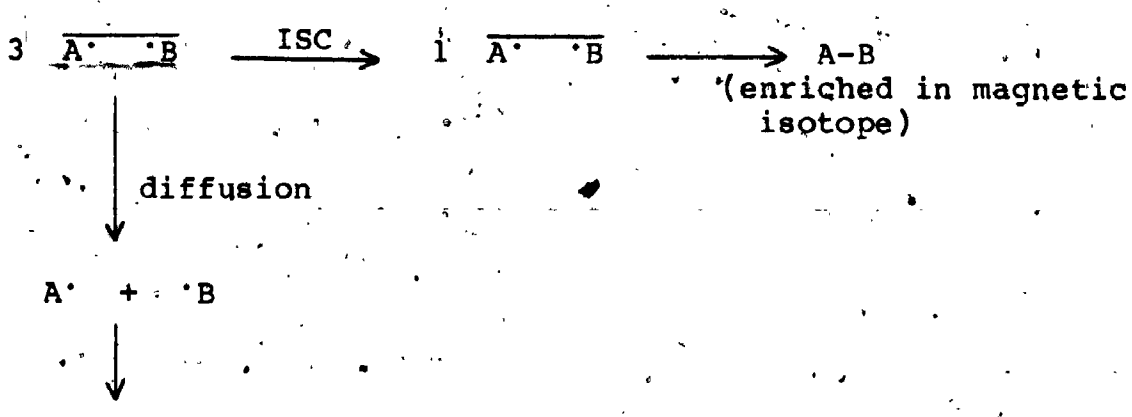

There are several requirements for efficient isotope separation by magnetic effects: (1) the hyperfine interaction must be large enough to allow ISC to be primarily determined by nuclear spins (i.e., other ISC mechanisms must be of lesser importance); (2) there must be sufficient time for the hfc interaction to develop; (3) the caged radical pair must separate to a distance where the hfc interaction is at least as large as the singlet-triplet energy difference; and (4) there must be formation of free radical products from, or transformation to a new radical

pair of $^3\overline{A\cdot\ \ \cdot B}$ to compete with ISC to $^1\overline{A\cdot\ \ \cdot B}$.

The ^{13}C enrichment which occurs during the photolysis of dibenzyl ketone[89,90,92] can be explained in terms of Scheme 3. The original acyl-benzyl radical pairs containing ^{13}C nuclei will undergo more rapid ISC to a singlet pair than will those containing ^{12}C nuclei. Escape from the solvent cage provides the required competitive pathway in solution. Therefore, the two cage products, regenerated dibenzyl ketone (8) and its isomer (20) (if present) will be enriched in ^{13}C. The free radical products formed after escape from the solvent cage will, on the other hand, contain more ^{12}C than did the original starting material.

Small amounts of ^{13}C enrichment have been observed in 8 recovered after partial photolysis in benzene or hexane.[83b,89]. The value for α, the single stage enrichment parameter, was ~1.04[83b] in benzene. Pines et al. have investigated the effect of solvent viscosity and temperature on the ^{13}C enrichment which occurs for photolysis of 8 in a variety of solvents.[92] They concluded that the nuclear magnetic isotope effect depended strongly on viscosity with maximum effects being observed at intermediate viscosities.

Turro and coworkers[83,90] have reported the results of an extensive series of investigations of ^{13}C enrichment for 8 photolyzed in aqueous micellar solutions. Substantial increases in the enrichment were observed for recovered ketone and its isomer, 20: $\alpha_{CO}(8) = 1.35$; $\alpha_{CH_2}(8) = 1.18$, and $\alpha'_{CO}(20) = 1.26$, where α' refers to the single stage enrichment parameter for 20 and the subscripts refer to the

Scheme 3

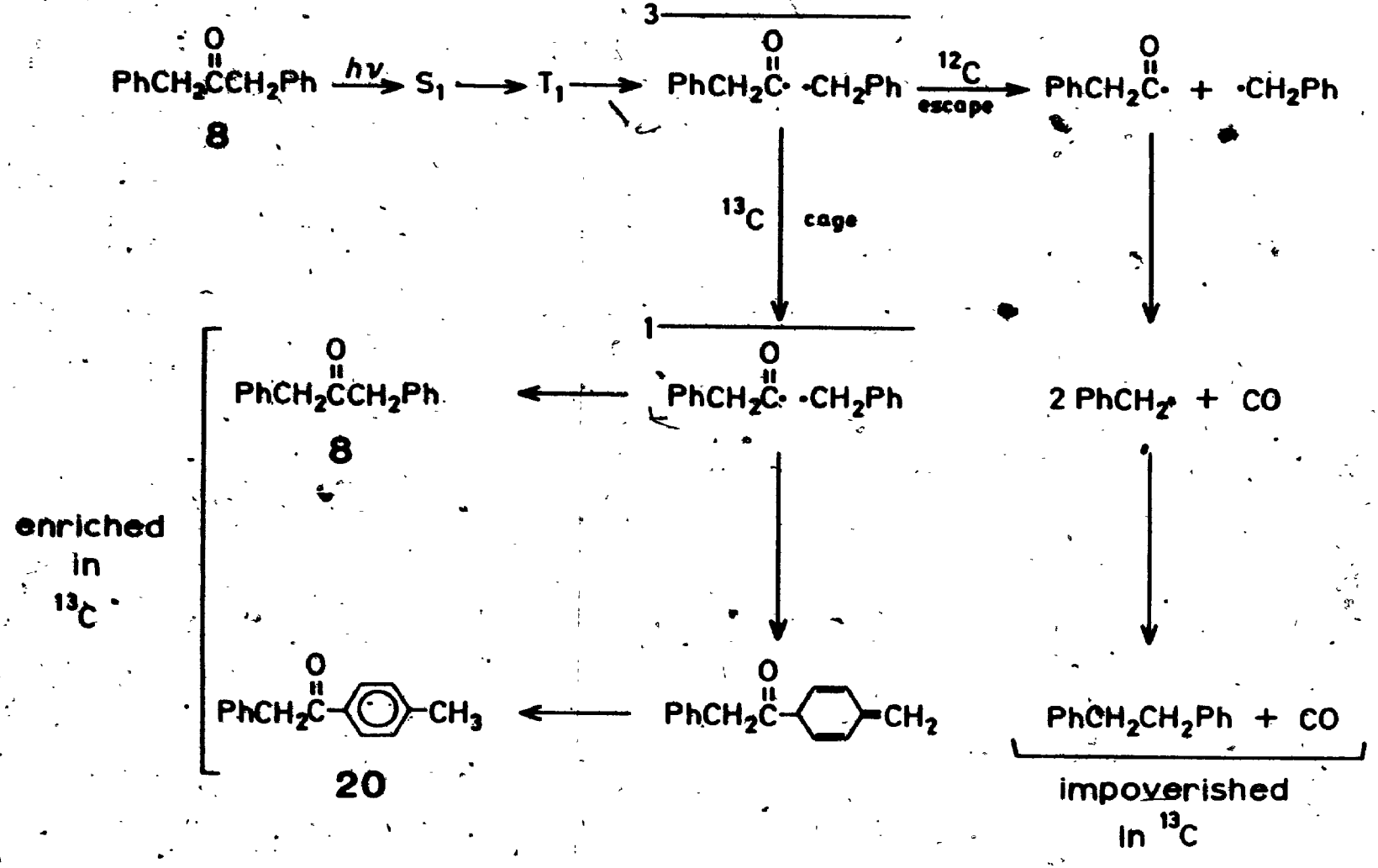
PhCH2CCH2Ph
8
hν
S1
T1
3
PhCH2C· ·CH2Ph
12C
escape
PhCH2C· + ·CH2Ph
13C
cage
1
PhCH2C· ·CH2Ph
2 PhCH2· + CO
PhCH2CCH2Ph
8
enriched
in
13C
PhCH2C
CH3
20
PhCH2C
CH2
PhCH2CH2Ph + CO
impoverished
in 13C

position of the ^{13}C enrichment.[83b] The larger enrichment at the carbonyl rather than the methylene carbon was as expected on the basis of the hfc constants (a)[90c] for ^{13}C at the various positions. Much smaller enrichments were detected by ^{13}C NMR for the aromatic protons.

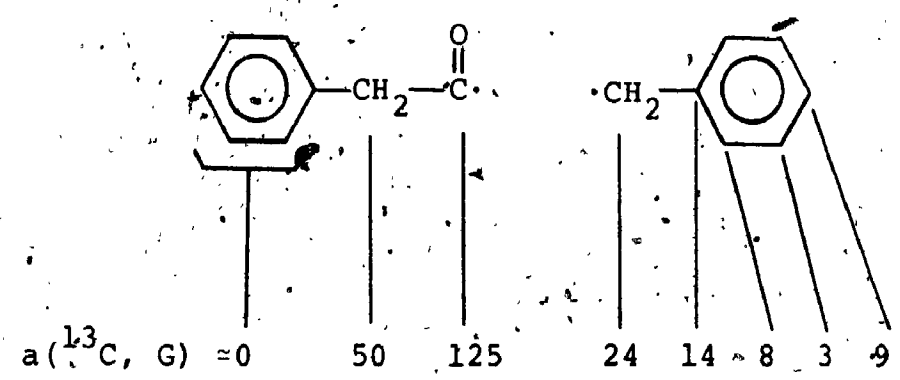

The effects of magnetic field[90b] and temperature[90c] on micellar ^{13}C enrichment were also examined. As expected, the enrichment at high magnetic fields (5-100 KG) decreased substantially from that observed at 0 G since the large Zeeman splitting of the triplet sublevels prevented hfc induced ISC from T_+ and T_- to S. Opposite temperature effects were observed for 8 and 20: for 8, α decreased from 1.38 at 27°C to 1.13 at 70°C but for 20, α' increased from 1.24 to 1.50 over the same temperature range. The results for 8 have been attributed to a diminished recombination efficiency caused by an increase in the decarbonylation rate at higher temperatures. Turro et al. have proposed that the efficient enrichment observed for dibenzyl ketone in micellar environments is due to the restricted space in

which the radical pair finds itself. The micelle provides a boundary which prevents the radical pair from diffusing too far apart and allows more time for hfc induced ISC to occur. Decarbonylation rather than diffusion (as in solution) is thought to provide the competing escape mechanism for the triplet radical pair in a micelle.

Epling and Florio[93] have photolyzed 8 adsorbed on a surface prepared by chemically bonding a hydrocarbon layer (using trichlorododecylsilane) to the surface of silica gel. They observed substantial ^{13}C enrichment in recovered 8; an α value of 1.66 was obtained. Since natural abundance ketone was used, this number refers to the total enrichment at all carbons, not only at the carbonyl. The authors concluded that the synthetic monolayer surface was analogous to a micelle in providing an artificial "reflecting boundary" which led to an enhanced magnetic isotope effect. The results to be presented below do not support such an interpretation.

The results obtained for photolysis of the substituted dibenzyl ketone, **16**, on silica gel had indicated some restriction to radical motion on the surface. It was, therefore, expected that the silica gel surface would also provide a suitable environment for the observation of substantial amounts of ^{13}C enrichment. Since the time-scale of the ^{13}C enrichment process is shorter than that for combination of benzyl radicals, the surface was expected to have more influence over the former process. Furthermore, the results obtained by Epling and Florio seemed more likely

to be a reflection of the silica gel surface properties rather than the micelle-like properties of the synthetic monolayer surface. Investigation of the ^{13}C enrichment on silica gel would indicate if this was the case. The aims of the present study were threefold: (1) to search for conditions for optimization of ^{13}C enrichment; (2) to obtain further information concerning the mechanism of the magnetic isotope effect in restricted environments; and (3) to understand more completely the diffusional motion of radical pairs on a silica gel surface.

3.2 Data Analysis

Since the amount of enrichment depends on the extent of conversion, it is useful to express the results in terms of a single stage isotope separation factor, α.[94] This parameter does not depend on the extent of conversion and, thus, allows comparison of isotope separation efficiencies for different experiments. Bernstein[94] has shown that, for competitive, first-order reactions of isotopically different species, the residual unreacted starting material becomes exponentially enriched in the slower reacting isotope. This may be applied to the competitive $^{12}C/^{13}C$ reactions in the photolysis of dibenzyl ketone, as shown by Turro et al.[83b] Since molecules containing ^{13}C proceed to products at a slower rate (i.e., more geminate recombination to regenerate starting material occurs for ^{13}C radical pairs) than do those containing ^{12}C, the residual unreacted ketone will become enriched in ^{13}C.

The parameter α is defined as the single stage separation factor [94] and may be computed from the measured quantities, S, the overall separation factor, and f, the fractional conversion. These are defined for carbon isotopes in equations 10 and 11 where the subscripts o and f

$$S = \frac{[^{13}C]_f[^{12}C]_0}{[^{12}C]_f[^{13}C]_0} \tag{10}$$

$$f = 1 - \frac{[^{12}C]_f + [^{13}C]_f}{[^{12}C]_0 + [^{13}C]_0} \tag{11}$$

refer to concentrations in the initial and recovered material. The conversion, f, is determined by GC; the separation factor, S, is obtained from the relative mass spectral intensities for the M/M+1 peaks at m/e 210 and 211 (see 6.9). The magnitude of α is then obtained from equation

$$\log S = \frac{\alpha-1}{\alpha}\left[\log\left(\frac{1+SR_0}{1+R_0}\right) - \log(1-f)\right] \tag{12}$$

$$R_0 = \frac{[^{13}C]_0}{[^{12}C]_0} \tag{13}$$

12 which can, for most purposes, be approximated by equation 14. In practice, α can be evaluated directly from (12) or (14) for each experiment or can be computed from the slope

$((\alpha-1)/\alpha)$ of a plot of log S against $-\log(1-f)$. Identical values of α (within experimental error) were obtained using

$$\log S = \frac{\alpha-1}{\alpha}\,[-\log(1-f)] \qquad (14)$$

either equation 12 or 14.

The above method for obtaining single stage enrichment parameters cannot be used to express isotope separation efficiencies for products formed in a competitive isotope reaction. When dibenzyl ketone is photolysed in restricted environments, an isomeric product, 1-phenyl-4'-methylacetophenone, 20, is produced. This isomer formed from geminate recombination of the initial radical pair is expected to be formed more often from ^{13}C ketone molecules than from ^{12}C-molecules as a result of the more rapid ISC in the radical pair containing ^{13}C. Any isomer formed is not diluted by a large pool of unreacted, and therefore unenriched, material as is the case for regenerated dibenzyl ketone. As a result, the ^{13}C enrichment, as measured by S, is much higher for 20 than for 8 at low conversions but increases more slowly with increasing conversion. The increase in S for 20 with conversion occurs because the ketone from which 20 is formed is being constantly enriched in ^{13}C as the reaction progresses.

In principle, measurement of S for 20 at very low conversions for which the ^{13}C enrichment for 8 is negligible

2

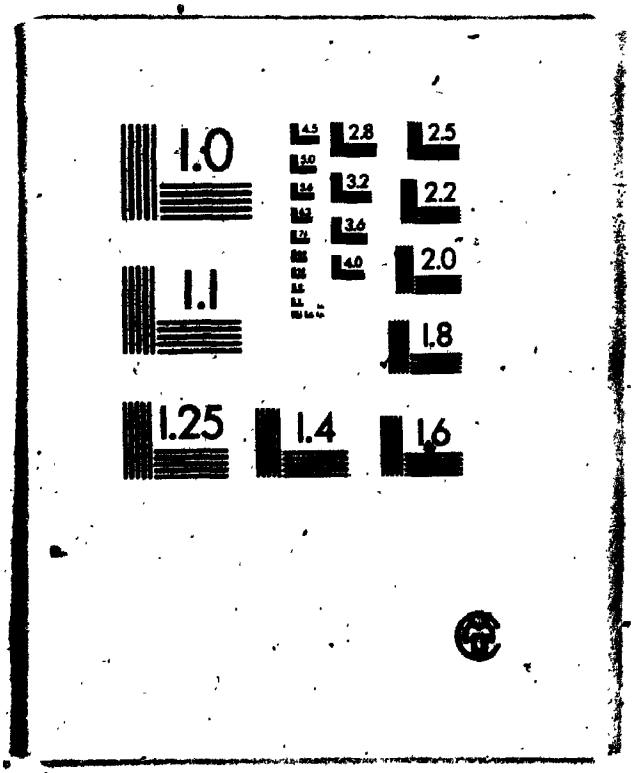

can yield directly the single stage enrichment parameter, α', for 2Ø. This approach has been used by Turro et al.;[90a] they have plotted log S against -log(1-f) for 2Ø and have extrapolated to zero conversion to obtain α' (α' = S, at zero conversion). A considerable number of points at low conversion are required to obtain α' in this way. A method based upon the overall separation factor, S, for 2Ø and the variation in $^{13}C/^{12}C$ ratios for 8 throughout the photolysis was, therefore, developed to allow calculation of the single stage enrichment factor (α') for 2Ø in the present studies.

The parameter α' may be defined by equation 15 where

$$\alpha' = \frac{k_{13}}{k_{12}} \tag{15}$$

k_{13} and k_{12} are the rate constants for the formation of ^{13}C and ^{12}C 2Ø, respectively. The rate of formation of 2Ø depends on the concentration of 8 (16); integration of both sides gives equation 17, the right side of which is equal to the total $[^{13}C_{2Ø}]$ after photolysis time t.

$$\frac{d[^{13}C_{2Ø}]}{dt} = k_{13}[^{13}C_8] \tag{16}$$

$$\int_0^t \frac{d[^{13}C_{2Ø}]}{dt}\,dt = \int_0^t k_{13}[^{13}C_8]dt \tag{17}$$

$$\therefore\ [^{13}C_{2Ø}]_{total,t} = k_{13}\int_0^t [^{13}C_8]dt \tag{18}$$

The above integral is expressed in terms of t; however, the variable must be changed to conversion, f, since the $^{13}C/^{12}C$ ratios for 8 can more easily be expressed as a function of f. Making the appropriate changes of variable and integration limits[96] yields equation 19. The $[^{13}C_8]$ at a

$$[^{13}C_{20}]_{total,f} = k_{13} \int_0^f [^{13}C_8]df \qquad (19)$$

particular conversion, f, may be expressed as in equation 20, where C_o is the initial total ketone concentration

$$[^{13}C_8]_f = (\text{fraction } ^{13}C_8)_f(1-f)C_0 \qquad (20)$$

(i.e., $^{12}C+^{13}C$ 8). The fraction of $^{13}C_8$ for any conversion, f, may be obtained from S at that conversion as illustrated in (21)-(24).

$$(\text{fraction } ^{13}C_8)_f = \frac{^{13}C_f}{^{13}C_f+^{12}C_f} \qquad (21)$$

Rearranging equation 9 gives

$$\frac{[^{13}C_f]}{[^{12}C_f]} = SR_0 \qquad (22)$$

$$\frac{SR_0}{1+SR_0} = \frac{[^{13}C]_f}{[^{13}C]_f+[^{12}C]_f} \qquad (23)$$

$$\therefore (\text{fraction } ^{13}C_8)_f = \frac{SR_0}{1+SR_0} \qquad (24)$$

Solving (14) for S and substituting in (24) gives

$$S = (1-f)^{((1/\alpha)-1)} \tag{25}$$

$$\therefore \text{(fraction } {}^{13}C_8)_f = \frac{R_0(1-f)^{((1/\alpha)-1)}}{1+R_0(1-f)^{((1/\alpha)-1)}} \tag{26}$$

Substitution of (26) in (20) gives

$$[{}^{13}C_8]_f = \frac{C_0R_0(1-f)^{1/\alpha}}{1+R_0(1-f)^{((1/\alpha)-1)}} \tag{27}$$

Equation 27 can now be substituted into (19):

$$[{}^{13}C_{20}]_{total,f} = k_{13}C_0R_0\int_0^f \frac{(1-f)^{1/\alpha}}{1+r_0(1-f)^{((1/\alpha)-1)}} \tag{28}$$

$$= k_{13}C_0R_0A$$

The same series of operations can be carried out for $[{}^{12}C_{20}]$ to give

$$[{}^{12}C_{20}]_{total,f} = k_{12}\int_0^f [{}^{12}C_8]df \tag{29}$$

$$\text{(fraction } {}^{12}C_8)_f = 1 - \text{(fraction } {}^{13}C_8)_f \tag{30}$$

$$= \frac{1}{1+SR_0} \tag{31}$$

$$\therefore [^{12}C_{20}]_{total,f} = k_{12}C_0 \int_0^f \frac{(1-f)}{1+R_0(1-f)((1/\alpha)-1)}\,dt \qquad (32)$$

$$= k_{12}C_0 B$$

Evaluation of the integrals in (28) and (32) then allows calculation of α':

$$\alpha' = \frac{k_{13}}{k_{12}} = \frac{[^{13}C_{20}]_{total,f}}{C_0 R_0 A} \times \frac{C_0 B}{[^{12}C_{20}]_{total,f}} \qquad (33)$$

$$[^{13}C_{20}]_{total,f} = C_T(\text{fraction } ^{13}C_{20})_f \qquad (34)$$

where C_T is the total concentration of 20.

$$[^{13}C_{20}]_{total,f} = \frac{C_T[^{13}C_{20}]}{[^{13}C_{20}]+[^{12}C_{20}]} \qquad (35)$$

$$[^{12}C_{20}]_{total,f} = \frac{C_T[^{12}C_{20}]}{[^{13}C_{20}]+[^{12}C_{20}]} \qquad (36)$$

$$\therefore \alpha' = \frac{[^{13}C_{20}]}{[^{12}C_{20}]} \times \frac{B}{R_0 A} \qquad (37)$$

The integrals A and B can be evaluated numerically for any experiment using the known values for α and f. The ratio $[^{13}C_{20}]/[^{12}C_{20}]$ is readily obtained from mass spectral

analysis (see 6.9). In practice there was no significant difference for α' values determined from α values calculated using either the exact or approximate equation (12 or 14, respectively). The above method for calculating α' has the advantage that it can be used to obtain an enrichment efficiency for a limited amount of data.

3.3 ^{13}C Enrichment on Silica Gel

Carbon 13 enriched ketone was used as the starting material for all measurements of ^{13}C enrichment resulting from photolysis of dibenzyl ketone, 8. Analysis of the $^{13}C/^{12}C$ ratios was much easier if enriched material was used; several preliminary experiments had indicated that there was considerable error in the mass spectral analysis if unenriched ketone was used. Dibenzyl ketone (90% ^{13}C in the carbonyl) was prepared from ^{13}C labelled phenylacetic acid and was mixed with an appropriate amount of natural abundance 8 to give ketone which contained 25% ^{13}C in the carbonyl position. All reported enrichments, therefore, refer to enrichment at the carbonyl and have been corrected for the natural abundance ^{13}C content at other positions as outlined in 6.9.

Substantial ^{13}C enrichment was observed in both dibenzyl ketone, 8, and its isomer, 20, recovered after partial photolysis of 8 on silica gel. The mass spectral results obtained for an experiment at 84.3% conversion are shown in Figure 5: the intensity at m/e 211 relative to that at 210 was greater for recovered 8 than for the

Figure 5. Mass spectra (molecular ion region only): A - dibenzyl ketone, 25% $^{13}C = O$, before photolysis; B - ketone recovered after photolysis to 84.3% conversion.

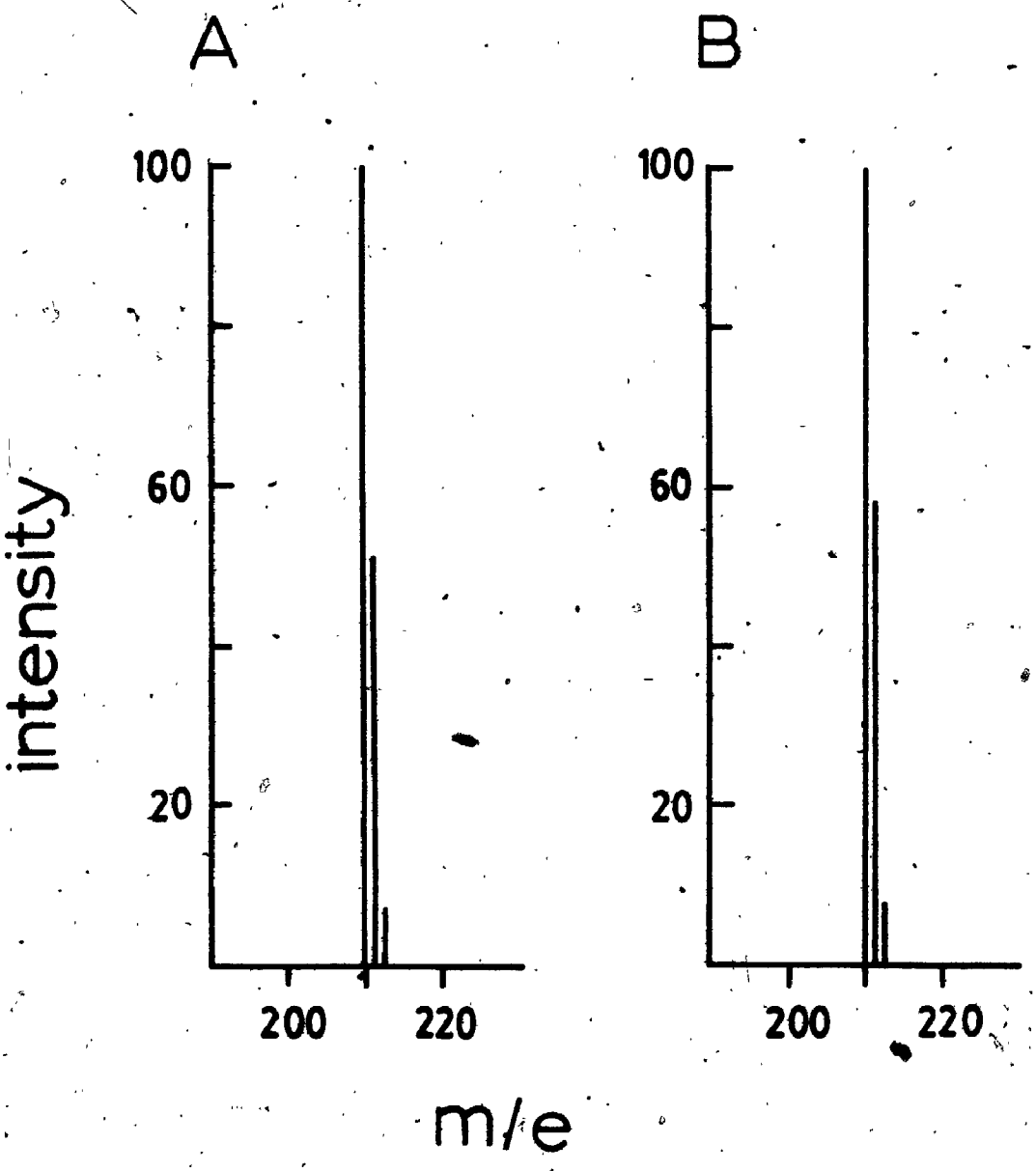
A
B
100
60
20
intensity
200
220
m/e

starting material. The ^{13}C contents of recovered 8 and 20 were 30.4% and 35.6%, respectively, from the mass spectral intensities. These results were confirmed by NMR analysis of the two ketones. The methylene protons of both show signals which are a combination of a singlet due to a ^{12}C carbonyl and a doublet centred at the same chemical shift. The latter arises from ^{13}C proton coupling for molecules containing a ^{13}C carbonyl. Integration of the singlet and the two satellites allowed determination of the ^{13}C content at the carbonyl. The methylene signals for starting material and for 8 and 20 recovered after 70.9% conversion are shown in Figure 6. The ^{13}C content determined from the NMR integration agreed well with that determined mass spectrally.

The ^{13}C contents in 8 and 20 recovered after photolysis on silica gel at 20°C are listed in Table 8. As expected, the ^{13}C content of ketone 8 increased steadily with conversion. The calculated values for α, the single stage enrichment factor, ranged from 1.12 to 1.18; the average was 1.14. The lower α values obtained at higher conversions may result from the overirradiation of enriched ketone caused by inhomogeneous photolysis on the silica gel surface. This explanation is substantiated by the fact that lower α values (α < 1.04) were obtained for experiments carried out to >98% conversion. The α values of ~1.18 for the lower conversions appear, therefore, to provide a more reliable measure of the ^{13}C enrichment efficiency on the silica gel surface. An α value of 1.13 was calculated from the slope of a plot of log

Figure 6. ^{1}H NMR spectra (methylene region only): A - dibenzyl ketone, 25% $^{13}C = O$, before photolysis; B - dibenzyl ketone recovered after photolysis to 70.9% conversion; C - 1-phenyl-4'-methylacetophenone recovered after photolysis of dibenzyl ketone to 70.9% conversion.

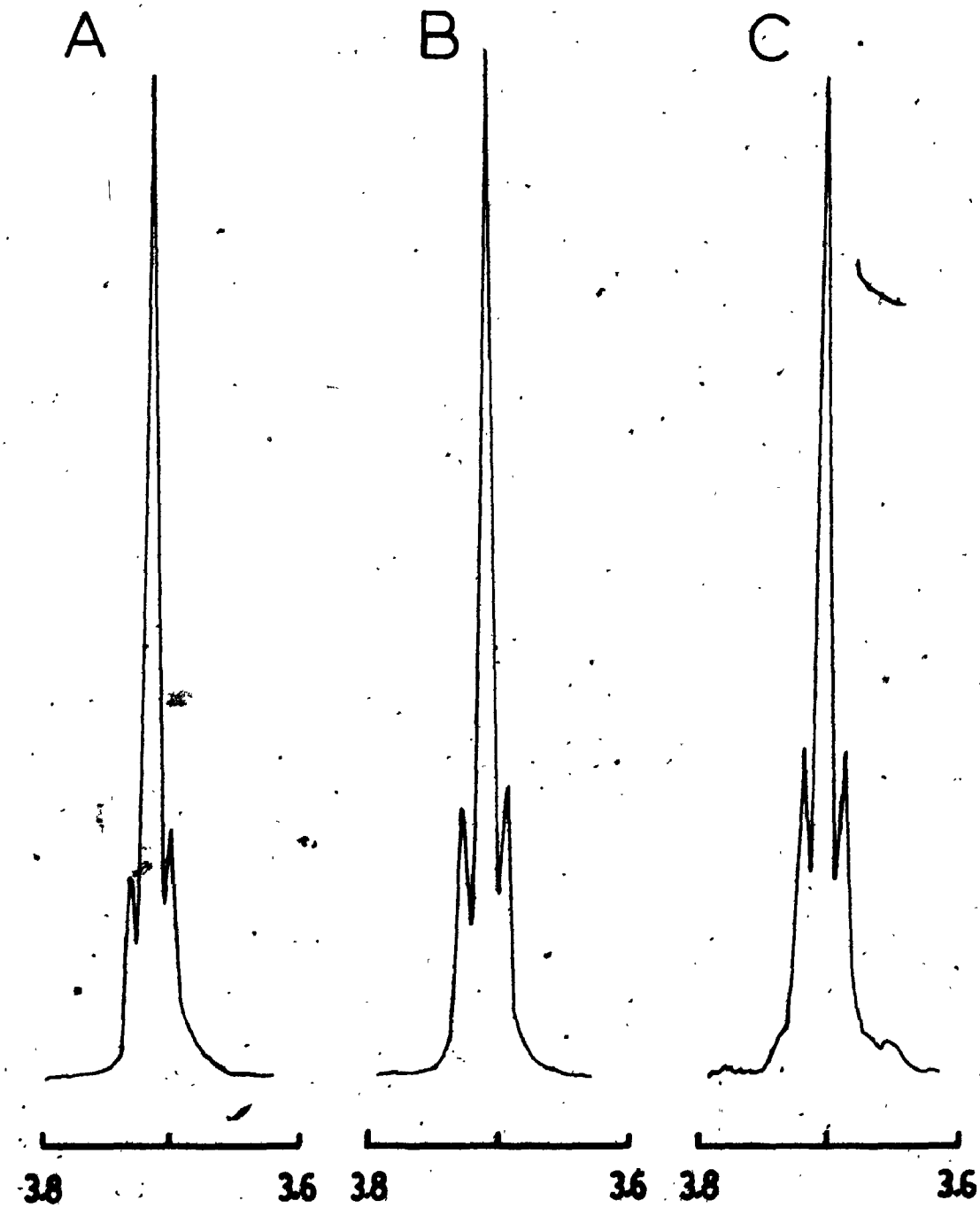
A
B
C
3.8
3.6
3.8
3.6
3.8
3.6

Table 8. ^{13}C enrichment for dibenzyl ketone, 8, and 1-phenyl-4'-methylacetophenone, 20,[a] recovered after photolysis of 8 on silica gel at 20°C.

Reaction conditions[b,c]	Conversion (%)	% ^{13}C at C=O[d] 8	20	α	α'
A	84.3	30.4	35.6	1.12	1.58
A	70.9	27.7	34.6	1.11	1.52
A	69.8	28.1	34.1	1.14	1.48
A	43.8	26.8	33.8	1.18	1.48
A	29.9	26.1	33.0	1.17	1.44
B,C	91.6	30.7	35.4	1.12	1.56
B,C	73.6	28.3	34.3	1.14	1.49
B	27.4	25.4	___[e]	1.08	___

[a] Yields of 20 were 2-3%, based on consumed starting material.

[b] 4.77×10^{-4} mol 8/g silica gel.

[c] A - silica gel used without drying;
B - silica gel dried as in 6.3.2, procedure B;
C - sample rotated in an ultrasonic bath to aid in sample mixing.

[d] The reported % ^{13}C values are approximately ±0.9 (3%); these produce α values of approximately ±0.03.

[e] Yield of 20 insufficient for isolation and analysis.

S versus -log(1-f) (Figure 7) for the data in Table 8 (excluding the last entry).

Comparison of the results obtained under various experimental conditions at 20°C (Table 8) showed that the ^{13}C enrichment was not affected by the water content of the silica gel or by the method of sample mixing. Lowering the photolysis temperature had little effect on α. At -55°C the observed enrichments (Table 9) were similar to those obtained at 20°C; α values were slightly higher for dry silica gel than for undried silica.

For isomer 20 the ^{13}C content was, as expected, already quite high at low conversions and did not increase very rapidly thereafter. For example, at 20°C the 33.0% ^{13}C content at 29.9% conversion increased to only 35.6% at 84.3% conversion (Table 8). The α' values calculated using the method outlined above were all ~1.5 for 20 recovered after photolysis at 20°C. For comparison, a plot of log S versus -log(1-f) was also constructed (Figure 8); extrapolation to zero assuming a linear relationship yielded on α' of 1.46 (correlation coefficient 0.96).

As for ketone 8, the enrichment obtained at 20°C for 20 was not affected by the dryness of the silica gel or the method of sample mixing. In contrast to results obtained for 8, changing the photolysis temperature from 20°C to -55°C substantially decreased the ^{13}C enrichment for 20. Values of α' at -55°C were ~1.1 as compared to ~1.5 at 20°C.

The above results indicate that, as predicted, the photolysis of 8 on dry silica gel does yield substantial ^{13}C

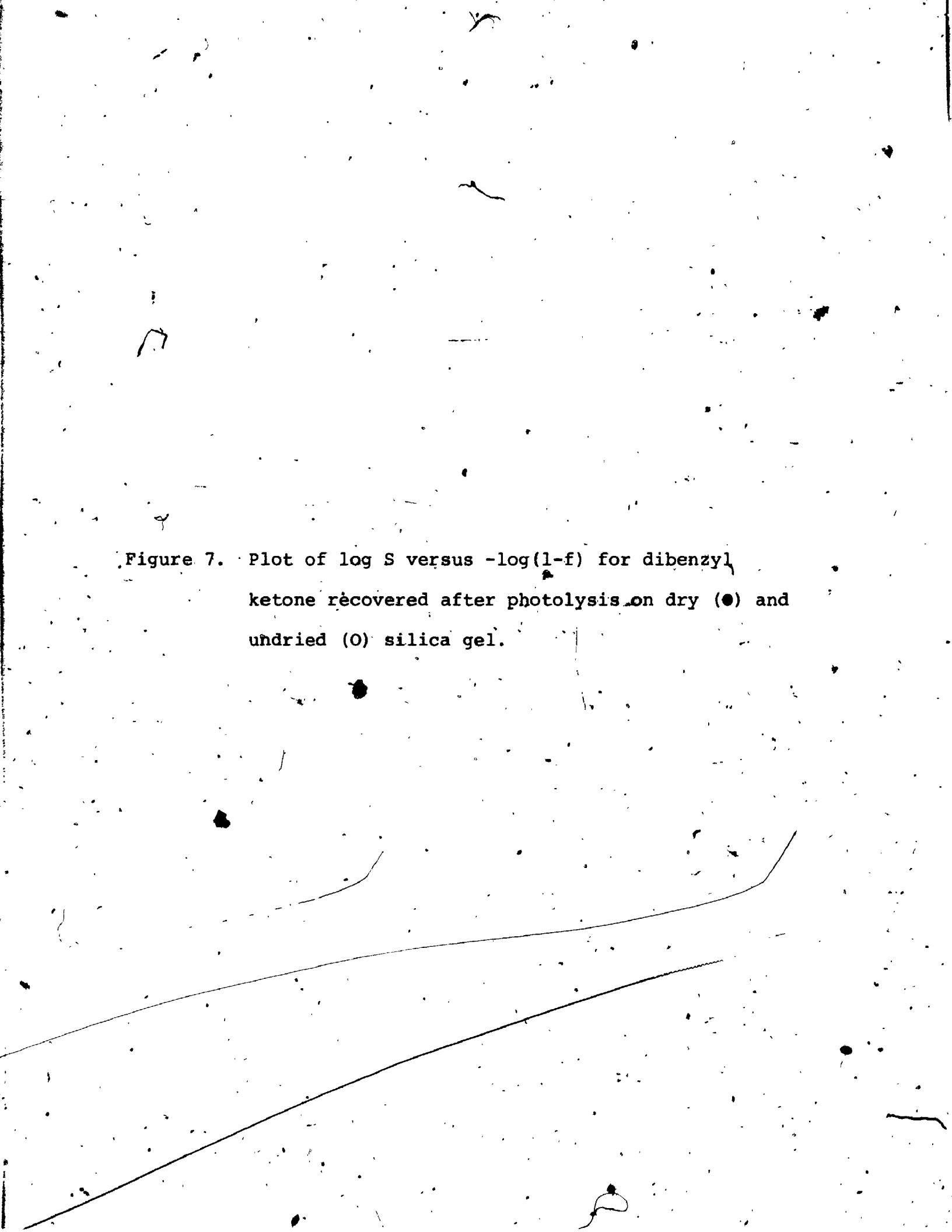

Figure 7. Plot of log S versus -log(1-f) for dibenzyl ketone recovered after photolysis on dry (●) and undried (O) silica gel.

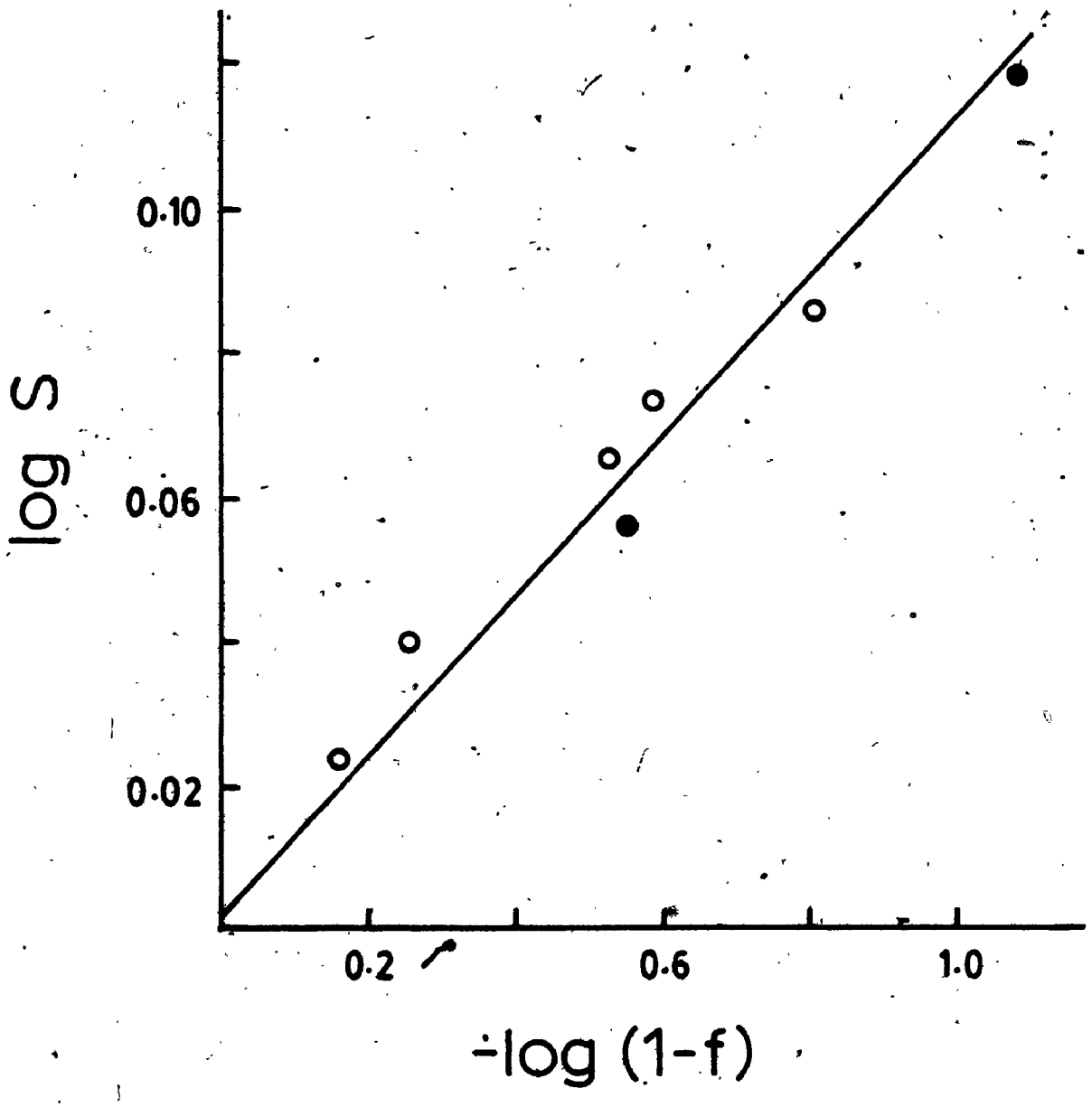
log S
0·10
0·06
0·02
0·2
0·6
1·0
-log (1-f)

Table 9. ^{13}C enrichment for dibenzyl ketone, 8, and 1-phenyl-4'-methylacetophenone, 20,[a] recovered after photolysis of 8 on silica gel at -55°C.[b]

Reaction conditions[c,d]	Conversion (%)	% ^{13}C at c=O			
		8	20	α	α'
A	66.8	26.9	28.2	1.09	1.14
A	28.7	25.5	25.8	1.07	1.03
B	74.0	28.9	30.1	1.22	1.20
B	50.2	27.3	28.1	1.18	1.12

[a] The yield of 20 was 3-5%, based on consumed material.

[b] At 20°C values of ~1.14 and ~1.5 were obtained for α and α' respectively.

[c] 4.77×10^{-4} mol 8/g silica gel.

[d] A - silica gel used without drying;
B - silica gel dried as in 6.3.2, procedure B.

Figure 8. Plot of log S versus -log(1-f) for 1-phenyl-4'-methylacetophenone recovered after photolysis of dibenzyl ketone on dry (●) and undried (O) silica gel.

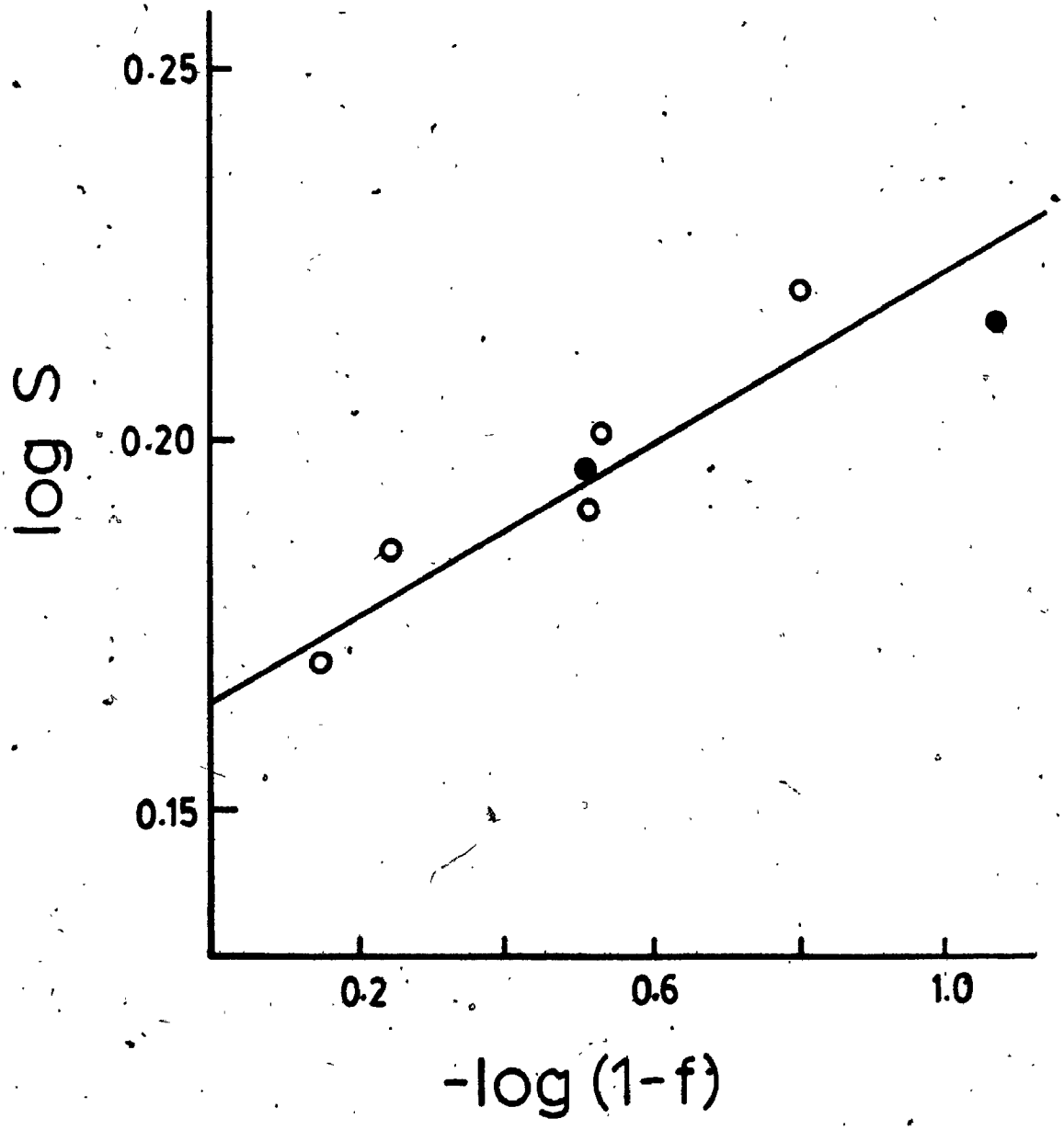
0.25
0.20
0.15
log S
0.2
0.6
1.0
-log (1-f)

enrichments in recovered ketones 8 and 20. Although the observed α values for 8 are larger than those in solution (α ~ 1.04), the enrichment for the surface reaction is less efficient than that for micellar photolysis (α ~ 1.25, see 3.5). Surprisingly, the enrichment in 20 is substantially higher than that for 8 at 20°C while at -55°C the two ketones show similar α and α' values.

3.4 ^{13}C Enrichment on Other Surfaces

Ketone 8 was photolyzed on several other types of surfaces to determine their effect upon ^{13}C enrichment. The results are summarized in Table 10. Firstly, 8 recovered after photolysis on a smaller particle size (6 μm rather than 0.2-0.5 mm) silica gel showed an enrichment (α ~ 1.13) similar to that already observed. Secondly, photolysis of 8 on neutral alumina also gave a similar α value (~1.1); however, the situation on alumina may be more complex than that on silica gel since the product recovery was only ~20% for the former. Isomer 20 was not detected among the reaction products for photolysis of 8 on either 6 μm silica gel or alumina. This suggests that a particular surface site may be instrumental in permitting the formation of 20 during photolysis on silica gel.

Thirdly, 8 was photolyzed on silica gel on which decanol had been coadsorbed. The decanol concentrations used corresponded to ~55% monolayer coverage, based on calculated molecular areas. The values obtained for both α and α' at 20°C and at -55°C were not appreciably different

Table 10., ^{13}C enrichment for dibenzyl ketone, 8 and 1-phenyl-4'-methylacetophenone recovered after photolysis of 8 on various surfaces at 20°C.

Surface	Conversion (%)	% ^{13}C at c=O			
		8	20	α	α'
6 μm Silica Gel[a]	67.1	27.6	___[f]	1.13	____
Silica Gel+Decanol[b]	43.6	27.0	33.0	1.20	1.42
Silica Gel+Decanol[c]	74.9	27.7	34.2	1.11	1.50
Silica Gel+Decanol[c,d]	54.1	27.1	27.9	1.15	1.12
Alumina[e]	27.3	25.4	___[f]	1.08	____
Alumina[e]	22.6	25.6	___[f]	1.12	____

[a] Average particle size, 6 μm; no drying; 4.60×10^{-4} mol 8/g

[b] 4.77×10^{-4} mol 8/g silica gel; 7.8×10^{14} mol decanol/g.

[c] 1.03×10^{-4} mol 8/g silica gel; 7.5×10^{-4} mol decanol/g.

[d] -55°C

[e] 1.5×10^{-4} mol 8/g alumina; alumina dried as in procedure A, 6.3.2; product recovery as dibenzyl 11 was <20%.

[f] 20 not detected by VPC (<0.2%).

from those for silica gel in the absence of decanol. Comparison of the present results for silica gel and silica gel plus decanol with those of Epling and Florio[93] suggest that it is the silica gel surface, not the bound hydrocarbon layer, which is responsible for the enhanced ^{13}C enrichment efficiency. It seems unlikely that the hydrocarbon layer makes the surface "micelle-like" as has been suggested.[93] It would be expected that radicals on a layer of hydrocarbon would be more mobile than those attached to silica gel and would, thus, be less likely to produce ^{13}C enriched material via the geminate recombination pathway. Although higher α values were obtained in the previous study,[93] it should be noted that these reflect the total enrichment at all carbons and are, consequently, expected to be higher than the present α values for carbonyl enrichment.

3.5 ^{13}C Enrichment in Micelles

For comparison with earlier work,[83b,90] ^{13}C enriched dibenzyl ketone was photolyzed in aqueous potassium dodecanoate. In previous micelle experiments a constant ketone : micelle ratio had been used. The present work was therefore designed to investigate the effect of variations in N (the average number of molecules/micelle) on the ^{13}C enrichment efficiency. The results shown in Table 11 indicated that α and α' values for the recovered ketones were not particularly sensitive to N. The high values for α' at high conversion could be due to photolysis of 2Ø and its further enrichment by recombination to regenerate 2Ø.

Table 11. ^{13}C enrichment for dibenzyl ketone, 8, and 1-phenyl-4'-methylacetophenone, 20,[a] recovered after photolysis of 8 in aqueous potassium dodecanoate.

N	Conversion (%)	α	α'
0.34[b]	98.0	1.19	1.73
0.43[b]	34.7	1.28	1.20
0.43[b]	39.2	1.19	1.23
1.17[c]	94.4	1.24	1.67
1.24[c]	54.7	1.37	1.20

[a] The yield of 20 was 8-10% and 2-4% for low and high conversion experiments, respectively.

[b] [surfactant] = 0.16 M

[c] [surfactant] = 0.08 M

The lower yields of 20 obtained at >80% conversion support this explanation. The observed enrichments are comparable to those found in other micellar systems.[83b,90]

Dibenzyl ratios for photolysis of the unsymmetrical ketone 16 in micellar solution (Table 5) changed from 1.0:48:1.0 (N = 0.35) to 1.0:6.4:1.2 (N = 0.85), indicating a large decrease in the amount of cage recombination. It might be expected that ^{13}C enrichment efficiencies would also decrease at higher N since radical escape from the geminate pair is thought to be responsible for the low α values in solution. The trend (at least for 8) appears to be in the opposite direction. This effect may be rationalized by considering that the dibenzyl ratios depend on events following decarbonylation; higher Ns may make escape of benzyl radicals from the micelle more likely without affecting significantly the partitioning between decarbonylation and recombination of the acyl-benzyl radical pair. It is this partitioning which Turro has suggested to be the key factor in enhancing the ^{13}C enrichment efficiency in micelles. The present results provide support for this hypothesis.

3.6 Comparison of Results

Consideration of α values for 8 on a variety of surfaces and in micelles indicates that both environments are effective in enhancing the ^{13}C enrichment. Since restrictions on the diffusion of the initial radical pair appear to be important in the enrichment process, the

results suggest that the silica gel surface provides a slightly less restricted environment than does a micelle. The dibenzyl ratios obtained upon photolysis of unsymmetrical dibenzyl ketones also indicate more restriction of radical motion by micelles than by the silica surface. However, the differences are much greater in the latter case. This is reasonable if the lifetimes of the radical pairs are considered. The acyl-benzyl radical pair involved in the ^{13}C enrichment process has a shorter lifetime than the benzyl radical pair and the surface will be much more effective in localising this shorter-lived radical pair. On the other hand, since both radical pair lifetimes are short with respect to radical exit from a micelle, the micelle can effectively localise both radical pairs until recombination occurs.

Substantially higher enrichments were observed for isomer 2Ø than for 8 at 2Ø°C. Similar differences have also been observed in micelles.[9Ø] Both 2Ø and 8 are derived from the same initial radical pair; the differences in enrichment may be a reflection of differences in the rates of processes leading to each ketone. It is also possible that surface sites which favor recombination to produce isomer 2Ø also permit more efficient ^{13}C enrichment.

The enrichment efficiency was considerably decreased for 2Ø at low temperature; however the α values for 8 were much less sensitive to the temperature, at least from -55 to 2Ø°C. It is plausible that an investigation of the photolysis over a wider temperature range* would reveal a

maximum α (or α') value at a particular temperature, as observed by Rines et al.[92] in solution. The variation of α with temperature in solution has been attributed to both viscosity effects and the variation in the decarbonylation rate with temperature. Turro has explained similar temperature effects in micelles on the basis of changes in the decarbonylation rate. The data obtained in the present study are not extensive enough to permit speculation concerning their origins. It might be expected that, if temperature effects are caused by changes in the decarbonylation rate, the maximum enrichment would occur at the same temperature for various environments.* It is unlikely that changes in the decarbonylation rate are entirely responsible for the observed effects; a combination of factors is more likely to be involved for any restricted environment.

The presence of a reflecting boundary has been suggested as an explanation for the efficient isotope enrichment in micelles[90] and on a surface with a bound hydrocarbon monolayer.[93] However, it is not obvious how this explanation applies to the surface. There does not seem to be any reason to prefer this hypothesis over a rationalization based upon the actual "stickiness" of the environment. On a surface there is no "wall" to prevent the radicals from diffusing apart; rather, the radicals are

---

* Experimental difficulties prevented the completion of such an investigation.

confined to a small space by virtue of their inability to overcome rapidly the surface-adsorbate interaction and move apart. This provides sufficient time for the development of the hyperfine coupling induced intersystem crossing required for ^{13}C enrichment.

CHAPTER 4

CIDNP STUDIES OF DIBENZYL KETONES

4.1 Introduction

Since its discovery in 1967, chemically induced dynamic nuclear polarization (CIDNP) has been widely used in mechanistic studies of organic chemistry and photochemistry. The use of this versatile technique in measuring the relative rates of Type I photolysis of a number of dibenzyl ketones will be described in this section.

CIDNP phenomena are observed only, although not always, for reactions involving a radical pair (or in some cases a biradical); they are detected as either an enhanced NMR absorption or an NMR emission spectrum. These anomalous NMR spectra result from nonequilibrium populations of the nuclear spin states. The radical pair theory[87,88] which provides the basis for understanding CIDNP effects states that the reactivity of a radical pair in solution depends on the spin states of nuclei present in the pair. This dependence arises from the fact that the nuclear spin states of a magnetic nucleus in a radical, due to hyperfine coupling interactions with the electron, influence the rate of intersystem crossing in the radical pair. An initially formed radical pair surrounded by a solvent cage which acts to hold it together has a number of processes available to it. If present in the singlet electronic state, the radical pair may recombine to form a cage product. However, a

triplet radical pair cannot react until intersystem crossing to the singlet has occurred. The process of diffusion, and resulting separation of the two radicals, therefore, competes with a cage reaction much more effectively for triplet pairs. Since the rate of intersystem crossing and, hence, the probability of diffusional separation of a radical pair is affected by the nuclear spin states of the radicals through the hyperfine coupling interaction, it is possible to see CIDNP effects due to the predominance of one spin state in a cage reaction product and the predominance of a second in escape products.

The properties of CIDNP spectra and the prediction of the signal directions are summarised in Kaptein's rules.[88] The net polarization (Γ_{ne}) for nucleus i on radical a (for the case where only one radical of the pair contains a magnetic nucleus) is given by

$$\Gamma_{ne}(i) = \mu \, \varepsilon \, \Delta g \, Ai \qquad \text{product sign} \begin{cases} + & \text{absorption} \\ - & \text{emission} \end{cases} \qquad (38)$$

where the product sign determines whether emission or enhanced absorption will occur. In (38) Ai refers to the hyperfine coupling constant for nucleus i and Δg is the difference in g-factors for the two radicals, $g_a - g_b$, where g_a is the radical containing the nucleus i. These two determine the magnitude of the hyperfine induced intersystem crossing. The parameter μ refers to the radical precursor

multiplicity and is + for a triplet precursor and for free, uncorrelated radicals and is - for a singlet precursor. The sign of ε is + for cage recombination products and - for noncage, escape products.

CIDNP spectra are not observed in all radical reactions. The observation of this phenomenon requires not only that there be sufficient time for the development of polarization of the nuclear spin states, but also that reaction occur before relaxation restores the normal distribution of the nuclear spins.

CIDNP spectra for dibenzyl ketone (8) photolysis were first measured by Fischer and coworkers.[66a,b] The CIDNP emissive character of the methylene protons could be explained using the Kaptein rule:[88] the phenylacetyl-benzyl radical pair is generated from a triplet state ($\mu > 0$), the recombination to regenerate 8 is a cage process ($\varepsilon > 0$), the benzyl radical methylene protons have a negative hyperfine coupling constant ($A_i < 0$) and the g factor of the benzyl radical (2.0025) is larger than that of the acyl radical (2.0007) ($\Delta g > 0$). Polarization was also observed for the decarbonylation product, dibenzyl, 11. The enhanced absorption for the methylene protons of 11 was consistent with product formation via a free radical mechanism ($\varepsilon < 0$) but from the same precursor, the phenylacetyl-benzyl radical pair.

Turro et al.[72] have also examined CIDNP spectra during photolysis of 8. In addition to the signals from 8 and 11, they observed a weak emission at 5.0 ppm which they assigned

to the tautomer (i.e., before rearomatization) of the isomeric 1-phenyl-4'-methylacetophenone, 20. Quantitative CIDNP spectra for 8 in the presence of sufficient thiol to trap free benzyl radicals were also measured. Although the absorptive polarization of the methylene protons of 11 formed from free radical combination disappeared completely at high scavenger concentrations, no emissive signals due to cage benzyl radical recombination were observed. These results provided further evidence for the lack of decarbonylation within the geminate radical pair.

Roth and Turro[95] have compared CIDNP spectra generated in homogeneous solutions to those observed in micelles for a monosubstituted dibenzyl ketone. Similar polarizations were observed in the two media. In homogeneous solution the spin sorting mechanism involves hyperfine dependent intersystem crossing and the subsequent competition between an electron spin dependent radical pair recombination and a spin independent diffusional separation of the radical pair. In a micellar environment there is a much greater reencounter probability for the radical pair. Turro et al. have suggested that decarbonylation rather than diffusion provides the competitive pathway necessary for the spin selection process in micelles.

The CIDNP spectra for the substituted ketone also showed an intensity difference for the signals from the two ketone methylene groups.[95] This effect was attributed to the preferential cleavage of the substituted benzyl-carbonyl bond. This and the investigations of phenylacetyl-benzyl

radical pair behaviour described in Chapters 2 and 3 led to the following CIDNP study of the relative rates of Type I cleavage of substituted dibenzyl ketones.

4.2 Results and Discussion

A series of monosubstituted dibenzyl ketones (25a-25e, Scheme 4) was prepared (see 6.2.5). Proton NMR spectra of each showed well separated singlets for the two sets of nonequivalent methylene protons. Photolysis of each ketone in the magnetic field of an NMR spectrometer produced CIDNP spectra which were qualitatively similar. The absorptions of the methylene protons of all starting materials were converted into emission and enhanced absorption signals were observed in the dibenzyl products. A complex absorption and emission pattern was also observed for the aromatic protons of each ketone. Spectra obtained for ketones 25a, 25b, and 25e are shown in Figures 9, 10 and 11. Different emission intensities were observed for the methylene protons of the substituted and unsubstituted benzyl groups for each ketone. For example, for 4-methoxydibenzyl ketone, 25a, the methoxybenzyl methylene protons exhibited much stronger emission than did the unsubstituted benzyl methylene protons (Figure 9). The situation was reversed for the 3-chloro ketone (Figure 10) for which the unsubstituted benzyl protons showed the stronger emission. Similar emission intensities were observed for both methylene groups of the 4-fluoro ketone, 25c (Figure 11). The methylene protons were assigned by comparison of their chemical shifts to that

Figure 9. ^1H NMR spectrum of 4-methoxydibenzyl ketone, 25a, ($CDCl_3$) in the dark (left) and during UV irradiation (right). Peaks at δ 3.65, 3.70 and 3.79 are assigned to 4-methoxybenzyl methylene, benzyl methylene and methoxy protons, respectively.


4.0
3.8
3.6
4.0
3.8
3.6

Figure 10. ^1H NMR spectrum of 3-chlorodibenzyl ketone, 25e, ($CDCl_3$) in the dark (left) and during UV irradiation (right). Peaks at δ 3.69 and 3.72 are assigned to 3-chlorobenzyl methylene and benzyl methylene protons, respectively.

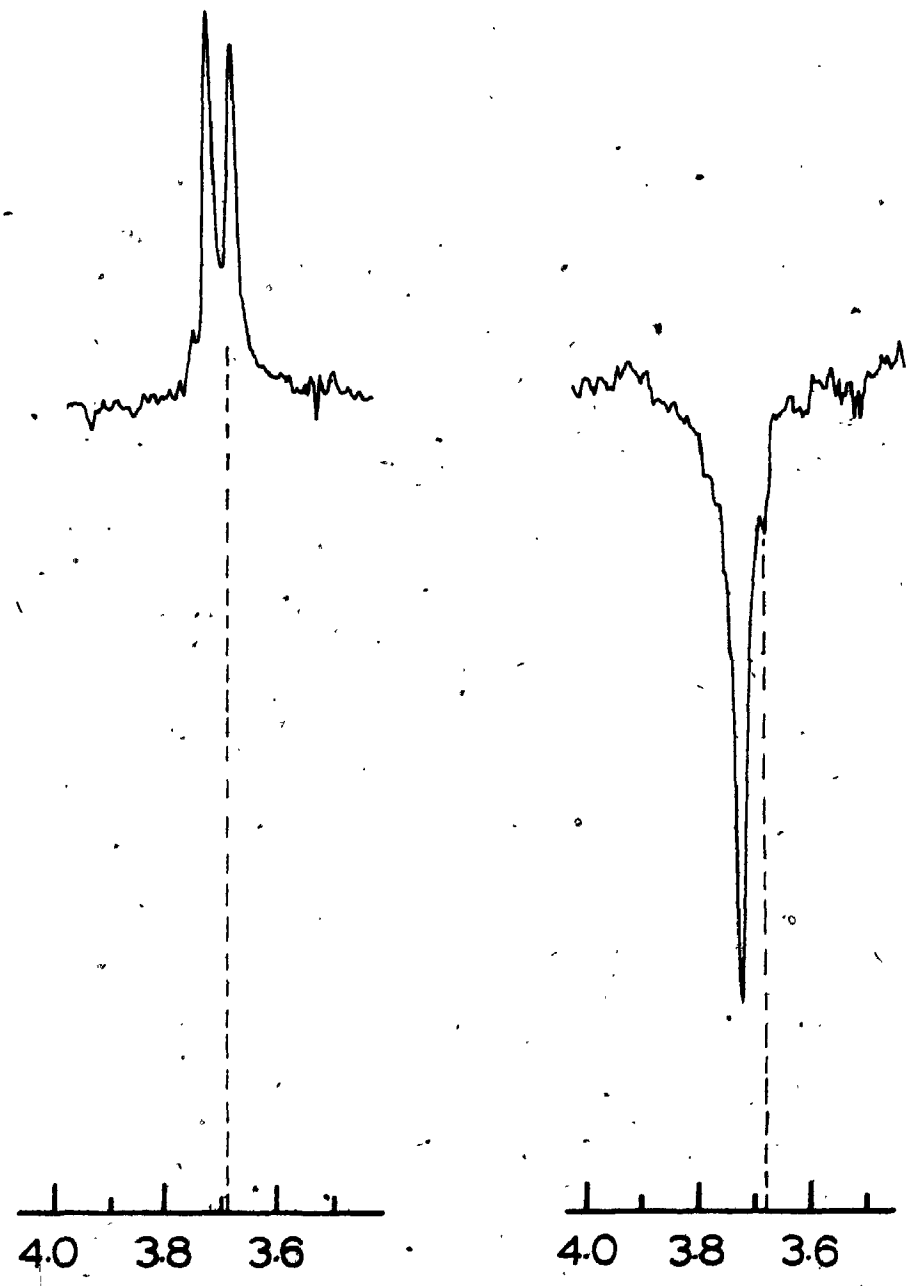
4.0
3.8
3.6
4.0
3.8
3.6

Figure 11. ^1H NMR spectrum of 4-fluorodibenzyl ketone, 25c, ($CDCl_3$) in the dark (left) and during UV irradiation (right). Peaks at 3.68 and 3.71 are assigned to 4-fluorobenzyl methylene and benzyl methylene protons, respectively.

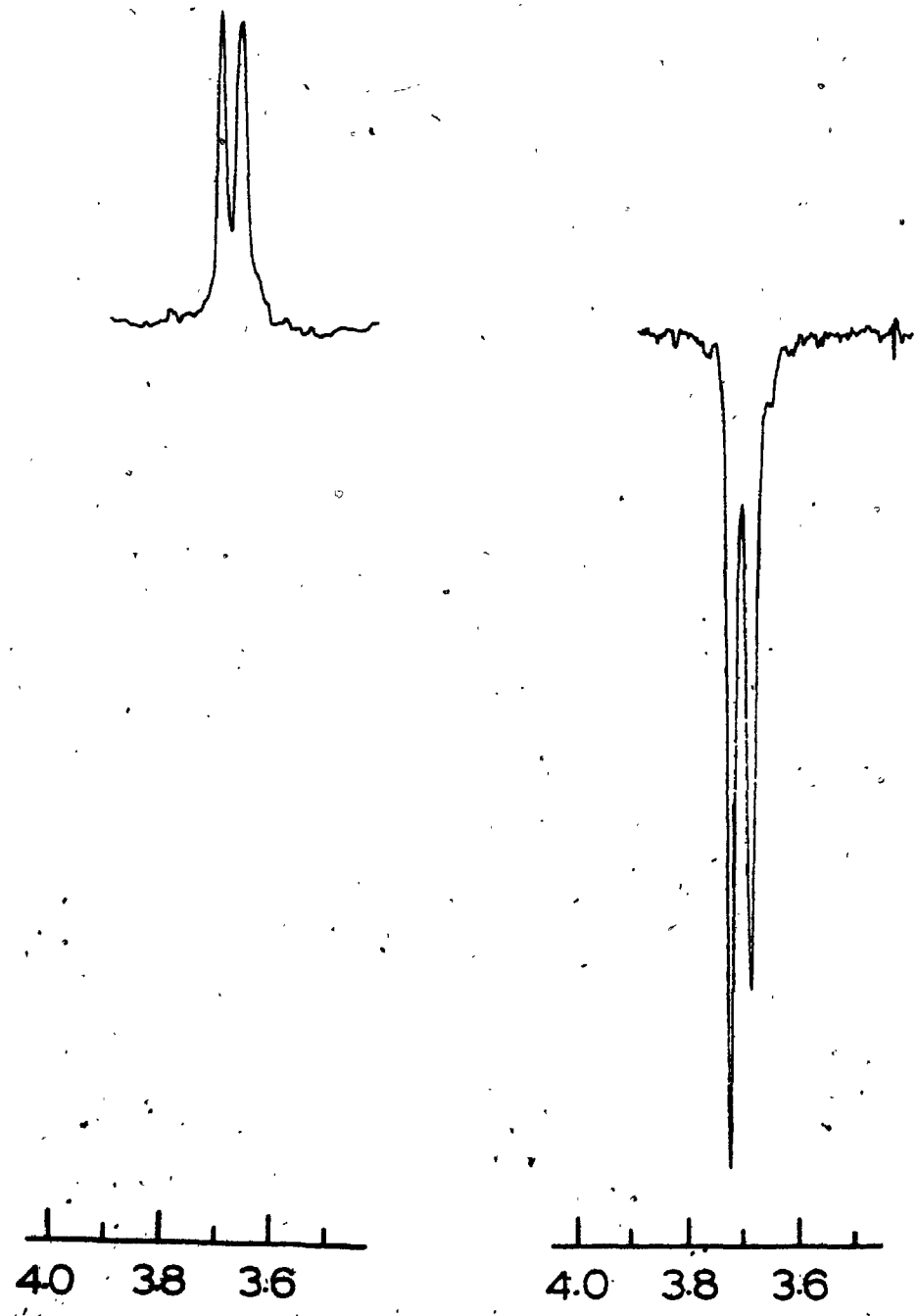
4.0
3.8
3.6
4.0
3.8
3.6

of the unsubstituted dibenzyl ketone, 8, and by addition of 8 to samples of each ketone. The statistical (1:2:1) dibenzyl product ratios obtained when substituted dibenzyl ketones were photolyzed failed to indicate the CIDNP nonequivalence of the methylene protons.

Photolysis of an unsymmetrical dibenzyl ketone can result in two possible competitive α cleavages, a and b (Scheme 4), although the same three final coupling products (dibenzyls 11, 26 and 27) will result in either case. Differences in the rates for pathways a and b will lead to unequal concentrations of radical pairs A and B. The different CIDNP signal intensities may then be derived from a larger concentration of one of the pairs resulting from preferred cleavage of one of the benzyl-carbonyl bonds.

The above explanation of the observed CIDNP phenomena is consistent with the available data. However, other interpretations must be considered and, if possible, eliminated. The magnitude of the observed emission signals may be influenced by (1) the relative quantum yields of cleavage, (2) the relative spin lattice relaxation times for the benzyl methylene protons and (3) the relative lifetimes of radical pairs A and B. It is unlikely that (1) is influencing the present CIDNP results since quantum yields for decarbonylation of several substituted dibenzyl ketones have been shown to be the same within experimental error.[65] Similarly, factor (2) is not responsible for the observed effects. Spin lattice relaxation times for the benzylic methylene protons of all ketones have been measured (Table

Scheme 4

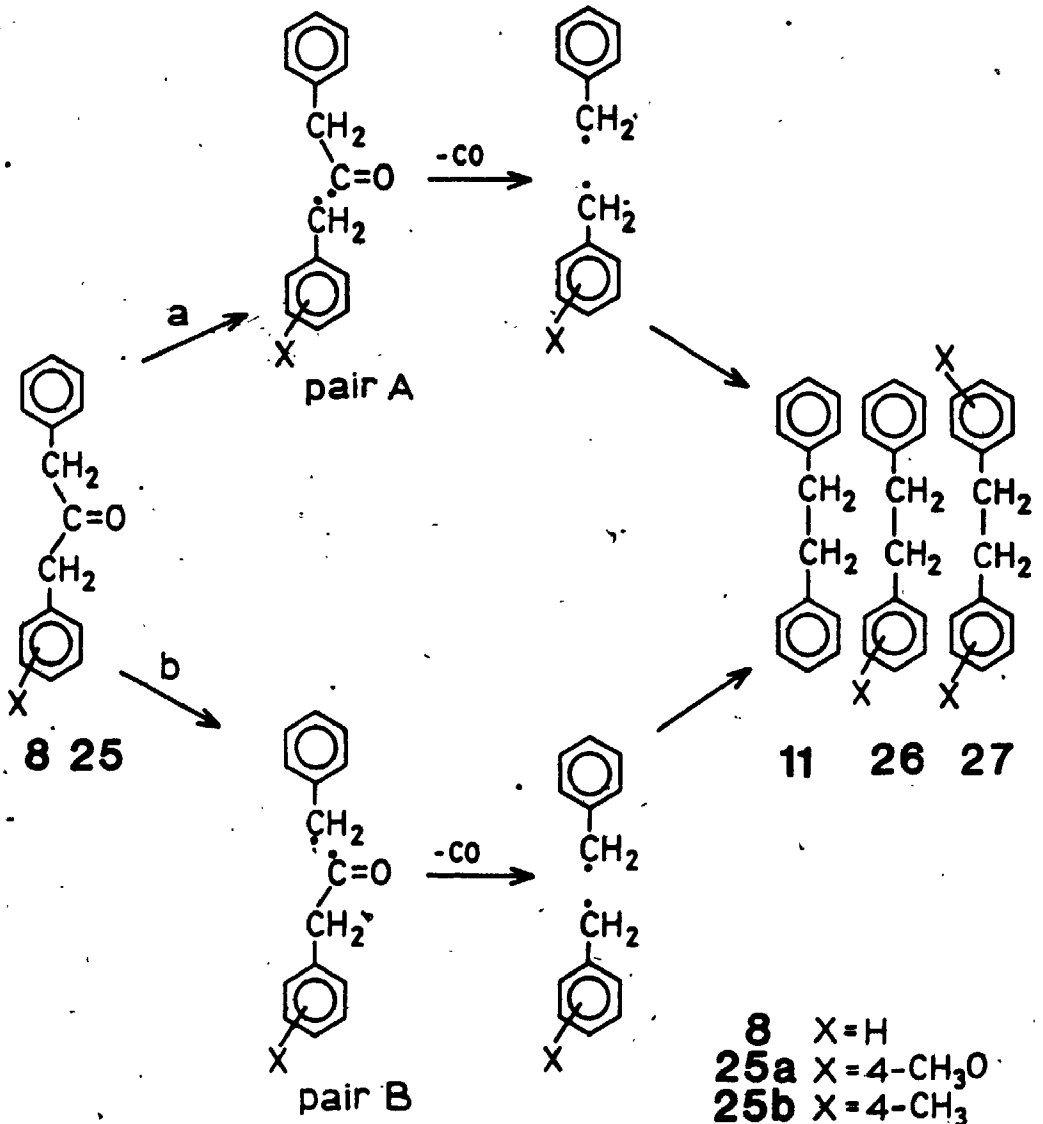
a
b
-CO
-CO
pair A
pair B
8 25
11 26 27
8 X=H
25a X=4-CH3O
25b X=4-CH3
25c X=4-F
25d X=4-Cl
25e X=3-Cl

12) and the relative emission intensities corrected accordingly. The measured relaxation times were similar (1.8-2.2 s) and did not significantly affect the results.

The relative lifetimes of radical pairs A and B are determined by several factors: (a) diffusion, (b) their recombination probabilities, (c) intersystem crossing rates and (d) their rates of decarbonylation. The diffusion behaviour may be considered to be identical for the two. The recombination probabilities (from the singlet) should also be the same. The intersystem crossing rates should not be markedly different for the two pairs since Δg is the same for both and the variation in the hyperfine coupling constants of the methylene protons of benzyl radicals is small.[‡,97] Although the β protons of the phenylacetyl radicals ($a_H \sim 1G$; $\Delta g < 0$) can also induce CIDNP effects, the contribution would be much smaller than that from the methylene protons. Hyperfine interactions with nuclei other than the methylene protons are also expected to have only minor influences on the amplitude of the methylene polarization since they are averaged to null with respect to the methylene protons and since the present CIDNP effect is basically due to Δg. The above reasoning leads to the conclusion that the intersystem crossing rates for pairs A and B should be similar.

---

‡ Hyperfine coupling constants for the methylene protons of benzyl radicals, X-Ph-CH_2·(X,hfc);[97] 4-MeO, -15.93 G; 4-Me, -16.07 G; 4-F, -16.43 G; H, -16.34 G; 4-Cl, -16.08 G.

Table 12. Spin lattice relaxation times (T_1) of the benzylic methylene protons for X-substituted dibenzyl ketones.

X	T_1(s)
4-MeO	1.8
4-Me	2.Ø
4-F	2.2
H	2.2
4-Cl	2.Ø
3-Cl	2.Ø

The possibility that differences in the decarbonylation rates for the substituted and unsubstituted acyl radicals are responsible for the varying CIDNP intensities is not so readily disproved. This interpretaton would assume equal rates of formation of pairs A and B but faster decarbonylation of the pair with the weaker CIDNP emisson. In this case, the relative rates of decarbonylation, not Type I fragmentation, would be monitored. The problem might, in principle, be resolved by repeating the experiments in micelles where the sorting mechanism responsible for CIDNP polarization has been postulated by Turro and Roth to be that of decarbonylation.[95] If the same results were obtained in micelles and in solution, it could be concluded that decarbonylation was responsible for the sorting mechanism in both cases. However, appreciably different results would indicate that the solution results reflect diffusional sorting and are, thus, not affected by decarbonylation.

CIDNP specta were measured during the photolysis of ketones **25a** and **25e** in potassium dodecanoate, sodium dodecyl sulfate and cetyltrimethylammonium bromide micelles. Although polarization of the methylene protons of the ketones was observed for each, sufficient resolution for quantitative measurement of the two methylene emission signals could not be obtained. The light and dark spectra obtained for **25a** in potassium dodecanoate are shown in Figure 12.

Despite this failure to exclude experimentally the

Figure 12. ^{1}H NMR spectrum of 4-methoxydibenzyl ketone in 0.08 M potassium dodecanoate in the dark (left) and during UV irradiation (right).

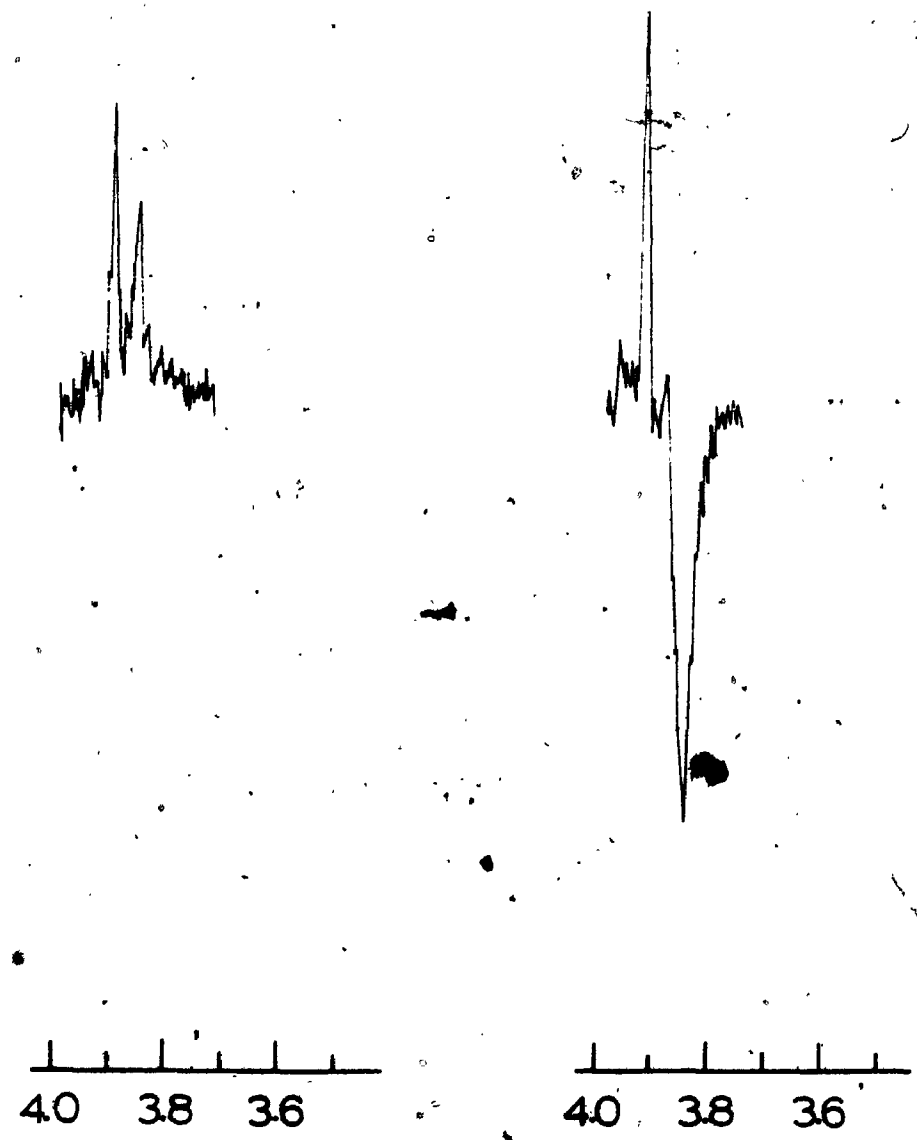
4.0
3.8
3.6
4.0
3.8
3.6

importance of decarbonylation, the original interpretation of the CIDNP results is favored for the following reasons. The measured lifetime of the phenylacetyl radical ($5-9 \times 10^{-6}$ s, depending on the solvent[73]) is considerably longer than the lifetime ($\sim 10^{-9}$ s) suggested for radical pairs in nonviscous solvents such as $CDCl_3$. The decarbonylation rate for substituted phenylacetyl radicals would have to be substantially greater than 10^5 s^{-1} to compete with diffusion and affect the relative concentrations of radical pairs A and B. Furthermore, it is generally believed that the quantum yield for dibenzyl formation is less than unity ($\Phi \sim 0.7$) because of efficient geminate recombination. If acyl radical decarbonylation were to compete effectively with recombination, the quantum yields would be expected to vary for different substituents; reported values are essentially the same.[65] This leads to the conclusion that the CIDNP nonequivalence of the methylene emission signals for substituted dibenzyl ketones is best explained by preferred cleavage of one of the benzyl-carbonyl bonds, as has been suggested previously for 25b.[95]

The CIDNP intensities for the substituted benzyl methylene protons relative to those of the unsubstituted benzyl group were used to estimate the relative rates of Type I cleavage of the substituted benzyl-carbonyl bonds. The relative rates obtained after correction of the intensities for variations in spin lattice relaxation times are listed in Table 13. The data were used to construct Hammett plots with σ^+,[98] σ[98] and $\sigma \cdot$[99] values, as shown in

Table 13. Relative rates of Type I reactions for substituted dibenzyl ketones.[a]

	k_X/k_H[b]	$\log(k_X/k_H)$	σ^+[c]	σ[c]	$\sigma\bullet$[d]
4-MeO	3.18	0.502	-0.78	-0.27	0.24
4-Me	1.53[e]	0.185	-0.31	-0.17	0.11
4-F	1.05	0.021	-0.07	0.06	-0.08
H	1	0	0	0	0
4-Cl	0.90	-0.045	0.11	0.23	0.12
3-Cl	0.52	-0.284	0.40	0.37	0.04

[a] Determined from the emission intensities which have been corrected for initial absorption intensities and spin-lattice relaxation times.

[b] Reproducible within ±5%.

[c] See reference 98.

[d] See reference 99.

[e] Hutton et al.[95] obtained 1.5.

Figure 13. A better fit was obtained with σ^+ values;

$\rho+ = -0.65$ correlation coefficient = 0.997

$\rho = -1.03$ correlation coefficient = 0.937

$\rho\cdot = 0.55$ correlation coefficient = 0.655 .

The negative $\rho+$ obtained for the σ^+ correlation implies a polar transition state which can be stabilized by electron-donating aromatic substituents. Similar correlations of free radical decomposition reactions with σ^+ have also been interpreted in terms of a transition state with ionic character. Lewis et al.[102a] have investigated the effect of nonconjugated aromatic substituents on the rate constants for deoxybenzoin α cleavage (39). The correlation with σ^+ ($\rho^+ = -1.1$) indicated the development of

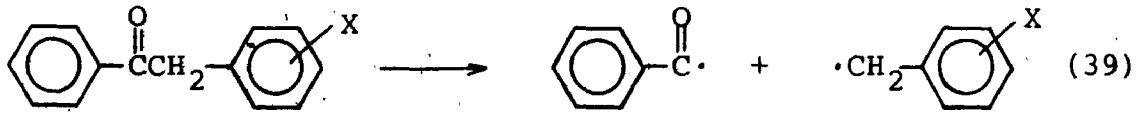

(39)

a partial positive charge at the α carbon. These authors have also observed that substituents at the α carbon in benzoin derivatives have a much more pronounced effect upon the rate of α cleavage[102b] than do substituents on the aromatic ring.

Walling and Clarke[103] have shown that the relative rates of alkoxy radical β-scission (40) also correlate with

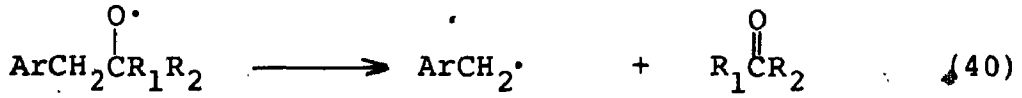

(40)

Figure 13. Hammett plot of log (k_x/k_H) versus substituent constant for α cleavage of substituted dibenzyl ketones: O, σ^+; ●, σ; □, $\sigma\cdot$.

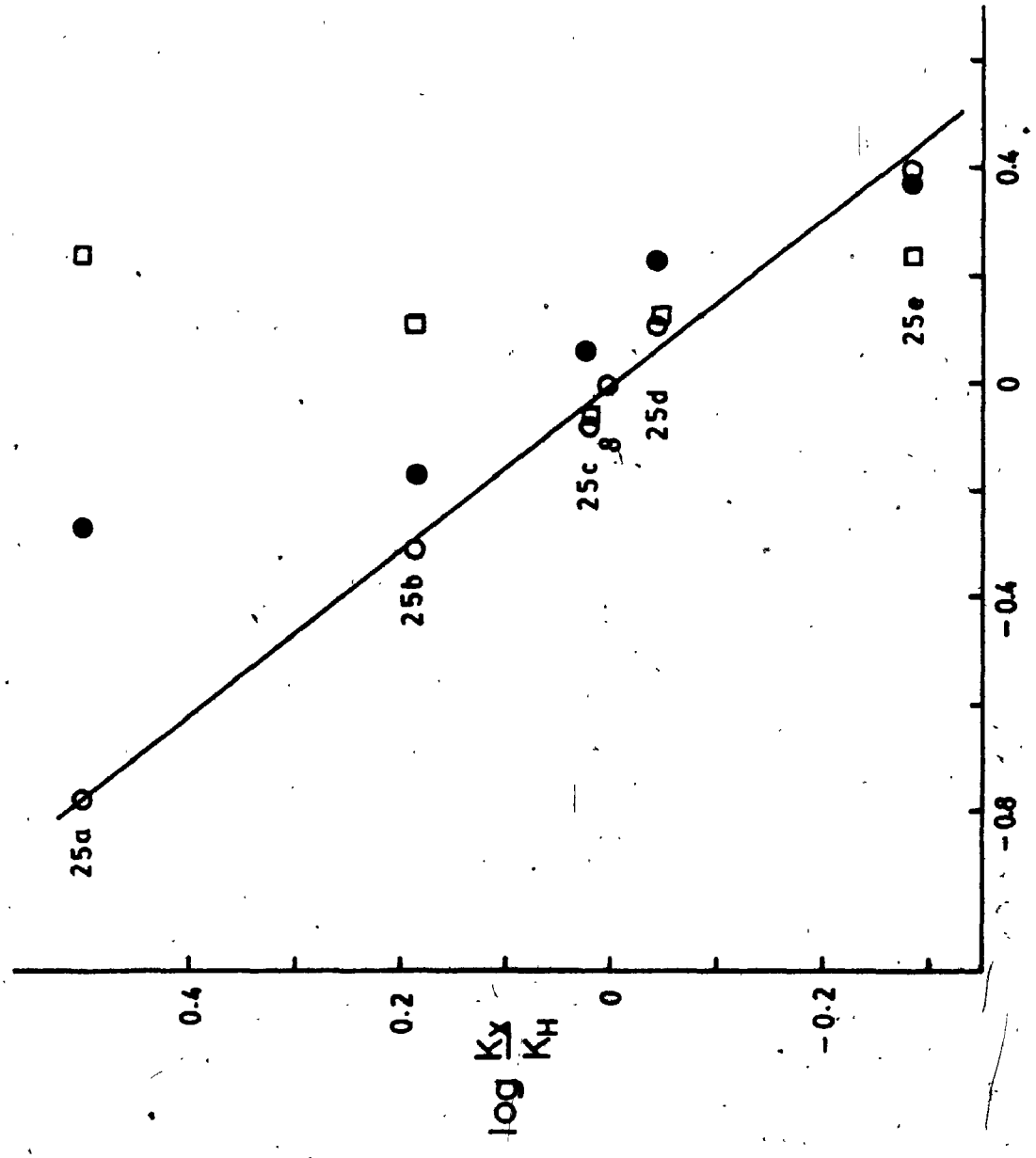
0.4
0.2
0
-0.2
log Kx/KH
25a
25b
25c
25d
25e
-0.8
-0.4
0
0.4
Substituent Constant

σ^+ ($\rho^+ = -1.\emptyset4$). The present results provide further support for the general parallel made between the α cleavages for alkoxy radicals and the n,π^* triplet states of ketones.[1Ø4]

The results for the α cleavage of dibenzyl ketones may be interpreted in terms of the development of partial ionic charge in the transition state, as shown below. The partial

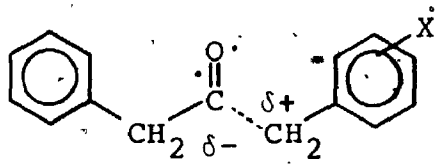

negative charge may be stabilized by the nonbonding orbital on oxygen and the partial positive charge by electron donating aromatic substituents. The smaller ρ^+ for this system may reflect the faster rate of homolysis as compared to those for alkoxy radicals and deoxybenzoins (~$1\emptyset^{1\emptyset}$ s^{-1} for dibenzyl ketones,[64,65] ~$1\emptyset^7$ s^{-1} for alkoxy radicals,[1Ø3] and ~$4 \times 1\emptyset^6$ s^{-1} for deoxybenzoins[1Ø5]).

CHAPTER 5

CYANOPROPYL RADICAL PAIRS

5.1 Introduction

Azobisisobutyronitrile, **28**, one of the most common and extensively studied free radical initiators, undergoes both thermal[106] and photochemical[107-110] homolysis to generate two cyanopropyl radicals and a nitrogen molecule (Scheme 5). In inert solvents the radicals either combine to yield tetramethylsuccinodinitrile, **29**, and dimethyl-N-(2-cyano-2-propyl) ketenimine, **30**, or disproportionate to produce isobutyronitrile, **31**, and methacrylonitrile, **32**. The symmetrical coupling product, **29**, arises from carbon-carbon coupling of two cyanopropyl radicals; carbon-nitrogen coupling gives the unsymmetrical product, **30**.

Thermolysis of **28** at 60-90°C in the absence of free radical scavengers yields approximately 60% **29**, 30% **30**, and 5-10% each of **31** and **32**.[106] At high conversions the yield of ketenimine **30** decreases substantially as a result of its thermal decomposition to **29** by a radical mechanism.[106b] The products result from cage as well as noncage processes for thermolysis of both the azo compound and the ketenimine.[106c]

The direct photolysis of **28** has been investigated by several groups.[29b,44,107-110] The reaction occurs efficiently ($\Phi \sim 0.45$ in benzene) to give product distributions[109a] (**29**, ~55%; **30**, ~40%; and **31** and **32**, ~5% each) which vary little with solvent or temperature.

Scheme 5

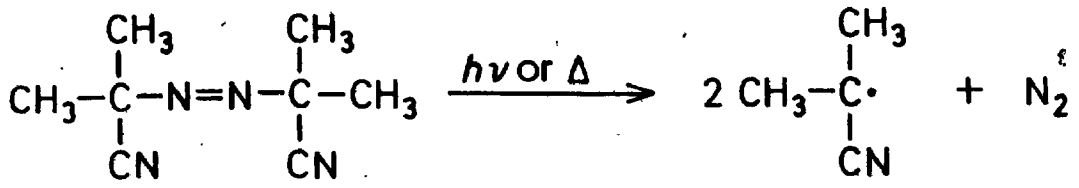

28

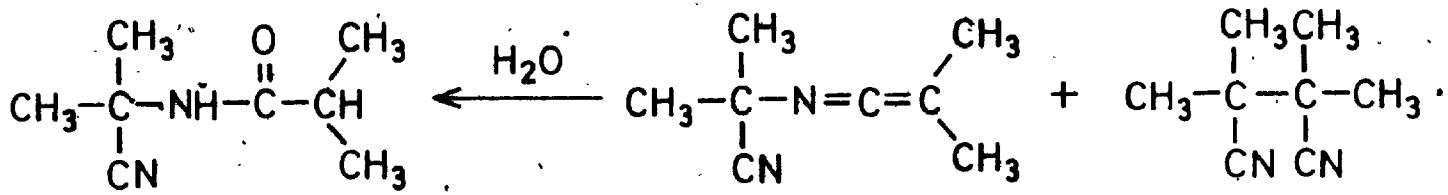

33 30 29

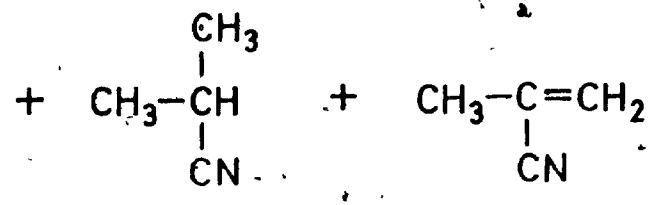

31 32

Photolysis of other tertiary azoalkanes has been shown to occur by isomerization to a thermally unstable cis azo compound which then decomposes.[111] However, McBride et al.[109a] have found no evidence for the formation of the cis azo isomer during low temperature irradiation of **28**. It is conceivable that the cis isomer is unstable even at the temperatures used;* nevertheless, the direct photochemical decomposition of **28** at present appears to provide a more reasonable explanation of the observations, since most cis azo compounds are detectable at low temperature and since some azoalkanes do undergo direct photochemical decomposition.

Engel et al. have shown that the photodecomposition of azobisisobutyronitrile can be sensitized with acetophenone (Φ = Ø.14), benzophenone (Φ = Ø.1Ø) and several other triplet sensitizers.[11Ø] Triplet sensitized photolysis was also observed for several other thermally labile azo compounds; for methyl azo-1,1-dimethyl-2-propene it was shown that triplet sensitized isomerization to a thermally labile cis isomer was not responsible for the photodecomposition. It remains to be demonstrated whether direct decomposition of a triplet state or photoisomerization to the cis isomer is occurring in the sensitized photolysis of **28** and other azoalkanes.

In contrast to results obtained in solution, McBride and coworkers[109] have observed that, in the photolysis of

---

* The temperature is not specified.[109a]

crystalline 28, disproportionation to give 31 and 32 accounts for from 70-95% of the radical reactions. Since much less disproportionation (~28%) occurred when 28 was photolyzed in a benzyl benzoate glass at -196°C, it seemed unlikely that the crystalline photolysis results were determined by the viscosity of the medium. Analysis of the crystal packing suggested the intervention of intermolecular dipolar interactions which could be used to explain qualitatively the observed behaviour. Photolysis of a variety of crystalline deuteriated samples showed that disproportionation occurred only for geminate radical pairs and was limited by the requirement that rotation about a C-C≡N axis occur to bring a methyl group into the proper orientation for hydrogen abstraction.

Leermakers et al.[29b,34] have investigated the photolysis of 28 in a silica gel-benzene slurry. They have claimed that only the symmetrical coupling product 29 was formed; a 90% isolated yield of 29 was reported for a preparative scale irradiation. Furthermore, although the disappearance of the azo compound during its photolysis in a slurry could be followed spectroscopically, no evidence for the formation of ketenimine 30, which absorbs strongly at 290 nm, was observed. The difference between the solution and slurry results was attributed to the nature of the binding between the radicals and the silica gel surface. The authors claimed that the cyano groups were bound to the surface's active sites and that, as a result, the cyanopropyl radicals were unable to rotate and recombine at

the nitrogen centre, as in solution. Consequently, the unsymmetrical coupling product was not formed and carbon-carbon coupling of the radicals to produce 29 was the only available pathway.

The above facts and interpretation appear to have been generally accepted.[109,112] In view of the results presented in Chapters 1 and 2 for a variety of adsorbed radicals, it appeared unlikely that the silica gel surface could impose such severe restrictions upon the rotational mobility of the cyanopropyl radicals. Furthermore, for the ratio of 28 to silica gel used a considerable amount of the azo compound would be expected to remain in the solvent where it would react in the usual manner to produce both 29 and 30. The photolysis of 28 in silica gel-benzene slurries and on dry silica gel was, therefore, examined. The results obtained require revision of the earlier proposals.

5.2 Stability of Ketenimine 29 on Silica Gel

The stability of ketenimine 30 on silica gel was first examined to ensure that conversion of 30 to 29, either thermally or photochemically, would not be a complication in the photolysis of adsorbed 28. Firstly, silica gel was added to a 0.113 M benzene solution of 30 in a 1 mm cuvette. The ketenimine absorption at 290 nm decreased gradually, as shown in Figure 14, indicating that it was not stable in the silica gel-benzene slurry. Similarly, addition of silica gel to a cuvette containing a benzene solution of 28 which had been irradiated to produce a sizable concentration of 30

Figure 14. UV absorption spectra of azobisisobutyronitrile, 28, in benzene and ketenimine 30 in benzene and in a benzene-silica gel slurry.

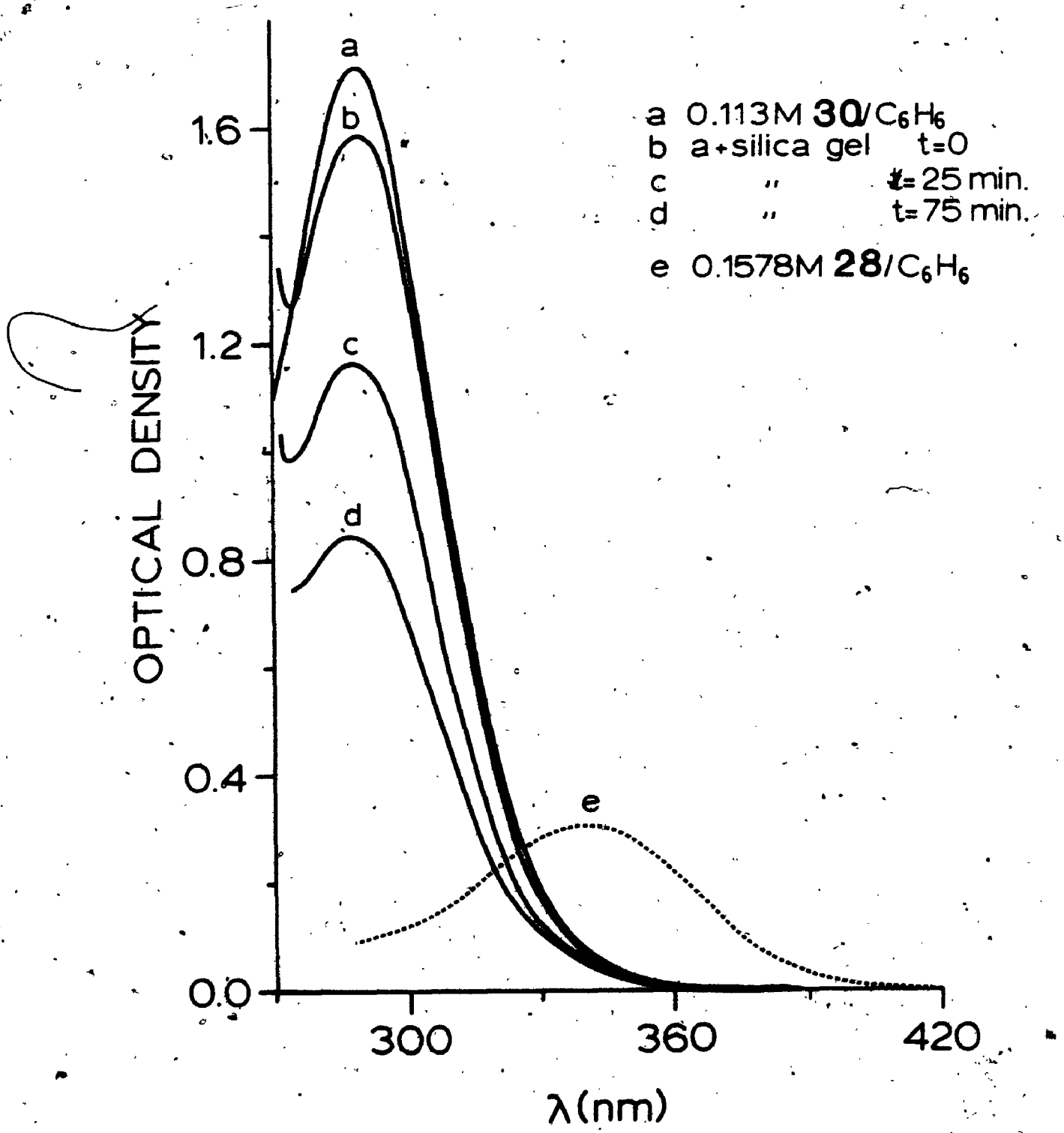
a 0.113M 30/C6H6
b a+silica gel t=0
c " t=25 min.
d " t=75 min.
e 0.1578M 28/C6H6
OPTICAL DENSITY
1.6
1.2
0.8
0.4
0.0
300
360
420
λ(nm)

resulted in a gradual decrease in the ketenimine absorption. Irradiation of 28 in a silica gel-benzene slurry showed only a small increase in absorption at 290 nm, although the absorption at 360 nm due to 28 decreased as expected. The spectrum did not change after leaving the sample in the dark for ~12 hours.

Preparative experiments were then carried out to determine what products were formed from 30 adsorbed on silica gel. Silica gel was added to a benzene solution of ketenimine and the resulting slurry was left in the dark at room temperature for 12 hours. The material extracted from the slurry was shown to be unchanged 30 (55%) and its hydrolysis product, N-(1-cyano-1-methylethyl)isobutyramide, 33 (45%), Scheme 5. An authentic specimen of this amide had been isolated previously from the thermolysis of 28 in water.[113] Substantial amounts of ketenimine hydrolysis were observed under various conditions; for example, on silica gel dried at 200°C before addition of 30 there was still >30% hydrolysis. In all cases the isolated amide accounted quantitatively for the amount of ketenimine decomposition.

Ketenimine 30 has been reported to be stable when irradiated in benzene through pyrex with a 450 W Hanovia lamp.[109] Its stability to irradiation in a silica gel-benzene slurry was examined to test for the formation of additional products under these conditions. After irradiation of 30 in a slurry for 4 hours, the material extracted was 27% amide and 70% ketenimine. No additional products were detected. Furthermore, the rate of

decomposition of 30 in a slurry was followed spectrophotometrically for two samples, one of which was kept in the dark while the second was irradiated (pyrex filter, 450 W mercury lamp). The ketenimine absorption for both decreased at approximately the same rate. These experiments indicated that irradiation of 30 gave no additional decomposition products and did not influence the rate of hydrolysis.

5.3 Photolysis of 28 in Silica Gel-Benzene Slurries

Irradiation of 28 in a silica gel-benzene slurry gave, contrary to earlier reports,[34] substantial amounts of the unsymmetrical coupling product, ketenimine 30, in addition to the amide derived from it, together with the dinitrile 29. In general, the sum of 30 and 33 represented ~50% of the isolated products (Table 14). These results were similar to those obtained for photolysis in solution except for the added complication of ketenimine hydrolysis. Analysis of the supernatant benzene layer showed that, prior to irradiation, a substantial amount (15-20%) of the azo compound was in the solvent. It is, therefore, probable that some photolysis occurred in the solvent phase. In any event, the silica gel clearly provides little restriction to the rotational motion of the cyanopropyl radicals.

The photolysis of 28 in a slurry under a variety of conditions was undertaken to determine whether or not the incompatibility of the present results with those obtained previously was caused by changes in the inadequately

Table 14. Photolysis of 28 in silica gel-benzene slurries.

Conditons[a,b]	Temperature (°C)	Product Distribution (mole %) 29	30	33
A,C	20	43	16	41
A,C	20	48	13	38
A,C	40[c]	57	2	43
A,D	20	50	13	37
B,C	20	55	14	30
B,C	52[c]	58	--	52
B,D	20	59	34	7
A,F,D	10	62	--	38
A,F,E	10	66	--	33

[a] Slurry concentrations were 0.281 mmol 28/g silica gel/2.0 mL benzene.

[b] A, medium pressure Hanovia Hg lamp
B, high pressure Hg lamp (shorter irradiation time)
C, Corning 7-60 filter (λ > 330 nm)
D, Pyrex filter
E, quartz filter
F, immersion well.

[c] <5% dark decomposition of 28 to 29 occurred under these conditions.

reported experimental procedure.[34] The data presented in Table 14 show that, except for variations in the amount of hydrolysis of **30**, similar product ratios were obtained in all cases. Changes in light intensity (high pressure versus medium pressure mercury lamp), irradiation temperature variations or the use of a Pyrex instead of a 330 nm cut-off filter had little effect. Two large scale photolyses of **28** in silica gel-benzene slurries in an immersion well, using either a Pyrex or quartz filter, both yielded substantial amounts of amide **33**. It was, therefore, concluded that the earlier observation[34] that restrictions to the rotational motion of adsorbed cyanopropyl radicals prevented the formation of ketenimine **30** was in error; the unsymmetrical ketenimine was formed upon photolysis of **28** in a slurry and was partially hydrolyzed to the corresponding amide on the silica gel surface. The product ratios indicate that the surface does not restrict the rotational movement of the radicals to a much greater extent than does a solvent cage.

5.4 Photolysis of 28 on Silica Gel

Samples of **28** adsorbed on dry silica gel at two coverages (25% and 5%, by calculation) were irradiated. The product distribution (Table 15) was qualitatively similar to that obtained in the slurry experiments with some hydrolysis of **30** again observed. However, the normal isolation procedure used in these and the previous experiments would have resulted in the loss of volatile compounds such as **31** and **32**. A specific search for these among the products from

Table 15. Photolysis of 28 on silica gel.[a]

Coverage[b]	Product Distribution (mole %)[c]		
	29	30	33
0.403 mmol/g	53	16	31
0.403 mmol/g	58	13	29
0.0812 mmol/g	63	25	12
0.0812 mmol/g	73	9	17

[a] Medium pressure Hanovia Hg lamp, Corning 7-60 filter (λ > 330 nm), 10°C; silica gel was not dried before use.

[b] 25% and 5%, by calculation.

[c] Product distribution based upon isolated material. Mass balances based on recovered, unphotolysed 28 were typically 85-90%.

irradiation of 28 on dry silica gel at 25% coverage showed the presence of ~5% 31. The similarity of the surface product ratios to those in solution and their difference from the results obtained for crystalline 28 indicate that restrictions to rotational motion on silica gel are not severe.

5.5 Geminate Recombination of Cyanopropyl Radicals

Translational movement of cyanopropyl radicals on the silica gel surface could be demonstrated by measuring the amount of nongeminate radical combination. The fraction of nongeminate combination could be determined from the product ratios from photolysis of either an unsymmetrical azo compound or a mixture of two azoalkanes. The latter approach was used here; equimolar mixtures of deuteriated and undeuteriated azobisisobutyronitrile were photolyzed and the deuterium content of the products was measured by mass spectrometry. If only geminate radical recombination occurred, then only R_H-R_H and R_D-R_D coupling products would result. Conversely, complete nongeminate combination would lead to free R_H· and R_D· which would yield a statistical mixture (1:2:1) of R_H-R_H, R_H-R_D and R_D-R_D. The presence of partially deuteriated products would demonstrate that some translational radical motion had occurred.

The demonstration of translational motion of adsorbed radicals using the above approach requires that the partially deuteriated products do not result from simultaneous photolysis of adjacent azoalkane molecules.

The intensity of the lamp used for irradiation of adsorbed 28 was such that the probability of a photon striking an adjacent molecule during the lifetime of a·cyanopropyl radical pair was negligible (<<1%). It may, therefore, be concluded that photolysis of nearest neighbours was not a complication in these experiments.

Deuteriated azobisisobutyronitrile was prepared from acetone-d_6;[109] equimolar mixtures of 28-d_0 and 28-d_{12} were then photolyzed. The symmetrical coupling product, 29, did not yield a measurable molecular ion peak and was, therefore, unsuitable for mass spectral deuterium analysis. The unsymmetrical ketenimine, 30, also gave a weak molecular ion and was difficult to separate from other products because of its propensity for hydrolysis and thermal decomposition. Consequently, the amide derived from 30 was separated from unreacted 28 and the other products and its deuterium content determined by mass spectral analysis (M^+ ~ 20% intensity).

A mixture of 28-d_0 and 28-d_{12} was first photolyzed in benzene so that the amount of geminate recombination in solution could be compared to that on the silica gel surface. The mass spectral molecular ion intensities at m/e 154 (33-d_0), 160 (33-d_6) and 166 (33-d_{12}) were obtained in the ratio of 65.1:41.4:100. This result clearly demonstrated that a substantial number of cyanopropyl radicals did not recombine with their original geminate radical partners in solution. However, the rather large discrepancy between the amount of 33-d_0 and 33-d_{12} was

unexpected; one possible interpretation was that an isotope effect on the mass spectral fragmentation was at least partially responsible.

To test for such a possibility, the deuteriated amide was prepared by hydrolysis of ketenimine formed from photolysis of 28-d_{12}. The mass spectral molecular ion intensities were then measured for an equimolar mixture of 33-dØ and 33-d_{12}. The ratio of 74.7:100.0 obtained (average of 3 determinations, 2Ø eV) indicated that there was indeed a substantial isotope effect on the mass spectral fragmentation for amide 33. Although this corresponds to a total isotope effect of $(k_H/k_D)_T = 1.34$, the effect per atom is small, $(k_H/k_D)_T^{1/12} = 1.02$. Similar secondary deuterium isotope effects have been reported for mass spectral fragmentations of, for example, the oxetane 34 molecular ion[114] (k_H/k_D = 1.03 per atom at 2Ø eV) and the enolic acetone ion, 35[115] (k_H/k_D = 1.1Ø per atom).

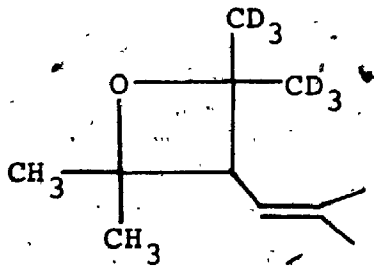

34

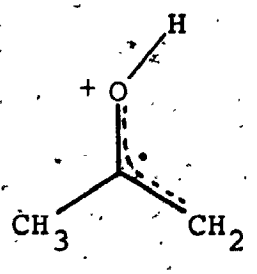

35

All mass spectral deuterium analysis data were corrected for the observed isotope effect so that the intensities could be related to the relative amounts of 33, 33-d_6 and 33-d_{12}. The corrected intensities, I'_{154} and

I'_{160}, were obtained using equations 41 and 42, respectively, where I_{154} and I_{160} are the mass spectral molecular ion intensities.

$$I'_{154} = \left(\frac{k_H}{k_D}\right)_T I_{154} \qquad (41)$$

$$I'_{160} \doteq \left[\left(\frac{k_H}{k_D}\right)^{1/12}\right]^6 I_{160} \qquad (42)$$

For photolysis of the equimolar mixture of 28 and 28-d_{12} in benzene the ratio of intensities at 154, 160 and 166 after correction was 84.7:47.2:100 (Table 16). A substantial number of radicals escape geminate recombination under these conditions.

Equimolar mixtures of 28-d_0 and 28-d_{12} were photolyzed on silica gel at two coverages (25% and 5%). The corrected mass spectral peak intensities for the amide recovered after photolysis are listed in Table 16. The amount of partially deuteriated amide formed by nongeminate radical combination decreased considerably from that obtained in benzene. For example, at 25% coverage the average ratio of 33-d_0:33-d_6:33-d_{12} was 81.5:15.7:100; changing the coverage to 5% had little effect on the amide ratios. Mixtures of deuteriated and undeuteriated azo compound were also photolyzed in silica gel benzene slurries. The fraction of amide 33-d_6 increased slightly from that on dry silica, but was still much lower than in benzene. This increase in escape from the original geminate partner was most likely caused by some

Table 16. Mass spectral peak intensities for amide 33 from the direct photolysis of equimolar mixtures of 28 and 28-d_{12}.

Conditions[a]	Intensities[b] 154	160	166
Benzene	84.7	47.2	100
Silica gel, 25% Coverage[c]	82.6	11.5	100
Silica gel, 25% Coverage	89.7	18.7	100
Silica gel, 25% Coverage	74.9	17.1	100
Silica gel, 25% Coverage	76.0	14.2	100
Silica gel, 25% Coverage	84.5	17.0	100
Silica gel, 5% Coverage[d]	83.0	15.8	100
Silica gel, 5% Coverage	88.6	16.2	100
Silica gel-Benzene Slurry[e]	90.9	23.0	100
Silica gel-Benzene Slurry	91.5	27.5	100

[a] Photolysis: 450 W Hanovia medium pressure mercury lamp, Corning 7-60 filter (330 nm cut off); 45-80% conversion; silica gel was not dried.

[b] Corrected for the secondary isotope effect on the mass spectral fragmentation. Error limits, ±0.5 → 0.8.

[c] 0.403 mmol/g

[d] 0.0812 mmol/g

[e] 0.397 mmol/g

photolysis in the solvent phase for the slurry experiments; however, the similar amounts of 33-d_6 formed on dry silica and in a slurry suggested that, for the latter, most of the photolysis had occurred for adsorbed molecules.

The above results may be more easily compared with each other and with other work by calculating the fraction of geminate recombination, β, using equation 43. The corrected

$$\beta = 1 - \frac{2[33\text{-}d_6]}{[33\text{-}d_0]+[33\text{-}d_6]+[33\text{-}d_{12}]} \qquad (43)$$

mass spectral peak intensities at 154, 160 and 166 are used to obtain [33-d_0], [33-d_6], and [33-d_{12}], respectively. β is defined as one minus the fraction of products formed by escape from the original geminate partner. Values of β in benzene, on silica gel and in silica gel-benzene slurries are listed in Table 17.

For photolysis in benzene the β value of 0.59 agrees well with the cage effect of 0.61 reported previously for photolysis of a similar azo compound, azobis-3-(methyl-1-butene).[110] For photolysis on dry silica gel and in silica gel-benzene slurries the substantially higher β values of 0.84 and 0.76 indicate that fewer radicals escape from their original partners before recombining. The silica gel surface must, therefore, restrict the translational motion of cyanopropyl radicals to a greater extent than it does their rotational movement. Nevertheless, ~15% of the radicals have sufficient mobility to escape from their original geminate partners. There is no evidence for

Table 17. Fraction of geminate recombination, β, for photolysis of 28.

Conditions[a]	β	βcorr[b]
Benzene, A	Ø.59	-
Benzene + sensitizer, B	Ø.13	Ø.1Ø
Benzene + sensitizer, B	Ø.19	Ø.16
Silica gel, 25% coverage[c], B	Ø.84	-
Silica gel, 5% coverage[d], B	Ø.84	-
Silica gel + sensitizer, B	Ø.31	-
Silica gel + sensitizer, B	Ø.31	-
Silica gel + sensitizer, C	Ø.78	-

[a] 45Ø W Hanovia medium pressure Hg lamp; silica gel was not dried before use;
A, Corning 7-6Ø filter (λ > 33Ø nm)
B, $NiSØ_4$ and $K_2CrØ_4$ filters
C, Corning 5-6Ø filter (λ > 355 nm).

[b] Corrected for direct photolysis.

[c] Average of 5 determinations.

[d] Average of 2 determinations.

restriction to radical movement by molecules of azobisisobutyronitrile since the β values are identical over the coverage range used.

5.6 Triplet Sensitized Photolysis of 28

A variety of triplet sensitizers have been shown to sensitize the photodecomposition of 28.[110] It was expected that substantial decreases in the fraction of geminate recombination would be observed for the sensitized photolysis on silica gel and in benzene if, as has been suggested, direct decomposition of a triplet state occurs for the sensitized photolysis of azo compounds. Decreases in the cage effect have been previously observed by Engel for the sensitized photolysis of azobis-3-(methyl-1-butene).[110]

Benzophenone was used as the sensitizer for the silica gel reactions because it has a moderate quantum yield for sensitization (Φ = 0.10) in solution and is less volatile than some of the other sensitizers which could have been used (e.g., acetophenone, Φ = 0.14). Before attempting the sensitized photolysis on the surface, both 28 and an equimolar mixture of 28-d$_0$ and 28-d$_{12}$ were photolyzed in benzene in the presence of benzophenone. Conditions were chosen so as to reproduce as closely as possible the previous triplet sensitization experiment with 28 and benzophenone.[110] The product ratios from 28 in the sensitized experiment were similar to those for the direct photolysis. For the mixture of 28-d$_0$ and 28-d$_{12}$ the mass

Table 18. Mass spectral peak intensities for amide 33 from the triplet sensitized photolysis of equimolar mixtures of 28 and 28-d_{12}.

Conditions[a]	Intensities[b]		
	154	160	166
Benzene, B[c]	143	186	100
Benzene, B	145	166	100
Silica Gel, B[d]	129	120	100
Silica Gel, B	121	116	100
Silica Gel, C	106	25	100

[a] 450 W Hanovia medium pressre Hg lamp; silica gel was not dried before use;
B, $NiSO_4$ and K_2CrO_4 filters
C, Corning 5-60 filter (λ > 355 nm).

[b] Corrected for the secondary isotope effect on the mass spectral fragmentation.

[c] 0.0314 M 28, 0.124 M benzophenone.

[d] 0.117 mmol 28/g, 0.441 mmol benzophenone/g.

spectral molecular ion intensities were as shown in Table 18. In one experiment the intensity ratio of 145:165:100 for the peaks at 154, 160 and 166 indicated a dramatic increase, relative to direct photolysis, in the amount of product formed by escape from the solvent cage. A β value of 0.19 may be calculated from the data (Table 17) but this must be corrected for the amount of direct photolysis which occurs. The correction may be done by considering the relative amounts of light absorbed by 28 and benzophenone at the irradiation wavelength and the quantum yields for direct and sensitized photolysis (0.45 and 0.10,[110] respectively), as outlined in 6.4. The corrected β value (0.13, average) shows that, for the triplet reaction, only ~13% of the radicals recombine in the solvent cage. Similar values (0.07-0.13, depending on the sensitizer) were obtained previously for the cage effect for the sensitized photolysis of azobis-3-(methyl-1-butene).[110]

The results obtained provide support for the proposed[110] direct decomposition of triplet azo compounds in the sensitized photolysis of 28 and other azoalkanes. If triplet sensitized isomerization to an unstable cis isomer which decomposed thermally were occurring, the amount of cage recombination would be expected to be similar to that obtained by direct photolysis; i.e., thermal decomposition of the cis isomer would generate a singlet radical pair as would direct photolysis (regardless of whether the latter process proceeds via direct decomposition of a singlet or via isomerization to a thermally labile cis isomer). The

different cage effects for direct and sensitized photolysis are, thus, attributed to the generation of radical pairs of different multiplicities in the two processes. The triplet pair must intersystem cross before it can recombine and, as a result, more of the radicals escape from the solvent cage for a triplet than for a singlet radical pair.

For the sensitized photolysis of 28 on silica gel the benzophenone and azo compound coverages were 34% and 7%, respectively (by calculation). The recovered amide contained a much larger amount of the partially deuteriated material than had been obtained for direct irradiation. For example, a ratio of 129:120:100 was obtained in one experiment, giving a β value of 0,31. Again, as for solution, some decomposition is expected to result from the direct photolysis of 28. However, the β values could not be corrected for direct photolysis on the surface since neither the extinction coefficients for 28 and benzophenone nor the relative quantum yields for the direct and sensitized processes under these conditions were known. The extinction coefficients and the direct quantum yields on the surface could probably have been determined with reasonable accuracy; however, there is presently no available technique for the measurement of surface quantum yields under the degassed conditions required for the determination of sensitized quantum yields. In any case, the results, even without correction, demonstrate that a large number of radicals recombine with other than their original partners in the triplet reaction. Correction for direct singlet

photolysis would only further increase the number.

It is tempting to attribute the difference between the direct and sensitized experiments on the surface to the multiplicity difference in the radical pairs formed by the two pathways. A singlet radical pair formed by direct photolysis would be less likely to diffuse apart before recombining than would a triplet pair generated by sensitization, since the latter must intersystem cross before it can recombine. Nevertheless, the possibility that the effects could be caused by the benzophenone acting as a surface additive rather than, or in addition to, a sensitizer should also be considered. For example, if the sensitizer occupied strong adsorption sites on which the azo compound would otherwise be adsorbed, then the cyanopropyl radicals would be more translationally mobile and a smaller amount of geminate recombination would result than in the absence of benzophenone. Similar effects of surface additives have been observed previously.[44]

To test for the above possibility, a sample of benzophenone and 28-dØ plus 28-d_{12} on silica gel was photolyzed at (primarily) 366 nm in air. At this wavelength most of the light is absorbed by 28 and in the presence of oxygen at least some of any benzophenone triplets formed should be quenched before energy transfer to 28 could occur. The recovered amide showed peaks at m/e 154, 160 and 166 in a ratio of 106:26:100 (Table 18); a β value of Ø.78 was calculated. This β value is only slightly lower than the value of Ø.84 obtained by direct photolysis. The difference

may result from some sensitized photolysis in this experiment. Alternatively, it may be derived from some effect of benzophenone as an additive. In any event, the results demonstrate that the primary role of benzophenone on the silica gel surface is that of a sensitizer. It may be concluded that the increased amount of geminate recombination in the presence of benzophenone reflects the triplet nature of the cyanopropyl radical pair. As observed previously for benzyl radicals, translational motion on the surface competes much more effectively with recombination for a triplet rather than for a singlet radical pair precursor.

For both the singlet and triplet reactions in benzene and on the silica gel surface nonequivalent amide-d_0:amide-d_{12} ratios were always obtained. Furthermore, the amount of 33-d_{12} was greater than that of 33-d_0 for the direct irradiations whereas the opposite trend was observed for the sensitized experiments. These effects may be a reflection of the larger hyperfine interaction in the nondeuteriated cyanopropyl radicals; d_0 radicals undergo more rapid hyperfine coupling induced intersystem crossing than do d_6 radicals. As a result, a singlet radical pair generated from 28-d_0 will intersystem cross more quickly to a triplet pair and will have a greater probability of diffusing apart than will a pair generated from 28-d_{12}. The opposite will occur for triplet radical pairs; a nondeuteriated radical will recombine with its original partner more often than will a radical generated from 28-d_{12}. A greater percentage

of geminate recombination will, thus, occur for singlet d_6 radical pairs than for singlet d_0 pairs; for triplet pairs, geminate recombination for d_0 pairs will be larger than for d_6 pairs.

The above explanation is consistent with the larger amounts of 33-d_{12} and 33-d_0 in the direct and sensitized experiments, respectively. However, it requires that there be a similar nonequivalence in the amounts of another deuteriated and nondeuteriated product. For example, there could be a difference in the ratios of carbon-carbon to carbon-nitrogen coupling for geminate and free radical recombination. If carbon-carbon coupling were increased for free radicals then, for the singlet reaction, the 29-d_0/29-d_{12} ratio should be >1 since there are more free R-d_0 radicals. Alternatively, the probability of disproportionation to yield 31 and 32 could be different for geminate and free radical recombinaton. The ~5% disproportionation observed both in solution and on silica gel for the singlet photolyses would be sufficient to account for the nonequivalent amide-d_0 and -d_{12} ratios in these experiments. The amounts of disproportionation in the sensitized reactions have not been determined. A small amount of an undetected product could also be important in either the cage or escape radical processes (mass balances on silica gel are typically ~90%). For example, the radicals which escape from their original partners may have new reaction pathways, such as reaction with a hydrogen

donor, available to them.

The possibility that a secondary isotope effect on the rate of ketenimine hydrolysis is responsible for the observed effects is unlikely since essentially complete ketenimine hydrolysis was observed for the deuterium experiments. Furthermore, such an isotope effect does not explain the difference between the singlet and triplet reaction.

Additional experiments are required to distinguish among the above possibilities. The differences in hyperfine induced intersystem crossing rates for d_0 and d_6 radicals, and the resulting variation in the amount of escape from the geminate pair, appears to provide a reasonable explanation for the available data.

CHAPTER 6

EXPERIMENTAL

6.1 General

6.1.1 Spectra:

Ultraviolet and visible spectra were recorded on either a Varian Cary 219 or 118 spectrophotometer using 1 cm or 1 mm quartz cuvettes.

Routine nuclear magnetic resonance spectra were recorded on a Varian T-60 spectrometer using tetramethylsilane as the internal standard. For more precise measurements and for CIDNP experiments a Varian XL-100 instrument was used. All reported chemical shifts were measured on this instrument.

Mass spectra were recorded on a Varian MAT 311A mass spectrometer.

6.1.2 Melting Points:

Melting points were measured on a Reichert hot stage or a Gallenkamp capillary apparatus and are uncorrected.

6.1.3 Gas Chromatography:

Quantitative and qualitative chromatography were done on either a Varian 1200 or 2400 instrument, both of which were equipped with a flame ionization detector and temperature programmer. A 10% SE30 on Chromosorb W column (5'x1/4", glass) was used for all analyses except for the separation of 1-phenyl-2'-methylacetophenone from dibenzyl

ketone. A Carbowax column (5'x1/4") was used for the latter. The carrier gas was helium, flow rate 40 ml/min. Operating conditions were as follows: analysis of products from the photolysis of 4-methylbenzyl-4-methoxyphenyl acetate, 4-methyl-4'-methoxydibenzyl sulfone and all dibenzyl ketones: injector temperature, 225°C; column temperature, 170-210°C (depending on material analyzed); detector temperature, 250°; analysis of products from the photolysis of dibenzyl sulfone and benzyl α-toluenesulfinate: injector temperature, 190°C: column temperature 170°C for 20 minutes, 176°C for 25 minutes; detector temperature, 250°; 1-phenyl-2'-methylacetophenone: injector temperature, 225°C; column temperature, 170°C; detector temperature, 250°C.

6.1.4 Gas Chromatography-Mass Spectrometry:

Gas chromatography-mass spectrometry was done on a Varian 1400 gas chromatograph interfaced with a Varian MAT 311A mass spectrometer and a Varian data system. The gas chromatograph was equipped with a flame ionization detector and a 5'x1/4" 10% SE30 on chromosorb W column.

6.1.5 Irradiation Apparatus:

All photolyses were carried out with one of the following lamps: 150 W or 1000 W XBO high pressure xenon lamp in a Photochemical Research Associates lamp housing with an elliptical mirror for focusing purposes (infrared water filters were placed directly in front of the lamp housings); 450 W Hanovia medium pressure mercury lamp in a

pyrex or quartz water cooled immersion well; a 100 W high pressure mercury lamp with a water filter; or a Rayonet reactor equipped with either 254.7 nm or 300 nm lamps.

6.2 Materials

6.2.1 Solvents:

All solvents used for solution photolyses or for preparation of silica gel samples were Fischer spectrograde. Methylene chloride was dried by refluxing over phosphorus pentoxide and was distilled directly before use for adsorption of compounds onto dry silica gel. Cyclohexane, acetone, dioxane and hexane were dried over molecular sieves. 2-propanol was dried by refluxing over magnesium/iodine and was then distilled. Benzene was refluxed over lithium aluminum hydride and then distilled through a 6" column for use in the sensitized solution photolyses of azobisisobutyronitrile; for other purposes it was dried over molecular sieves. Methanol was not dried before use.

Deuteriochloroform for CIDNP experiments was dried over molecular sieves. Anhydrous ether (Fisher) was used as received or distilled from lithium aluminum hydride when dry ether was required. Water for micelle solutions was triply distilled (second distillation from potassium permanganate). All other solvents were reagent grade and were used as received.

6.2.2 Adsorbents:

Merck silica gel 60, 35-70 mesh, was used in all

experiments unless otherwise stated. This silica had a particle size range of Ø.2-Ø.5 mm and a surface area* of 560 m^2/g.

Dehydroxylated silica gel was prepared by heating the above silica slowly over a 6 hour period to 750°C and leaving it at that temperature for 48 hours at atmospheric pressure in an open container. The sample was then evacuated for 2 hours at ~Ø.1 torr and cooled slowly to room temperature while still under vacuum. The dehydroxylated silica gel was stored in a desiccator over phosphorus pentoxide until required and was dried (procedure B, 6.3.2) before a sample was adsorbed.

Silica gel, 5 μm particle size, was used as received.

Alumina, neutral (Fisher, Brockman Activity 1) was dried for 12 hours at 200°C, Ø.1 torr and stored in a desiccator before use.

6.2.3 Surfactants:

Potassium dodecanoate was prepared from dodecanoic acid and potassium hydroxide in methanol and was purified by recrystallization from methanol. The critical micelle concentration (CMC) was determined from a plot of conductivity versus surfactant concentration. The values obtained in the absence and presence of 4-methylbenzyl-4-methoxyphenyl acetate, Ø.Ø23Ø M and Ø.Ø225 M, respectively, indicated that the CMC was unaffected by dissolving the

---

*Determined by Dr. K. Okada[44] by the methanol adsorption method of Hoffman et al.[76]

ester in the micellar solution. The results agreed well with the literature value of 0.024 M for the CMC of potassium dodecanoate.[116]

Sodium dodecyl sulfate and cetyl trimethyl ammonium bromide were used as received.

6.2.4 Commercially available compounds:

Dibenzyl ketone: Dibenzyl ketone (ICN pharmaceutical) was recrystallized from petroleum ether (40-60°) or from ether (at -78°): m.p. 30.5-32°C. It was stored in the dark in a dessicator at ~0°C.

Dibenzyl Sulfone: Dibenzyl sulfone (Fairfield Chemical Company) as received contained a considerable amount of dibenzyl sulfoxide. The mixture was oxidizd with 3-chloroperbenzoic acid and the sulfone obtained recrystallized three times from 95% ethanol to give white plates: m.p. 153-155°C (literature,[117] 155°C).

Pinacol: Pinacol (Aldrich Chemical Company) was dried before use by the following procedure. Two separate 15 ml portions of benzene were added to 5 g pinacol and the benzene was removed by distillation. Calcium hydride was then added to the pinacol, the mixture was heated at 100°C for 4 hours and the pinacol was distilled under reduced pressure, the second fraction being used for all silica gel experiments.

Cyclohexanediol: Cyclohexanediol (Aldrich) was a mixture of cis and trans isomers and was recrystallized twice from acetone.

Decanol: Decanol was distilled before use.

Azobisisobutyronitrile: Azobisisobutyronitrile was recrystallized several times from absolute ethanol at temperatures not exceeding 50°C and was stored at 0°C in the dark: m.p. 101.5-102.5°C (literature,[107] 101-102°C); NMR (δ, $CDCl_3$; C_6D_6) 1.72 (s); 1.16 (s).

Benzophenone: Benzophenone was recrystallized twice from hexane.

6.2.5 Compounds synthesized:

4-Methylbenzyl-4-methoxyphenyl acetate (12): The following literature procedure[68b] for the preparation of ester 12 was used.

4-Methylbenzyl alcohol (5.003 g; 0.041 mol), 4-methoxyphenylacetic acid (6.807 g; 0.041 mol) and 138 mg of 4-toluenesulfonic acid were refluxed for 6 hours in 35 ml benzene with removal of water by azeotropic distillation using a Dean-Stark apparatus. The mixture was washed with aqueous Na_2CO_3, the aqueous layer back extracted with benzene and the benzene layers dried over anhydrous magnesium sulfate. A 93% yield of a yellow oil was obtained. Crystallization from ether at -77°C gave pure 12 as white crystals: m.p. 31.5-32°C (literature,[68b] 32-32.5°C). The ester was stored in a desiccator at 0°C in the dark.

1-(4-methylphenyl)-3-(4-methoxyphenyl)-2-propanone (16): A general literature procedure[118] employed for the synthesis of other unsymmetrically substituted dibenzyl ketones was

used.

4-Methylbenzylmagnesium chloride was prepared by slowly adding, under a positive pressure of nitrogen, a solution of 11.2 g (0.08 mol) 4-methylbenzyl chloride in 20 ml anhydrous ether to 0.08 mol magnesium in 20 ml anhydrous ether. The addition was carried out at a rate sufficient to maintain a gentle reflux. After the addition was complete, the dark green solution of the Grignard reagent was refluxed for 10 minutes and then transferred from the residual magnesium through a glass wool plug into a second flask by means of a positive pressure of nitrogen. The solution was diluted to 120 ml with ether and cooled in an ice bath. Dry (heated 5 hours at 200°C under vacuum) cadmium chloride, 0.064 mole, was added with vigorous stirring over a 10-15 minute period and the resulting dark yellow mixture was stirred with cooling for 2 hours.

4-Methoxyphenylacetyl chloride was prepared by heating 0.04 mole of the corresponding acid with 2.1 molar equivalents of thionyl chloride at 40-50°C for one hour and then at ~90°C for an additional hour. The excess thionyl chloride was removed by distillation, followed by repeated distillations of benzene from the residue. A solution of the acid chloride in 3 volumes of dry ether was added to the cold cadmium reagent over a 5 minute period. The mixture was stirred in an ice bath for 8 hours and then hydrolyzed with 20% sulfuric acid and ice. The ether layer was separated and the aqueous phase was extracted twice with ether. The combined ether layers were washed with water and

then with 10% $NaHCO_3$ solution and left overnight without drying. The ether solution was extracted four times more with $NaHCO_3$ and the combined bicarbonate solutions were extracted twice with ether. The total ether extracts were then washed with water and dried. The product obtained after solvent removal was a yellow oil (10.1 g) which contained ~30% dibenzyl. The ketone was crystallized from ether at -77°C and then recrystallized several times to give white crystals: m.p. 48-49°C; NMR (δ, $CDCl_3$) 7.1-6.8 (m, 8H), 3.79 (s, 3H), 3.65 (s, 2H), 3.64 (s, 2H), 2.33 (s, 3H); UV (cyclohexane) λ_{max} 275 nm (ε 1575 M^{-1} cm^{-1}).

Monosubstituted Dibenzyl ketones, 25a, 25b, 25c, 25d, 25e:

The procedure outlined above for 16 was used to synthesize 25a, 25b, 25c, 25d and 25e (all known compounds) from the appropriately substituted benzyl chloride and phenylacetyl chloride. Physical data are listed below. The preparation of 1-phenyl-3-(4-trifluoromethylphenyl)-2-propanone was also attempted using this procedure but difficulties in preparing the 4-trifluoromethylbenzyl magnesium chloride were encountered. Several attempts to synthesize the ketone by condensation of 4-trifluoromethylbenzyl cyanide and ethylphenylacetate[119] were also unsuccessful and the matter was not pursued any further.

1-(4-methylphenyl)-3-phenyl-2-propanone (25b): m.p. 31-32°C (literature,[118] 31-31.5°C); NMR (δ, $CDCl_3$) 7.34-6.98 (m, 9H), 3.70 (s, 2H), 3.67 (s, 2H), 2.31 (s, 3H).

1-(4-methoxyphenyl)-3-phenyl-2-propanone (25a): m.p. 46.5-

47.5°C (literature,[118] 47.5-48°C); NMR (δ, $CDCl_3$) 7.35-6.81 (m, 9H), 3.79 (s, 3H), 3.70 (s, 2H), 3.65 (s, 2H).

1-(4-chlorophenyl)-3-phenyl-2-propanone (25d): m.p. 40-41°C (literature,[118] 40.5-41°C); NMR (δ; $CDCl_3$) 7.36-7.00 (m, 9H) 3.72 (s, 2H), 3.68 (s, 2H).

1-(3-chlorophenyl)-3-phenyl-2-propanone (25e): m.p. 30-32°C (literature,[118] b.p. only given); NMR (δ, $CDCl_3$) 7.39-6.99 (m, 9H) 3.72 (s, 2H), 3.69 (s, 2H).

1-(4-fluorophenyl)-3-phenyl-2-propanone (25c): m.p. 35-36°C (literature,[118] 36-36.5°C); NMR (δ, $CDCl_3$) 7.33-6.97 (m, 9H) 3.71 (s, 2H), 3.68 (s, 2H).

1,3-Diphenyl-2-propanone-2-^{13}C: The labelled ketone was prepared by the method of Coan and Becker.[120]

^{13}C labelled phenylacetic acid (90% ^{13}C=0, Merck Sharp & Dohme) was esterified by refluxing 2.5 g (0.0182 mol) acid with 3.06 ml concentrated H_2SO_4 and 30 ml ethanol for four hours. This ester was used directly in the condensation with phenylacetonitrile. A mixture of the ester and 1.73 g (0.0148 mol) nitrile was added slowly (over ~50 minutes) with stirring to a refluxing sodium ethoxide solution (0.68 g sodium in 9 ml ethanol). After refluxing for four hours, the mixture was cooled and poured into 35 ml water. The aqueous layer was extracted with 3-12 ml portions of ether and the ether discarded. The aqueous layer was acidified with 10% hydrochloric acid and extracted with 3 additional 12 ml portions of ether. The ether solution was then extracted once with 6 ml water, twice with 12 ml portions of 10% $NaHCO_3$ and once with water.

The diphenylacetoacetonitrile obtained was decarboxylated by heating in 7.9 ml 60% sulfuric acid for 2 hours at 95°C followed by 24 hours at 105-108°C.‡ After cooling, the solution was poured into ice water and extracted three times with ether. The ether layers were washed as above. The product ketone was obtained as a red oil, overall yield ~60%. The crude material was purified by bulb to bulb distillation followed by two crystallizations from 40-60° petroleum ether: m.p. 32.5-33.5°C; NMR (δ, $CDCl_3$) 7.33-7.09 (m, 10H), 3.71 (s, $H_2C^{12}C{=}O$) superimposed with 3.71 (d, $H_2C^{13}C{=}O$; J (^{13}C,H), 6.2 Hz). The ratio of the satellite to the central peak integrals (9:1) was in agreement with the mass spectral determination of the carbonyl ^{13}C content.

4,4'-Methoxymethyldibenzyl sulfone (17):

A solution of 0.015 moles 4-methylbenzyl chloride in 20 ml ethanol was added dropwise to a refluxing solution of 0.015 moles 4-methoxybenzyl thiol and 0.020 moles potassium hydroxide (85%) in 100 ml ethanol. The solution was stirred for 30 minutes and then extracted three times with chloroform. The combined extracts were washed once with each of 25% potassium hydroxide, water and brine. The sulfide obtained as a yellow oil after solvent drying and removal was oxidized without further purification. Hydrogen peroxide (9.8 ml, 30%) was added dropwise to a solution of the sulfide in 86 ml 1:1 acetic acid/acetic anhydride. The

‡Higher temperatures gave large amounts of tarry material and little of the required ketone.

mixture was stirred for 90 hours at room temperature and then poured over 100 g ice. A white precipitate formed and was collected by filtration and washed with water. Recrystallization from ethanol gave white plates: m.p. 141-142°C; NMR (δ, $CDCl_3$) 7.33-6.86 (m, 8H), 4.07 (s, 2H), 4.05 (s, 2H), 3.81 (s, 3H), 2.36 (s, 3H); UV (ethanol) λ_{max} 274 nm (ε 1521 M^{-1} cm^{-1}); mass spectrum (70 eV) m/e (relative intensity) 290 (0.4), 226 (6), 121 (100).

1-phenyl-4'-methylacetophenone (20):

The ketone was prepared by Friedel Crafts acylation of toluene using phenylacetyl chloride and aluminum chloride and was purified by chromatography on silica gel (10% ether in hexane) followed by recrystallization from methanol to give white crystals: m.p. 108-109°C (literature,[121] 107.5°C); NMR (δ, $CDCl_3$) 7.95-7.19 (m, centred at 7.57, 4H), 7.28 (s, 5H), 4.24 (s, 2H), 2.39 (s, 3H).

1-phenyl-2'-methylacetophenone (21):

The ketone was prepared from benzyl chloride and 2-toluic acid using the procedure[118] outlined for substituted dibenzyl ketones but with the following modification. The mixture was stirred for only 2 hours in the ice bath after addition of the acid chloride and was then stirred for 2 hours at room temperature. The product was purified by flash chromatography on silica gel (3:2 benzene:hexane) to give a pale yellow oil:[122] mass spectrum (70 eV) m/e (relative intensity) 210 (1), 119 (99), 91 (100), 65 (83); NMR (δ, $CDCl_3$) 7.6-6.9 (m, 9H), 4.1 (s, 2H), 2.4 (s, 3H).

Benzyl-α-toluenesulfinate (22):

α-Toluenesulfonyl chloride was reduced using 2 equivalents of sodium sulfite[123] to α-toluenesulfinic acid which was converted directly to the α-toluenesulfinyl chloride using thionyl chloride. Condensation of the sulfinyl chloride (0.022 mol) with benzyl alcohol (0.02 mol) in the presence of pyridine (0.08 mol) gave the crude sulfinate in 61% yield. Recrystallization from hexane gave white plates: m.p. 49.5-50°C (literature,[124] 51-52°C); NMR (δ, $CDCl_3$) 7.3 (m, 8H), 5.06, 4.94 (s, 1H each, AB system, J = 11.8 Hz), 4.08, 4.01 (s, 1H each, AB system, J = 13.1).

Azobisisobutyronitrile-d_{12} (28-d_{12}): The literature procedure[125] for the preparation of the undeuterated material[109b] was used.

Acetone-d_6 (0.078 mol) was added slowly to a cooled solution of hydrazine sulfate (0.0437 mol) and sodium cyanide (0.0875 mol) in 56 ml D_2O. The mixture was stoppered and stirred in the dark for two days after which the white crystalline product was collected and washed with water. The product was then oxidized with bromine water. The deuterated azobisisobutyronitrile so obtained was recrystallized twice from absolute ethanol to give white needles: m.p. 107-108°C. The mass spectrum (97.8% d_6, 2.2% d_5) showed an atom % enrichment of 99.6%.

Tetramethylsuccinodinitrile (29):

The nitrile was prepared by thermolysis of 28 in benzene at ~85°C and was recrystallized from methanol: m.p. 169-170°C (literature,[107] 169°C); NMR (δ, $CDCl_3$; C_6D_6) 1.55

(s); 0.92 (s).

Dimethyl-N-(2-cyano-2-propyl) ketenimine (30):

The ketenimine was prepared by photolysis of 28 in benzene (medium pressure mercury lamp, Corning 7-60 filter). Removal of 29 was accomplished by precipitation from cyclohexane. The crude ketenimine was purified by repeated distillation (20-25°C, 0.01 torr): UV (benzene) λ_{max} 291, ε 151.5 M^{-1} cm^{-1} (literature,[108] 150.5); NMR (δ, $CDCl_3$; C_6D_6) 1.73 (s, 6H), 1.58 (s, 6H); 1.44 (s, 6H), 1.20 (s, 6H).

N-(1-cyano-1-methylethyl)isobutyramide (33):

The amide was prepared by hydrolysis of ketenimine 30 in a silica gel-benzene slurry and was purified by recrystallization from benzene: m.p. 106-107°C (literature,[113] 108°C); NMR (δ, $CDCl_3$; C_6D_6) 5.5 (s (broad), 1H), 2.36 (septet: J = 3.6 Hz, 1H), 1.70 (s, 6H), 1.20 (s, 3H), 1.13 (s, 3H); 4.6 (s (broad), 1H), 1.68 (septet: J = 3.5 Hz, 1H), 1.13 (s, 6H), 0.94 (s, 3H), 0.88 (s, 3H).

N-(1-cyano-1-methylethyl) isobutyramide-d_{12} (33-d_{12}):

The deuterated amide was prepared by hydrolysis of 30-d_{12} obtained from photolysis of 28-d_{12} and was recrystallized from benzene: m.p. 105-106°C.

6.3 Procedures for Silica Gel Experiments

6.3.1 Adsorption isotherms:

The same procedure was followed for the measurement of adsorption isotherms for ketone 16 and ester 12. Silica gel (dried at 200°C and stored in a desiccator over phosphorus pentoxide) samples (1.00 g) were placed in dry, stoppered 25

ml Erlermeyer flasks. Cyclohexane solutions of 12 (or 16) in the 0.09 M to 0.26 M concentration range were added and the slurries were equilibrated by stirring for 15 minutes. A 2.5 ml aliquot of the cyclohexane solution was then removed and diluted to an appropriate volume for UV analysis of the equilibrium substrate concentration in the cyclohexane. The amount of substrate required for complete monolayer coverage was determined by extrapolation from a plot of mmole adsorbed/gram silica gel against equilibrium solution concentration (Figures 3 and 4). Monolayer coverages for 12 and 16 were the same (0.9 mmol/g) within experimental error.

6.3.2 Drying procedures:

A number of silica gel drying techniques were investigated before a satisfactory method was found. Ester 12 and ketone 16 were the first adsorbed molecules to be investigated and the results for these molecules were found to vary considerably (but never reproducibly) with the method used to dry the silica gel before sample adsorption. It was necessary to dry the silica and then adsorb the substrate without reexposing the sample to the atmosphere at any time in order to obtain reasonable material balances and reproducible product ratios. A number of attempts to determine the reason for the low (10-20%) dibenzyl product recovery and irreproducible ratios for photolysis of 12 or 16 on wet silica gel were unsuccessful. Additional products were not found in sufficient amounts to account for the

missing material.

This sensitivity to the silica drying procedure was not observed for photolyses of other molecules examined. For example, mass balances in excess of 90% were obtained when dibenzyl ketone was photolyzed on silica gel regardless of the surface water content. Since the problem was only evident for 12 and 16 the matter was not pursued any further after a satisfactory drying procedure was developed. The three silica gel pretreatment procedures used are outlined below.

A. Silica gel was dried at 200°C at <1 torr for 24 hours. The samples were then cooled and placed in small tightly closed containers which were stored in a desiccator over phosphorus pentoxide. Silica gel dried in this manner rapidly picked up moisture upon exposure to the air during weighing and transferring and gave irreproducible results when used for photolysis of 12 and 16. It is unlikely that this method produces silica gel which is any drier than that which is not dried since the uptake of water occurs quite rapidly. Therefore, this procedure had no advantage over the use of undried silica and was used only in the initial investigations and for adsorption isotherm measurements.

B. Silica gel samples were dried immediately before each experiment and were not exposed to the atmosphere again during sample preparation. This was accomplished by heating a preweighed silica sample at 200°C at ~1 torr for >5 hours in compartment A of the cell shown in Figure 15. After heating, the sample was cooled under vacuum and stopcocks D

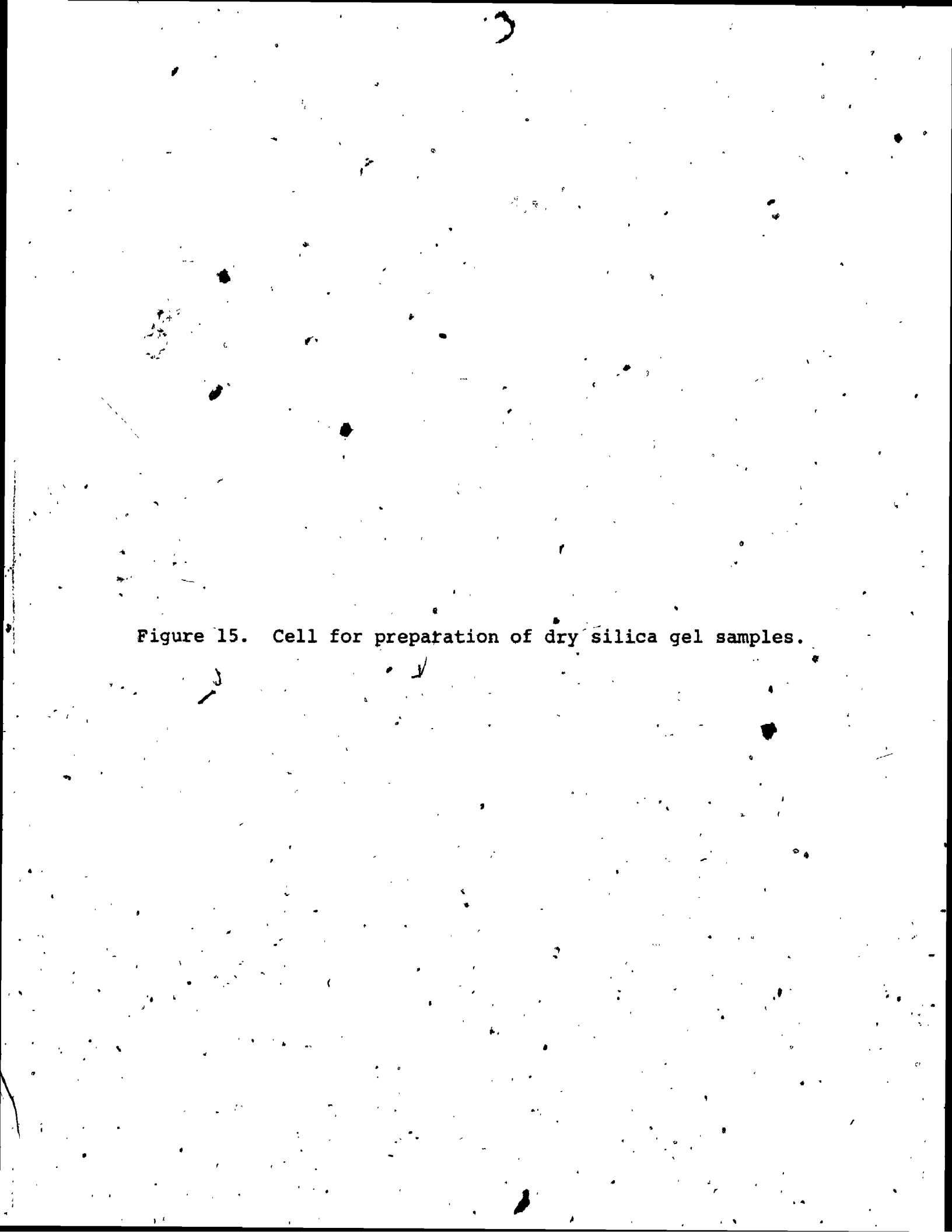

Figure 15. Cell for preparation of dry silica gel samples.

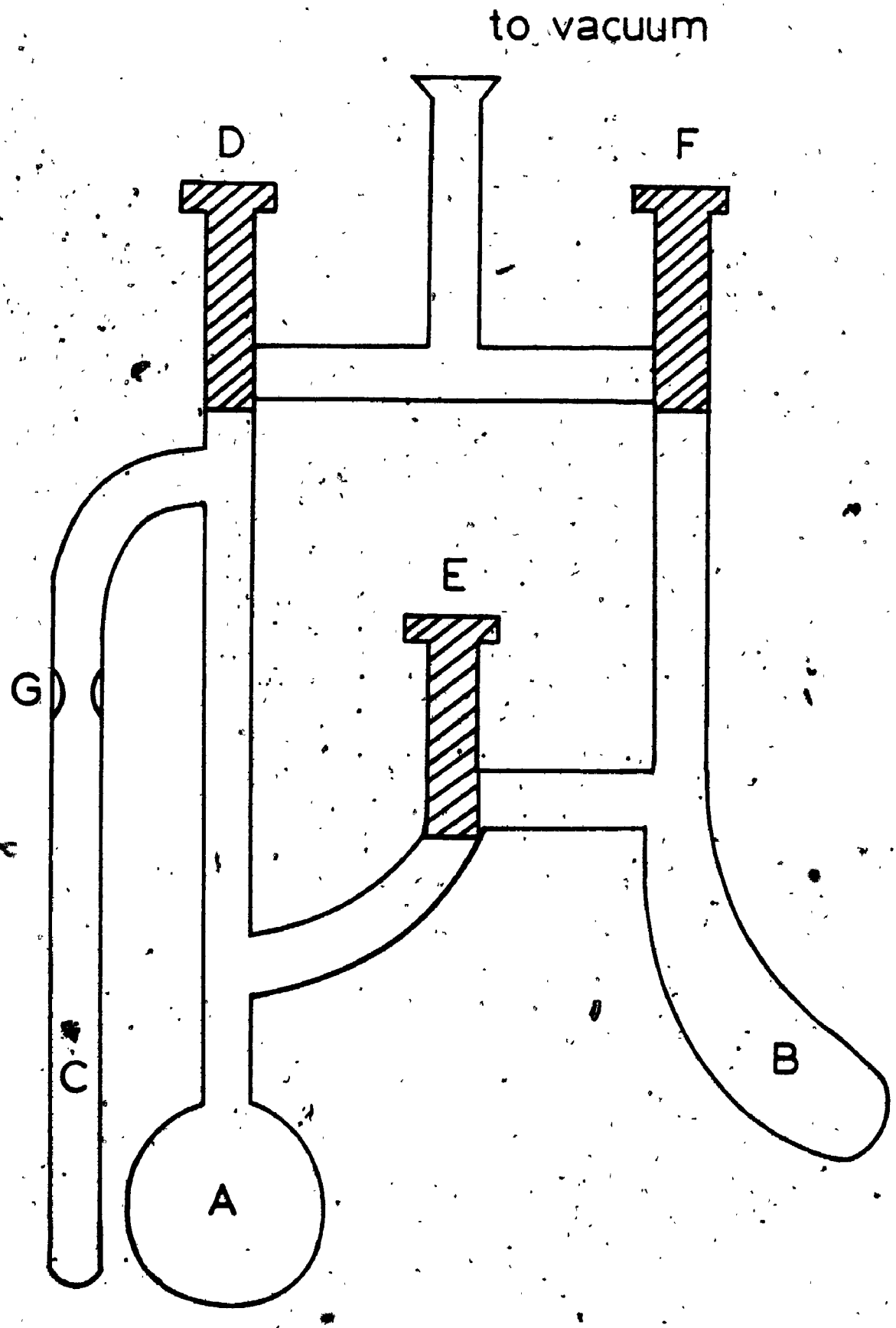
to vacuum
D
F
E
G
C
A
B

and E were closed. The substrate was then adsorbed as outlined in 6.3.3.

C. Silica gel was used without any predrying treatment. There appeared to be no difference between this silica gel and that which had been dried and stored as in A and then reequilibrated with water.

6.3.3 Adsorption of compounds:

Compounds were adsorbed on the surface by evaporation of the solvent from a slurry of silica gel and a solution of the substrate. Methylene chloride was used unless the compound was insoluble in this solvent. The use of a less polar solvent such as cyclohexane for compound adsorption did not affect the results. For silica gel treated as in A or C above the following procedure was used. A solution of the compound to be adsorbed was added to a weighed sample of silica gel in a round bottom flask. After solvent removal on a rotary pump, the free flowing solid was transferred to an irradiation cell. The sample was then evacuated on the rotary pump for 15 minutes before being degassed. Residual unadsorbed material in the round bottom flask was dissolved and the amount determined quantitatively by VPC. Except for high coverage experiments, there was <1% unadsorbed material remaining in the flask.

Slight modifications in the above adsorption procedure were necessary for preparation of samples on dry silica gel, prepared by procedure B (6.3.2). With the dried and cooled silica gel isolated (under vacuum) in compartment A of the

cell shown in Figure 15, a solution of the compound to be adsorbed was added through F to compartment B. After brief degassing of the solution, F was closed, E was opened and the solution was poured onto the silica gel sample. Compartment B was then rinsed with fresh solvent by closing E, adding ~2 ml solvent, degassing the solvent and adding it to the silica gel slurry. The solvent was removed (E and F open, D closed) to give a free flowing sample. All stopcocks were then closed and the cell was attached to a vacuum line and degassed (D open). After degassing, the sample was transferred to the irradiation tube C which was sealed at point G.

When two compounds were to be adsorbed, the additive or sensitizer was always added first and the solvent completely removed before addition of the compound to be photolyzed. The amounts of unadsorbed additive were not quantitatively analyzed but were estimated qualitatively by GC to be <5%.

6.3.4 Degassing procedures:

All silica gel samples were degassed to $<10^{-5}$ torr by three or more freeze-thaw cycles (liquid nitrogen). Since it appeared doubtful that gases adsorbed on the surface could be removed by this degassing procedure, a more efficient technique was used for some of the later experiments. This involved degassing the samples at 10^{-5} torr at 25°C for 1 1/2-2 hours. A comparison of the two methods for identical samples of sulfone 17 adsorbed on silica gel showed that the product ratios obtained upon

photolysis of this substrate were unaffected by the degassing procedure.

The degassed samples were usually sealed under vacuum. However, sample cooling for low temperature irradiations was found to be very inefficient for evacuated samples. For example, irradiation of an evacuated sample in a methanol/dry ice bath (-78°C) resulted in internal sample temperatures in excess of 20°C. (The temperatures were measured on a thermometer which had been placed in the irradiation cell with the bulb well covered with silica gel before the sample was degassed and sealed.) This sample overheating problem was eliminated by adding dry, deoxygenated nitrogen to the degassed sample before the tube was sealed. Under these conditions the sample temperature was stable, although typically 10-20° higher than the cooling bath temperature, during the irradiation period. As a result, nitrogen was added after the sample had been degassed for all low temperature experiments. Since less intense lamps were used for most of the irradiations at room temperature, the presence or absence of nitrogen did not affect the internal sample temperature. All samples of 12, 16 and 17 irradiated at 20°C were degassed and sealed under vacuum; nitrogen was added to all others before they were sealed.

6.3.5 Stability of adsorbed molecules:

The stability of substrates 8, 10, 12, 16, 17 and 28 on dry silica gel was examined. Each was adsorbed on silica

gel and degassed using the normal procedure for a sample to be irradiated. The sample was then stored in the dark at 25°C for 24 hours before desorption of the adsorbed material. In all cases the quantitative recovery (NMR or GC analysis) and the absence of decomposition products indicated that the compound was stable on the surface.

Dibenzyls 13, 14 and 15 were similarly shown to be stable on silica gel. The stability of the products from photolysis of azobisisobutyronitrile and benzyl-α-toluene sulfinate is discussed in sections 6.7.6 and 6.7.4, respectively.

6.3.6 Sample irradiation:

Sample mixing during irradiation was accomplished by rotation of the sample cell (a quartz or Pyrex tube) using a rotary evaporator motor. When the 150 W xenon lamp was used, the light was focused to a spot of approximately the same diameter as the sample tube (1.5-2.5 cm) 20 cm from the lamp housing; the end of the tube was centred in this area. Cooling the sample with cold running water during the irradiation maintained an internal temperature of 20±2°C. For irradiation of solid samples, the Rayonet reactor was placed on its side and the sample tube was rotated in the center of the reactor and air cooled (25-30°C internal temperature). When the 450 W Hanovia lamp was used, the sample was water cooled and rotated 1 cm in front of the immersion well (or the filter, if used).

All low-temperature irradiations were performed with

3 3

OF / DE

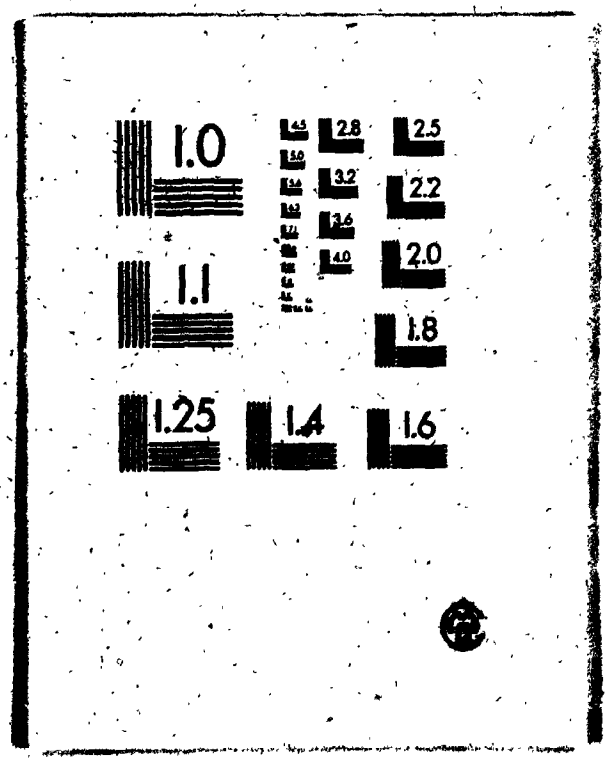

the 1000 W xenon lamp. The light from the lamp was focused on one end of a 16 mm quartz light pipe and the sample tube was rotated with its end directly under and as close as possible to the other end of the light pipe. Both the tube and the end of the light pipe were immersed in a cooling bath (either methanol/dry ice or liquid nitrogen). The sample was cooled for ~20 minutes prior to irradiation. Internal temperatures were either $-55\pm5^{\circ}C$ or $-165\pm10^{\circ}C$ during the irradiations. The light pipe system was also used for room temperature photolyses with the 1000 W lamp; cold running water was used for sample cooling in this case.

Irradiation times varied considerably depending upon the molecule photolyzed and the conversion required. In general, reproducible conversions could be obtained if the experimental set up was not changed between experiments.

6.3.7 Desorption of adsorbed material:

Adsorbed materials were removed from the silica gel by extraction with an appropriate solvent. For photolyzed samples of all molecules except the sulfones 10 and 17, 100 ml of diethyl ether were used for extraction; for samples of 10 and 17, 100 ml of methylene chloride or chloroform were used. The silica was placed in a sintered glass funnel and small portions of solvent were added. The slurry was stirred briefly and the solvent was allowed to drain through slowly, with the use of suction to remove the last of the liquid from the silica. After addition of all the solvent, the filtrate was concentrated to a 3-5 ml volume by

distillation through a 6" column (GC product analysis) or was evaporated to dryness on a rotary evaporator (NMR product analysis).

The efficiency of this extraction procedure was tested in two ways. Firstly, additional washing of the surface with either the original solvent or with a more polar solvent (e.g., methanol) gave no additional material detectable by GC. Secondly, soxhlet extraction of the silica sample for several hours showed no advantages over the above extraction procedure.

6.3.8 Silica gel-solvent slurries:

Slurries were prepared by adding an appropriate volume of a benzene solution of the compound to a weighed sample of silica gel (no predrying unless otherwise specified); a solvent to silica gel ratio of 2.0 ml/g was used. The slurries were not degassed but were stirred and air cooled during irradiation.

For UV experiments the slurry was prepared by adding silica gel to a 1 mm cuvette containing a benzene solution of the substrate. The slurry was stirred as much as possible to remove air bubbles and provide an even distribution of the adsorbed molecules.

6.4 Solution Preparation and Photolyses

Solutions of the substrate to be irradiated were degassed by purging with dry nitrogen for 30 minutes. The solvents used were dried and/or purified as outlined in 6.2.1. Relevant concentrations and irradiation wavelengths

are reported as footnotes in the tables of results for the various substrates. All solutions, except those irradiated at low temperature, were air cooled during irradiation. Where necessary, the solvent was concentrated by distillation (GC analysis) or removed on a rotary evaporator (NMR analysis) before product analysis.

Samples of azobisisobutyronitrile plus sensitizer were the only exception to the above procedure. These were degassed by 4 freeze-thaw cycles to pressures of $<10^{-5}$ torr and then sealed. The samples were irradiated with a 450 W Hanovia lamp with an inner nickel sulfate filter (250 g/L, 1.6 cm path length) and an outer potassium chromate filter (0.270 g/L K_2CrO_4 plus 1 g/L Na_2CO_3, 1 cm path length).

The amount of direct photolysis occurring for the triplet sensitization experiments (0.0318 M 28 plus 0.124 M benzophenone (B) in benzene) was determined by the following procedure.

$$\frac{A_{28}}{A_B} \quad \frac{\ell\varepsilon_{28}[28]}{\ell\varepsilon_B[B]}$$

The extinction coefficients and absorbance ratios at the three wavelengths (medium pressure Hg lamp) transmitted by the filter system were as shown:

λ (nm)	ε_{28} ($M^{-1}cm^{-1}$)	ε_B ($M^{-1}cm^{-1}$)	A_{28}/A_B
302	2.5	166	.004
313	5	69	.019
334	13	124	.027

The relative light intensities, after correction for the transmittance of the filter system, at 302 nm, 313 nm and 334 nm were 0.72, 4.62 and 0.19; the amount of light absorbed by 28 was then calculated:

$$\frac{0.72}{5.53}(0.4\%) + \frac{4.62}{5.53}(1.9\%) + \frac{0.19}{5.53}(2.6\%) = 1.7\%$$

The reported values for the direct and sensitized photolysis quantum yields then allow calculation of the relative amounts of direct and sensitized photolysis:

direct: $0.45(\pm 10\%)(0.017) = 0.0077 \pm 10\%$.

sensitized: $0.1(\pm 10\%)(0.983) = 0.0983 \pm 10\%$.

Therefore, 7±1.4% direct photolysis occurs in the sensitized reaction.

The β values obtained may then be corrected for direct photolysis:

$$\beta_{dir}(.07) + \beta_{corr}(.93) = \beta_{sens}$$

where β_{dir} and β_{sens} are determined from the direct and sensitized amide deuterium ratios.

6.5 Micellar Solution Preparation and Photolyses

An appropriate amount of substrate was added to a 0.08 M solution of potassium dodecanoate in triply distilled water. The mixture was sonicated for 1-2 hours to dissolve the substrate completely. The micellar solution was then transferred to an irradiation vessel and degassed by purging

with nitrogen for 30 minutes. Samples were irradiated either in a Rayonet reactor or with a 450 W Hanovia lamp.

The following extraction procedure was used for isolation of the photolysis mixtures. The micelle solution was diluted to <0.02 M (i.e., below the CMC value) and was extracted three times with ether. The formation of emulsions during the extraction procedure was minimized by the addition of sodium chloride to the aqueous phase. The ether layers were washed once with 10% Na_2CO_3 and once with water and were dried over anhydrous $MgSO_4$. The extract was concentrated by distillation.

6.6 Quantitative Product Analysis

6.6.1 GC:

Products from the photolysis of all dibenzyl ketones, benzyl phenyl acetates and dibenzyl sulfones were analyzed quantitatively by GC. A known amount of an appropriate internal standard was added to the concentrated reaction mixture and the solution was diluted to a 5 or 10 ml volume. The sample was then analyzed by GC for the desired compounds, taking the average of three or more injections for each determination. Internal standards and column temperatures for analysis of reaction mixtures from photolysis of the various substrates were as follows: 12 and 16, tetracosane, 185°C; 8, eicosane, 170°C; 17, tetracosane, 185°C for 15 minutes followed by 200°C for 25 minutes; 10 and 22, docosane, 170°C for 20 minutes followed by 176°C for 25 minutes.

For quantitative determinations of the material present a calibration curve was constructed for each compound to be analyzed. At least 4 solutions of different substrate and internal standard concentrations were prepared and analyzed by GC. The peak areas were determined by weight. The response factor, C, for a compound X was then obtained as the slope of a plot of mol X/mol standard versus peak area X/peak area standard. The response factor was used to calculate the amount of X in a reaction mixture, as shown in equation 44.

$$\text{mol X} = C\left(\frac{\text{peak area X}}{\text{peak area standard}}\right)\ (\text{mol standard}) \qquad (44)$$

6.6.2 NMR:

Product mixtures from the photolysis of azobisisobutyronitrile were analyzed quantitatively by NMR. After removal of the solvent from the reaction mixture, dibenzyl was added as an internal standard and the mixture was dissolved in deuteriated chloroform and its NMR spectrum recorded and integrated. The average of 2 or 3 integrations and the known amount of added standard were used to calculate the amounts of each compound present. In some cases the chloroform was removed and the sample was redissolved in deuteriated benzene and reanalyzed; some signals were better separated in this solvent so this provided an added check for the analysis.

6.6.8 Mass spectrometry:

The deuterium content of amide 33 recovered after photolysis of equimolar mixtures of 28 and 28-d_{12} was determined mass spectrally. The amide was isolated from the reaction mixture by chromatography (silica gel plates, 10% methanol in benzene as eluent) before analysis. A standard amide sample (1:1 33-d_0 : 33-d_{12}) was always run directly before the sample so that the intensities at m/e 154 and 160 could be corrected for the secondary isotope effect on the mass spectral fragmentation.

6.7 Qualitative Product Analysis

6.7.1 Photolyses of 12, 16 and 17:

The products from a preparative scale photolysis of ester 12 were separated by chromatography (silica gel, 10% diethyl ether in hexane). The three dibenzyls obtained were recrystallized from methanol and the identity of each established by comparison of its melting point and NMR and mass spectra to those reported in the literature:[68b] 4,4'-dimethyldibenzyl, 13, m.p. 81.5-82°C (literature[68b] 78-81°C); 4,4'-dimethoxydibenzyl, 15, m.p. 126-127°C (literature[68b] 124-127°C); and 4-methoxy-4'-methyldibenzyl, 14, m.p. 61.5-63°C (literature[68b] 61-62.5°C).

Dibenzyls 13, 14 and 15 were similarly isolated from reaction mixtures produced by photolysis of ketone 16 and sulfone 17 (diethyl ether in hexane, 10% and 20%, respectively).

6.7.2 Dibenzyl ketone (8) photolysis:

Recrystallization from methanol of the material resulting from photolysis of 8 on silica gel to >95% conversion gave dibenzyl, 11, m.p. 51-51.5°C (literature[117] 52.2°C), with an NMR identical to that of an authentic sample. Rearranged ketones, 1-phenyl-4'-methylacetophenone, 20, and 1-phenyl-2'-methylacetophenone, 21, formed during photolysis of 8 on silica gel were isolated by both flash chromatography (silica gel, 3:2 benzene:hexane as eluent) or chromatography on plates (silica gel, 10% ethyl acetate in petroleum ether as eluent). The order of elution was (first to last) dibenzyl, 21, 20 and unreacted ketone 8. The identity of 20 was established by comparison of its GC retention time (two columns; coinjection with an authentic sample) and its NMR and mass spectra with those of an authentic sample prepared synthetically. The identity of 21 was established by comparison of its GC retention time and NMR and GC/MS spectra to those of an authentic sample, also prepared synthetically.

6.7.3 Dibenzyl sulfone (10) photolysis:

Products produced by photolysis of dibenzyl sulfone on silica gel were separated by chromatography (silica gel plates, 25% ethyl acetate in petroleum ether). The order of elution (first to last) was dibenzyl, sulfinate 22 and unreacted sulfone, 10. The sulfinate was identified by comparison of its GC retention time (2 columns) and NMR spectrum with that of an authentic sample.

6.7.4 Benzyl-α-toluenesulfinate (22) photolysis:

Reaction mixtures produced by photolysis of 22 in solution and on silica gel were analyzed qualitatively by NMR and GC (coinjection with authentic samples). Products were not isolated.

6.7.5 Azobisisobutyronitrile (28) photolysis:

The products from a preparative scale photolysis of 28 on silica gel were separated by flash chromatography on silica gel using benzene to elute the less polar material and 10% methanol in benzene to elute amide 33. The order of elution was (first to last) 28, tetramethylsuccinodinitrile (29) and 33. Dinitrile 29 was recrystallized from methanol and its identity established by comparison of its melting point and NMR and mass spectra with those of an authentic sample prepared by solution photolysis of 28. Amide 33 was identified by comparison of its melting point and NMR and mass spectra to those of an authentic sample prepared by hydrolysis of 30. Since ketenimine 30 hydrolyses on silica gel, it was not isolated from surface photolysis mixtures. It was, however, detected in small amounts by NMR for most photolysis mixtures.

The presence of isobutyronitrile, 31, among the products from photolysis of 28 on silica gel was demonstrated by the following procedure. A sample of 28 adsorbed on silica gel was photolyzed to ~100% conversion. The sample was extracted with 40 ml methylene chloride and the solvent was then concentrated to ~1 ml by distillation

through a 6 inch Vigreux column. Deuteriated methylene chloride (2 ml) was added through the top of the column. The solution was again concentrated to a 1 ml volume, and the column was rinsed with an additional 1 ml of deuteriated solvent. The solution was then analyzed by GC and NMR; both showed the presence of 31. This extraction and distillation procedure was shown to give quantitative recovery of 31 adsorbed on silica gel. Since 28 decomposes thermally to yield small amounts of 31, the procedure could only be used for high conversion experiments.

6.7.6 Ketenimine 30 Hydrolysis

5 ml of a 0.113 M benzene solution of 30 was added to 2.8 g silica gel (no predrying). The mixture was stirred thoroughly and was left at 25°C in the dark for 15 hours. The silica gel was then extracted with 100 ml ether. Solvent removal followed by NMR analysis showed the presence of amide 33, 45%, and unreacted 30, 55%. A similar experiment using the dry cell procedure (6.3.2) resulted in ~30% hydrolysis of 30 to the amide.

6.8 CIDNP Experiments

Samples of dibenzyl ketones for CIDNP spectra were all ~0.01 M in deuteriochloroform and were deaerated by purging the solution with nitrogen for 15 minutes. The light source was a 200 W mercury-xenon lamp; the light was passed through a water filter and focused on the top of a quartz light pipe, the end of which was immersed in the sample solution in an NMR tube spinning in the probe of an XL-100 A

spectrometer. Irradiation times of 10-30 seconds were typical and data were collected by both CW and FT scans. Spectra obtained are shown in Figures 9, 10, 11 and 12.

The dibenzyl ratios from the photolysis of the 4-methoxy substituted ketone 25a in $CDCl_3$ were examined by GC. The three dibenzyls were present in a 1:2:1 ratio (assuming that all show the same response, which is reasonable based on the GC behaviour of other dibenzyls).

CIDNP spectra were also measured for the 4-methoxy and 3-chloro substituted ketones, 25a and 25e, in potassium dodeconoate (0.112 M), sodium dodecyl sulfate (0.110 M) and cetyl trimethyl ammonium bromide micellar solutions. Although emission of the methylene protons was clearly visible for both ketones in each of the micellar solutions, sufficient resolution of the two methylene signals for quantitative measurement of the relative amounts of emission could not be obtained (see Figure 12 for the results obtained for 25a in potassium dodecanoate). Similarly, spectra of ketone 16 in $CDCl_3$ or in aqueous potassium dodecanoate showed only partial resolution of the two methylene signals, as shown in Figure 16 for 16 in $CDCl_3$.

Attempts to detect CIDNP effects during the photolysis of ester 12, sulfone 17 and azobisisobutyronitrile (direct and benzophenone sensitized) were unsuccessful.

6.9 ^{13}C Enrichment Experiments

All photolyses of dibenzyl ketone for ^{13}C enrichment measurements used ketone which was 25% ^{13}C in the carbonyl

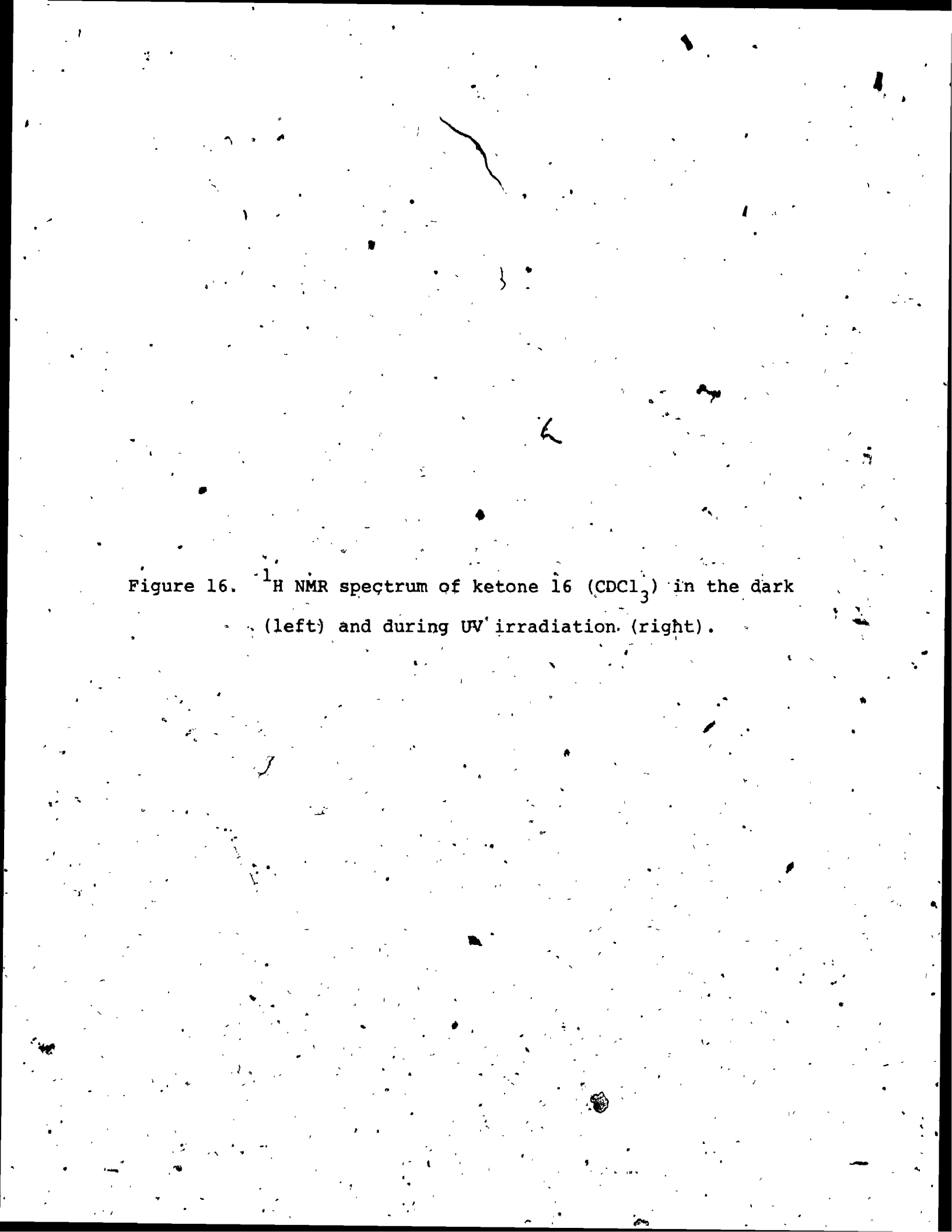

Figure 16. ^1H NMR spectrum of ketone 16 ($CDCl_3$) in the dark (left) and during UV irradiation (right).

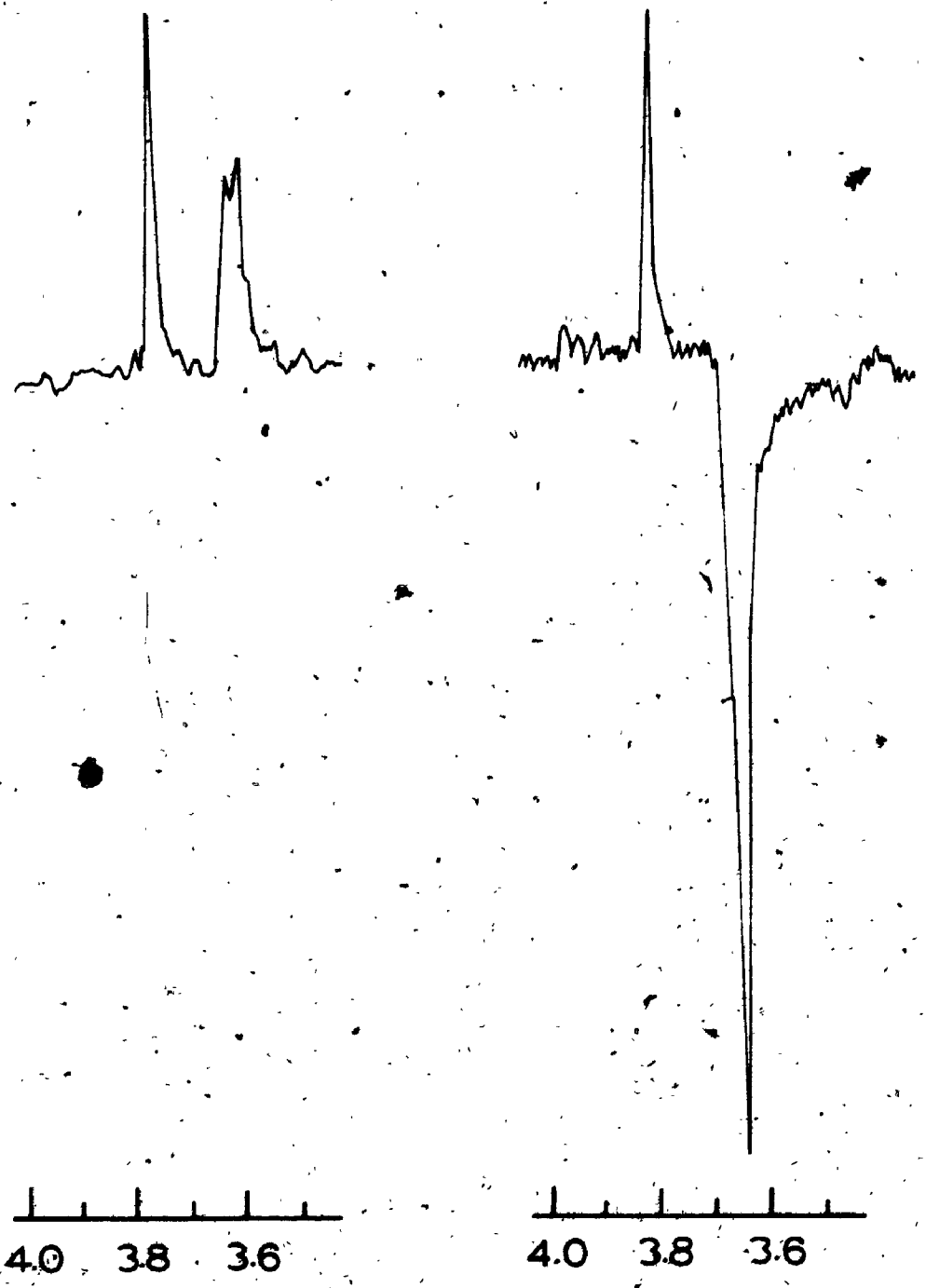
4.0
3.8
3.6
4.0
3.8
3.6

position. A 1000 W xenon lamp was used for all irradiations of solid samples; the sample preparation and extraction procedures were as outlined in 6.3 and all samples were degassed and nitrogen was added before sealing. Micelle samples were prepared and degassed as in 6.5. These samples were stirred and irradiated through pyrex with a 450 W Hanovia medium pressure mercury lamp. After GC analysis to determine the extent of conversion, the reaction mixtures were separated by chromatography (silica gel plates, 10% ethyl acetate in petroleum ether). The samples of 8 and its isomer 20 so obtained were analyzed by GC/MS for ^{13}C content.

The average of ~10 intensity determinations across the width of the VPC peak was used in all ^{13}C analyses. For 8 the analysis was obtained from the molecular ion peaks at m/e 210 and 211. The analysis for 20 was obtained from the mass fragment peaks at m/e 119 and 120 since only a very weak molecular ion peak was obtained for this ketone. The mass spectral intensity ratios for both 8 and 20 were corrected for natural abundance of ^{13}C at other than the carbonyl carbon. In addition, a standard sample of 8 (25% ^{13}C = 0) was always analyzed before samples of recovered 8 were run. Comparison of the % ^{13}C calculated for the standard with that determined mass spectrally allowed correction of the data for instrumental variations. A sample calculation for the determination of α (8) is given below (6.9.1).

The calculation of α' was done as outlined in 3.2; the

integrals were evaluated using a numerical integration procedure based on Simpson's Rule and summing over a sufficiently large number of intervals that any further increase did not change the value of the reported number. The mass spectral intensities for 2Ø could not be corrected for instrumental variations since an enriched sample of this ketone was not available. A sample calculation for the determination of α' is given in 6.9.2.

6.9.1 Calculation α:

The theoretical relative intensities for the mass spectral peaks for M^+ (21Ø) and M^++1 (211) for dibenzyl ketone containing 1ØØ(1-x)% $^{13}C{=}O$ may be calculated as

$$I_{21Ø} = X \tag{45}$$

$$I_{211} = 1-x + x[14(N.A._{^{13}C})+14(N.A._{^{2}H})+1(N.A._{^{17}Ø}) \tag{46}$$

where the second term in (46) is the correction for the natural abundance (N.A.) contributions for ^{2}H, ^{17}O, and ^{13}C (at other than the carbonyl, i.e., 14 other carbons).

$$I_{211} = 1-x + x[14(Ø.Ø112)+14(Ø.ØØØ149)+Ø.ØØØ374] \tag{47}$$

$$= 1 - Ø.84Ø7\ x \tag{48}$$

Normalizing to $I_{21Ø}$ = 1ØØ gives

$$I_{211} = 1ØØ/x - 84.Ø7 \tag{49}$$

The relative intensities considering only the $^{13}C{=}O$ are

$I_{210} = x$ and $I_{211} = 1-x$; normalizing to $I_{210} = 100$ gives

$$I_{211} = 100/x - 100 \qquad (50)$$

Subtracting equation 50 from 49 gives the correction factor, y, needed to correct for the natural abundance contributions from ^{13}C, ^{2}H and ^{17}O to the $M^{+}+1$ peak (for <u>any</u> % $^{13}C=O$):

$$y = 15.93 \qquad (51)$$

The mass spectral data were used to calculate α in the following way (for the experiment at 84.3% conversion, Table 8).

	I_{210}	I_{211}	$I_{211}-y$
recovered ketone 8	100	57.04	41.11
25% $^{13}C=O$ 8	100	49.70	33.77

$$[^{13}C]_f = \frac{41.11}{141.11} \qquad [^{13}C]_0 = \frac{33.77}{133.77}$$

$$[^{12}C]_f = \frac{100}{141.11} \qquad [^{12}C]_0 = \frac{100}{133.77}$$

$$S = \frac{[^{13}C]_f[^{12}C]_0}{[^{12}C]_f[^{13}C]_0}$$

$$\log S = \frac{\alpha-1}{\alpha}\left[\log\left(\frac{1+Sr_0}{1+R_0}\right) - \log(1-f)\right]$$

Since $R_0 = 0.333$, $f = 0.843$

$$\alpha = 1.12$$

The use of the actual mass spec number rather than the calculated one for I_{211} for the initial ketone before photolysis corrects for any instrumental variations which cause deviations from the theoretical intensities. Correction of I_{211} for the recovered ketone by subtraction or by a ratio method gave α values which were within ±0.01 of the value obtained by the above method.

6.9.2 Calculation α':

The theoretical relative intensities for the peaks at 119 and 120 for isomer 20 were used to determine the necessary correction factor, z, for the natural abundance contributions of ^{13}C, ^{2}H and ^{17}O to I_{120}. For 20 which contains 100(1-x)% $^{13}C{=}O$

$$I_{119} = x \tag{52}$$

$$I_{120_0} = 1-x + x[7(0.0112)+7(0.000149)+0.000374] \tag{53}$$

Normalizing to $I_{119} = 100$ gives

$$I_{120} = 100/x - 92.02 \tag{54}$$

Similarly, the normalized intensities considering only the $^{13}C{=}O$ are $I_{119} = 100$ and

$$I_{120} = 100/x - 100 \tag{55}$$

Subtracting (55) from (54) gives the correction factor, z

$$z = 7.99 \qquad (56)$$

A sample α' calculation for the experiment at 84.3% is given below

	I_{210}	I_{211}	$I_{211}-y$
ketone 20	100	63.24	55.25

$$\therefore \quad \frac{[^{13}C_{20}]}{[^{12}C_{20}]} = 0.553$$

From equation 37, chapter 3,

$$\alpha' = \frac{[^{13}C_{20}]}{[^{12}C_{20}]} \times \frac{B}{R_0 A} \qquad (37)$$

where B and A refer to the integrals

$$A = \int_0^f \frac{(1-f)^{1/\alpha}}{1+R_0(1-f)^{((1/\alpha)-1)}} \qquad (57)$$

$$B = \int_0^f \frac{(1-f)}{1+R_0(1-f)^{((1/\alpha)-1)}} \qquad (58)$$

For evaluation by a numerical integration program, integrals A and B were rearranged by making the substitution b = 1-f to give

$$A = \int_1^{1-f} \frac{b^{1/\alpha}}{1+R_0(b)^{((1/\alpha)-1)}}\, db \qquad (59)$$

$$B = \int_1^{1-f} \frac{b}{1+R_0(b)^{((1/\alpha)-1)}} \qquad (60)$$

For f = 0.843, R_0 = 0.333, α = 1.12,

$A = 0.05918 \qquad B = 0.05635$

$$\therefore \alpha' = 0.553 \times \frac{0.05635}{0.333(0.05918)} = 1.58$$

REFERENCES

1. H.P. Boehm, Advances in Catalysis, 16, 179 (1966).

2. K.K. Unger, "Porous Silica, J. Chromotogr. Library", V. 16; Elsevier Scientific Publishing Company: Amsterdam, 1979.

3. R.K. Iler, "The Chemistry of Silica"; John Wiley & Sons, Inc.: New York, 1979; Ch. 6.

4. J.J. Fripiat and J. Uytterhoeven, J. Phys. Chem., 66, 800 (1962).

5. Reference 2, pp. 60-61.

6. A.V. Kiselev and V.I. Lygin, "Infrared Spectra of Surface Compounds"; Keterpress Enterprises: Jerusalem, 1975.

7. V. Ya. Davydov, L.T. Zhuravlev and A.V. Kiselev, Russ. J. Phys. Chem., 38, 1108 (1964).

8. J.B. Peri and A.L. Hensley, J. Phys.Chem., 72, 2926 (1968).

9. C.J. Armistead, A.J. Tyler, F.H. Hambleton, S.A. Mitchell and J.A. Hockey, J. Phys. Chem., 73, 3947 (1969).

10. I. Tsuchlya, J. Phys. Chem., 86, 4107 (1982).

11. J.A. Hockey and B.A. Pethica, Faraday Soc. Trans., 57, 2247 (1961).

12. S.Y. Chuang and S.J. Tao, J. Chem. Phys., 54, 4902 (1951).

13. A.V. Bondarenko, V.F. Kiselev et al., Proc. Acad. Sci. SSSR, Phys. Chem. Sect., Engl. Transl., 136, 157 (1961).

14. References to original literature may be found in reference 2, pp. 78-83.

15. L.R. Snyder, J. Phys. Chem., 67, 2622 (1963).

16. W. Pohle, J. Chem. Soc., Faraday Trans. 1, 78, 2101 (1982).

17. M.R. Basila, J. Chem. Phys., 35, 1151 (1961).

18. (a) L.R. Snyder and J.W. Ward, J. Phys. Chem., 70, 3941 (1966).
(b) J.R. Dacey, Ind. Eng. Chem., 57, 27 (1965).

19. D.O. Hayward and B.M.W. Trapnell, "Chemisorption"; Butterworths: London, 1964.

20. A. Ron, M. Tolman and O.J. Schnepp, J. Chem. Phys., 36, 2449 (1962).

21. B. Boddenberg, R. Haul and G. Oppermann, J. Colloid and Interface Science, 38, 210 (1972).

22. D. Fiat, J. Reuben and M. Tolman, J. Chem. Phys., 46, 4453 (1967).

23. I.D. Gay, J. Phys. Chem., 78, 38 (1974).

24. (a) G.P. Lozos and B.M. Hoffman, J. Phys. Chem., 78, 2110 (1974);
(b) C. Maller and B.M. Hoffman, Ibid., 80, 842 (1976).

25. (a) V.I. Evreinov, V.B. Golubev and E.V. Lunina, Russ. J. Phys. Chem., 49, 564 (1975);
(b) A.K. Selivanovskii, V.B. Golubev, E.V. Lunina and B.V. Strakhov, Ibid., 50, 990 (1976).

26. (a) M. Fujimoto, H.D. Gesser, B. Garbutt and A. Cohen, Science, 154, 381 (1966);
(b) M. Fujimoto, H.D. Gesser, B. Garbutt and M. Shimizer, Ibid., 156, 1105 (1967);
(c) J. Turkevich and Y. Fujita, Ibid., 152, 1619 (1966);
(d) G.B. Garbutt and H.D. Gesser, Can. J. Chem., 48, 2685 (1970).

27. M. Robin and K.N. Trueblood, J. Am. Chem. Soc., 79, 5158 (1957).

28. H. Moesta, Discuss. Faraday Soc., 58, 244 (1974).

29. (a) P.A. Leermakers and H.T. Thomas, J. Am. Chem. Soc., 87, 1620 (1965);
(b) P.A. Leermakers, H.T. Thomas, L.D. Weis and F.C. James, Ibid., 88, 5075 (1966).

30. (a) D. Fassler and W. Guenther, Z. Chem., 17, 429 (1977);
(b) D. Fassler and W. Guenther, Ibid., 18, 69 (1978).

31. J. Griffiths and H. Hart, J. Am. Chem. Soc., 90, 5296, (1968).

32. R.L. Cargill, W.A. Bundy, D.M. Pond, A.B. Sears, J. Saltiel and J. Winterle, Mol. Photochem., 3, 123 (1971).

33. E.F. Kiefer and D.A. Carlson, Tetrahedron Lett., 1617 (1967).

34. P.A. Leermakers, S.D. Weis and H.T. Thomas, J. Am. Chem. Soc., 87, 4403 (1965).

35. M. Anpo, T. Wada and Y. Kubokawa, Bull. Chem. Soc. Japan, 50, 31 (1977).

36. (a) M. Anpo and Y. Kubokawa, J. Phys. Chem., 78, 2442; 2446 (1974);
(b) M. Anpo, S. Hirohashi and Y. Kubokawa, Bull. Chem. Soc. Japan, 48, 985 (1975);
(c) M. Anpo, T. Wada and Y. Kubokawa, Ibid., 48, 2663 (1975).

37. D. Avnir, P. de Mayo and I. Ono, J. Chem. Soc., Chem. Commun., 1109 (1978).

38. P. de Mayo, A. Nakamura, P.W.K. Tsang and S.K. Wong, J. Am. Chem. Soc., 104, 6824 (1982).

39. J.E. Leffler and J.J. Zupancic, Ibid., 102, 259 (1980).

40. J.E. Leffler and J.T. Barbas, Ibid., 103, 7768 (1981).

41. H. Ishida, H. Takahashi and H. Tsubomura, Bull. Chem. Soc. Japan, 43, 3130 (1970).

42. (a) D. Oelkrug and M. Radjaipour, Z. Phys, Chem. (Frankfurt Am Main), 123, 163 (1980);
(b) D. Oelkrug, M. Radjaipour and H. Erbse, Ibid., 88, 23 (1974);
(c) D. Oelkrug, H. Erbse and M. Plauschinat, Ibid., 96, 283 (1975).

43. D. Oelkrug, G. Schrem and L. Andra, Ibid., 106, 197 (1977).

44. R.K. Bauer, R. Borenstein, P. de Mayo, K. Okada, M. Rafalska, W.R. Ware and K.C. Wu, J. Am. Chem. Soc., 104, 4635 (1982).

45. (a) K. Hara, P. de Mayo, W.R. Ware, A.C. Weedon, G.S.K. Wong and K.C. Wu, Chem. Phys. Letters, 69, 105 (1980);
(b) R.K. Bauer, P. de Mayo, W.R. Ware and K.C. Wu, J. Phys. Chem., 86, 3781 (1982).

46. C. Francis, J. Lin and L.A. Singer, Chem. Phys. Lett., 94, 162 (1983).

47. P.L. Piciulo and J.W. Sutherland, J. Am. Chem. Soc., 101, 3123 (1979).

48. R.W. Kessler and F.J. Wilkinson, J. Chem. Soc., Faraday Trans. 1, 77, 309 (1981).

49. J.L. Ruhlen and P.A. Leermakers, J. Am. Chem. Soc., 89, 4944 (1967).

50. H. Werbin and E.T. Strom, Ibid., 90, 7296 (1968).

51. D. Donati, M. Fiorenza and P. Sarti-Fantoni, J. Heterocycl. Chem., 16, 253 (1979).

52. P. de Mayo, K. Okada, M. Rafalska, A.C. Weedon and G.S.K. Wong, J. Chem. Soc., Chem. Commun., 820 (1981).

53. C. Eden and Z. Shaked, Isr. J. Chem., 13, 1 (1975).

54. (a) V. Slawson, Lipids, 11, 472 (1976);
(b) G.S. Wu, R.A. Stein and J.F. Mead, Ibid., 14, 644 (1979).

55. A.W. Adamson and V. Slawson, J. Phys. Chem., 85, 116 (1981).

56. T.R. Evans, A.F. Toth and P.A. Leermaker, J. Am. Chem. Soc., 89, 5060 (1967).

57. C. Balny, K. Djaparidze and P. Dorizon, C.R. Acad. Sci., Ser. C, 265, 1148 (1967).

58. H.D. Bruer and H. Jacob, Chem. Phys. Lett., 73, 172 (1980).

59. L.D. Weis, T.R. Evans and P.A. Leermakers, J. Am. Chem. Soc., 90, 6109 (1968).

60. (a) H.G. Hecht and J.L. Jensen, J. Photochem., 9, 33 (1978);
(b) H.G. Hecht and R.L. Crackel, Ibid., 15, 263 (1981).

61. K. Otsuka, M. Fukaya and A. Morikawa, Bull. Chem. Soc. Japan, 51, 367 (1978).

62. D. Fassler, R. Gade and W. Guenther, J. Photochem., 13, 49 (1980).

63. S. Lazare, P. de Mayo and W.R. Ware, Photochem. Photobio., 34, 187 (1981).

64. P.S. Engel, J. Am. Chem. Soc., 92, 6074 (1970).

65. W.K. Robbins and R.H. Eastman, Ibid., 92, 6067, 6077 (1970).

66. (a) B. Blank, P.G. Mennitt and H. Fischer, Spec. Lect. 23rd Congr. Pure Appl. Chem., 4, 1 (1971);
(b) H. Langhals and H. Fischer, Chem. Ber., 111, 543 (1978);
(c) M. Lehni, H. Schuh and H. Fischer, Int. J. Chem. Kinet., 11, 705 (1979).

67. T.O. Meiggs, L.I. Grossweiner and S.I. Miller, J. Am. Chem. Soc., 94, 7986 (1972).

68. (a) R.S. Givens and W.F. Oettle, Ibid., 93, 3301 (1971);
(b) R.S. Givens and W.F. Oettle, J. Org. Chem., 37, 4325 (1972);
(c) B. Matuszewski, R.S. Givens and C. Neywick, J. Am. Chem. Soc., 95, 595 (1973);
(d) R.S. Givens, B. Matuszewski, N. Levi and D. Leung, Ibid., 99, 1896 (1977).

69. A.A.M. Roof, H.F. van Woerden and H. Cerfontain, J. Chem. Soc., Perkin Trans. II, 841 (1980).

70. (a) R.S. Givens and B. Matuszewski, Tetrahedron Lett., 861 (1978);
(b) J.H.-S. Liu, "Mechanistic and Exploratory Studies: SO_2 Photoextrusion and β,γ-Unsaturated Carbonyl Photochemistry", Ph.D. Dissertation, University of Kansas, 1980.

71. G.E. Robinson and J.M. Vernon, J. Chem. Soc., Perkin Trans. I, 1682 (1977).

72. G.F. Lehr and N.J. Turro, Tetrahedron, 37, 3411 (1981).

73. (a) L. Lunazzi, K.U. Ingold and J.C. Sciano, J. Phys. Chem., 87, 529 (1983);
(b) N.J. Turro, I.R. Gould and B.H. Baretz, Ibid., 87, 531 (1983).

74. W. Braun, L. Rajbenhach and F.R. Eirich, Ibid., 66, 1591 (1962).

75. R. Kaptein, J. Brokken-Zijp and F.J.J. de Kanter, J. Am. Chem. Soc., 94, 6280 (1972).

76. S.L. Murov, "Handbook of Photochemistry"; Marcel Dekker, Inc.: New York, 1973.

77. R.L. Hoffmann, D.G. McConnell, G.R. List and C.D. Evans, Science, 157, 550 (1967).

78. R.K. Bauer, P. de Mayo and W.R. Ware, unpublished results.

79. B.H. Baretz and N.J. Turro, J. Am. Chem. Soc., 105, 1309 (1983).

80. N.J. Turro and W.R. Cherry, Ibid., 100, 7431 (1978).

81. N.J. Turro, M.F. Chow, C.J. Cheung, Y. Tanimoto and G.C. Weed, Ibid., 103, 4574 (1981).

82. J.C. Scaiano, E.B. Abuin and L.C. Stewart, Ibid., 104, 5673 (1983).

83. (a) N.J. Turro, D.R. Anderson and B. Kraeutler, Tetrahedron Lett., 21, 3 (1980);
(b) N.J. Turro, M.F. Chow, C.J. Cheung and B. Kraeutler, J. Am. Chem. Soc., 103, 3886 (1981).

84. C.R. Hall and D.J.H. Smith, Tetrahedron Lett., 3633 (1974).

85. J. Salteil and L. Metts, J. Am. Chem. Soc., 89, 2232 (1967).

86. (a) R.G. Lawler and G.T. Evans, Ind. Chem. Belg., 36, 1087 (1971);
(b) G.T. Evans and R.G. Lawler, Mol. Phys., 30, 1085 (1975).

87. F.J. Adrian, "Chemically Induced Magnetic Polarization", (eds) L.T. Muus, P.W. Atkins, K.A. McLauchlan and J.B. Pedersen; D. Reidel Publishing Co.: Dordrecht, Holland, 1977; p. 77.

88. R. Kaptein, Adv. Free Radical Chem., 5, 381 (1975).

89. (a) A.L. Buchachenko, E.M. Galimov, V.V. Ershov, G.A. Nikiforov and A.D. Pershin, Dokl. Akad. Nauk SSSR, 228, 379 (1976).
(b) A.L. Buchachenko, Russ. J. Phys. Chem., 51, 1445 (1977).

90. (a) B.Kraeutler and J.J. Turro, Chem. Phys. Lett., 70, 266 (1980);
(b) N.J. Turro, M.F. Chow and B.Kraeutler, Ibid., 73, 545 (1980);
(c) N.J. Turro, D.R. Anderson, M.F. Chow, C.J. Cheung and B. Kraeutler, J. Am. Chem. Soc., 103, 609 (1983).

91. For a review of magnetic effects see: N.J. Turro, Proc. Natl. Acad. Sci. USA, 80, 609 (1983).

92. L. Sterna, D. Ronis, S. Wolfe and A. Pines, J. Chem. Phys., 73, 5493 (1980).

93. G.A. Epling and E. Florio, J. Am. Chem. Soc., 103, 1237 (1981).

94. R.B. Bernstein, J. Phys. Chem., 56, 893 (1952).

95. R.S. Hutton, H.D. Roth, B. Kraeutler, W.R. Cherry and N.J. Turro, J. Am. Chem. Soc., 101, 2227 (1979).

96. The integrals $\int_a^b f(x)dx$ and $\int_\alpha^\beta g(u)du$ are equivalent for a function $f(x)$, continuous when $a \leq x \leq b$ when $\phi(u)$ has a continuous derivative and $\phi(\alpha) = a$, $\phi(\beta) = b$ and $a \leq \phi(u) \leq b$ for $\alpha \leq u \leq \beta$ or $\beta \leq u \leq \alpha$ and the substitution $x = \phi(u)$ changes $f(x)dx$ to $g(u)du$.

97. P. Neta and R.H. Schuler, J. Phys. Chem., 77, 1368 (1973).

98. J. March, "Advanced Organic Chemistry: Reactions, Mechanisms and Structures"; McGraw-Hill: New York, 1977; p. 253.

99. σ values are controversial. Those used here are defined by Leigh et al.[100] based on some data of Creary.[101]

100. W.J. Leigh, D.R. Arnold, R.W.R. Humphreys and P.C. Wong, Can. J. Chem., 58, 2573 (1980).

101. X. Creary, J. Org. Chem., 45, 280 (1980).

102. (a) F.D. Lewis, L.H. Hoyle and J.G. Magyar, Ibid., 40, 488 (1975);
(b) F.D. Lewis, R.T. Lauterbach, H.G. Hein, W. Hartmann and H. Rudolph, J. Am. Chem. Soc., 97, 1519 (1975).

103. C. Walling and R.T. Clark, Ibid., 96, 4530 (1974).

104. (a) P.J. Wagner, Topp. Curr. Chem., 66, 1 (1976);
(b) N.J. Turro, "Modern Molecular Photochemistry"; Benjamin/Cummings: Menlo Park, CA, 1978; p. 528.

105. J.P. Fouassier and A. Merlin, Can. J. Chem., 57, 2812 (1979).

106. (a) M. Talât-Erben and S. Bywater, J. Am. Chem. Soc., 77, 3710 (1955);
(b) G.S. Hammond, O.D. Trapp, R.T. Keys and L.J. Neff, Ibid., 81, 4878 (1959);
(c) G.S. Hammond, C.H. Wu, O.D. Trapp, J. Warkentin and R.T. Keys, Ibid., 82, 5394 (1960) and references therein.

107. R. Back and C. Sivertz, Can. J. Chem., 32, 1061 (1955).

108. P. Smith and A.M. Rosenberg, J. Am. Chem. Soc., 81, 2037 (1959).

109. (a) J.M. McBride, Ibid., 93, 6302 (1971);
(b) A.B. Jaffe, K.J. Skinner and J.M. McBride, Ibid., 94, 8510 (1972).

110. P.S. Engel, D.J. Bishop and M.A. Page, Ibid., 100, 7009 (1978).

111. For a recent review of azo alkane photochemistry see: P.S. Engel, Chem. Rev., 80, 99 (1980).

112. (a) H. Werbin and E.T. Strom, J. Am. Chem. Soc., 90, 7296 (1968).
(b) L. Eberson, Electrochim. Acta, 12, 1473 (1967).

113. R.M. Haines and W.A. Walters, J. Chem. Soc., 3221 (1958).

114. G. Jones, II and L.P. McDonnell, J. Chem. Soc., Chem. Commun., 36 (1976).

115. F.W. McLafferty, D.J. McAdoo, J.S. Smith and R. Kornfeld, J. Am. Chem. Soc., 93, 3720 (1971).

116. J.H. Fendler and E.J. Fendler, "Catalysis in Micellar and Macromolecular Systems"; Academic Press: New York, 1975.

117. CRC Handbook of Chemistry and Physics; CRC Press: Ohio, 1974.

118. R.C. Elderfield and K.L. Burgess, J. Am. Chem. Soc., 82, 1975 (1960).

119. S.B. Coan and E.I. Becker, Ibid., 76, 501 (1954).

120. S.B. Coan and E.I. Becker, "Organic Synthesis", Collect. V. IV; John Wiley & Sons, Inc.: New York, 1968; pp. 174, 176.

121. O. Behagel and H. Ratz, Chem. Ber., 72, 1257 (1939).

122. R.R. Otter and R.L. Shriner, J. Am. Chem. Soc., 73, 887 (1951).

123. S. Smiles and C.M. Bere, "Organic Synthesis", Collect. V.I; John Wiley & Sons, Inc.: New York, 1941; p. 7.

124. Q.E. Thompson, J. Org. Chem., 30, 2703 (1965).

125. (a) C.G. Overberger, M.T. O'Shaughnessy and H. Schalit, J. Am. Chem. Soc., 71, 2661 (1949);
(b) A.W. Dox, Ibid., 47, 1471 (1925).

END

1 9H0 3 1 8 4

FIN